Damping of low frequency oscillations in ac/dc power systems using hvdc converter control
by Prince Alfred Emmanuel

A thesis submitted in partial fulfillment of the requirements for the degree of Doctor of Philosophy in Electrical Engineering
Montana State University

Abstract:
This thesis is concerned with the problem of damping of low frequency oscillations in ac/dc power systems using hvdc converter control. One objective of this thesis is to evaluate the performance of nonconventional hvdc controllers and small signal modulation schemes with reference to damping of these oscillations. Another objective is to develop an adaptive control strategy to enhance the damping.

Various nonconventional control strategies as available in the literature, are presented and are compared with the conventional control strategy. A Prony based evaluation of the nonconventional controllers is also carried out to study their effectiveness in damping low frequency oscillations. The performance of the different nonconventional control schemes is evaluated by conducting time-domain simulation studies on a 42-bus, 17-machine test system that includes a dc line model.

Various small signal modulation schemes are discussed, and a Prony-based analysis is used to obtain the ac modulating signal which offers the best promise for damping. A modified Prony analysis is developed to identify systems which contain a feedforward or throughput term in their linear model. Using the results of the modified Prony analysis, a modulation compensator is designed and implemented in the simulation. Also, the effectiveness of the modulating compensator for damping low frequency oscillations is examined on the basis of a time domain simulation on the test system. Also, a combination of real and reactive power modulation, using firing angle control at the rectifier and SVC control at the inverter, is presented for enhancing the damping of low frequency oscillations.

Lastly, a supplementary adaptive modulation scheme is presented. In this scheme the modulating signal is determined by an adaptive controller. Implementation of adaptive current modulation and adaptive rectifier firing angle modulation are reported, and time-domain simulation results on the test system are presented.

DAMPING OF LOW FREQUENCY OSCILLATIONS IN AC/DC POWER SYSTEMS USING HVDC CONVERTER CONTROL

by

Prince Alfred Emmanuel

A thesis submitted in partial fulfillment
of the requirements for the degree

of

Doctor of Philosophy

in

Electrical Engineering

MONTANA STATE UNIVERSITY
Bozeman, Montana

October 1991

APPROVAL

of a thesis submitted by

Prince Alfred Emmanuel

This thesis has been read by each member of the thesis committee and has been found to be satisfactory regarding content, English usage, format, citations, bibliographic style, and consistency, and is ready for submission to the College of Graduate Studies.

10/25/91
Date

D. A. Pierre
Chairperson, Graduate Committee

Approved for the Major Department

10/28/91
Date

Head, Major Department

Approved for the College of Graduate Studies

11/5/91
Date

Henry L Parsons
Graduate Dean

STATEMENT OF PERMISSION TO USE

In presenting this thesis in partial fulfillment of the requirements for a doctoral degree at Montana State University, I agree that the Library shall make it available to borrowers under rules of the Library. I further agree that copying of this thesis is allowable only for scholarly purposes, consistent with "fair use" as prescribed in the U.S. Copyright Law. Requests for extensive copying or reproduction of this thesis should be referred to University Microfilms International, 300 North Zeeb Road, Ann Arbor, Michigan 48106, to whom I have granted "the exclusive right to reproduce and distribute copies of the dissertation in and from microfilm and the right to reproduce and distribute by abstract in any format."

Signature 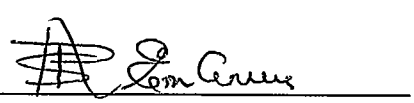

Date 10/25/91

ACKNOWLEDGEMENTS

I wish to thank my graduate advisor, Dr. Donald Pierre, for sharing his knowledge and wisdom during my studies, research and writing of this thesis. I would also like to thank Dr. Hashem Nehrir and Dr. Jim Smith for their helpful suggestions and guidance concerning the research. Special acknowledgements are made to the above three for their patience and knowledge while providing corrections to the thesis. My thanks also go to Dr. Dan Trudnowski for allowing me to use his Prony Identification Software Package, and to Mr. Tom Short for developing a method of integrating controllers in the power-system simulation package.

The financial support of the Electrical Power Research Institute, the Bonneville Power Administration, the Montana Electrical Power Research Affiliates, the Montana State Engineering Experiment Station, and the Department of Electrical Engineering at Montana State University, is gratefully appreciated.

Finally, I would like to thank my parents for their encouragement and support all through my life.

TABLE OF CONTENTS

TABLE OF CONTENTS--Continued

TABLE OF CONTENTS--Continued

LIST OF TABLES

LIST OF FIGURES

LIST OF FIGURES--Continued

LIST OF FIGURES--Continued

LIST OF FIGURES--Continued

LIST OF FIGURES--Continued

LIST OF FIGURES--Continued

LIST OF FIGURES--Continued

ABSTRACT

This thesis is concerned with the problem of damping of low frequency oscillations in ac/dc power systems using hvdc converter control. One objective of this thesis is to evaluate the performance of nonconventional hvdc controllers and small signal modulation schemes with reference to damping of these oscillations. Another objective is to develop an adaptive control strategy to enhance the damping.

Various nonconventional control strategies as available in the literature, are presented and are compared with the conventional control strategy. A Prony based evaluation of the nonconventional controllers is also carried out to study their effectiveness in damping low frequency oscillations. The performance of the different nonconventional control schemes is evaluated by conducting time-domain simulation studies on a 42-bus, 17-machine test system that includes a dc line model.

Various small signal modulation schemes are discussed, and a Prony-based analysis is used to obtain the ac modulating signal which offers the best promise for damping. A modified Prony analysis is developed to identify systems which contain a feedforward or throughput term in their linear model. Using the results of the modified Prony analysis, a modulation compensator is designed and implemented in the simulation. Also, the effectiveness of the modulating compensator for damping low frequency oscillations is examined on the basis of a time domain simulation on the test system. Also, a combination of real and reactive power modulation, using firing angle control at the rectifier and SVC control at the inverter, is presented for enhancing the damping of low frequency oscillations.

Lastly, a supplementary adaptive modulation scheme is presented. In this scheme the modulating signal is determined by an adaptive controller. Implementation of adaptive current modulation and adaptive rectifier firing angle modulation are reported, and time-domain simulation results on the test system are presented.

CHAPTER 1

INTRODUCTION

The relative merits of high voltage direct current (hvdc) transmission and alternating current (ac) transmission are well known [1-5]. The biggest advantage of dc is the high speed control capability of the dc controller which offers various possibilities including very fast control of dc power to stabilize the overall system and fast fault isolation in the case of dc feeding the fault. High speed control of the dc controller can be used for dynamic stabilization of low frequency oscillations (less than 3 Hz) referred to as electromechanical power system oscillations. These electromechanical oscillations are stimulated by disturbances in the system and result in energy exchanges between generators and other network components of the power system. There are two types of electromechanical oscillations: local modes (0.8 to 3 Hz) and interarea modes (0.2 to 0.8 Hz) [6,7]. A local mode of oscillation occurs when a single generator swings against the system while an interarea mode of oscillation occurs when a group of generators swing together against other groups of generators. They are quite significant in the case of a large system connected by long and relatively weak interties. These oscillations can limit the amount of power which can be

transferred over these interties and can reduce the life of generators, transformers and other network components. Sometimes even a small scale outage occurring during the oscillations can cause the system to become unstable and separate. Also there is a danger of these undamped oscillations initiating or aggravating a cascade outage [6]. Although power systems possess natural positive damping capability, the response of power system controls to the synchronizing swings associated with these low frequency modes can produce sufficient negative damping to cancel the natural positive damping of the system. Thus damping of these low frequency modes is necessary for proper operation of the power system. This has been the subject of much research lately. A detailed description of these electromechanical modes of oscillations is covered in [7], while in [6] justification and motivation for improving the damping of these oscillations is given.

Several power system devices can be utilized for damping these oscillations. They include Static Var Compensators (SVC), Power System Stabilizers (PSS), High Voltage DC (HVDC) Controllers [6,7], and electronically controlled braking resistors. The high speed control capability of the dc controller makes it a proper candidate for assisting in dynamic stabilization of these oscillations. Thus, one objective of this thesis is to evaluate the performance of the hvdc con-

trollers, both conventional and nonconventional, including modulation controllers. Another objective is to determine adaptive control strategies for damping low frequency oscillations. Since power systems are nonlinear and time-varying in nature, they are suitable candidates for application of adaptive control strategies [6-7].

Hvdc Transmission

Basically, the hvdc transmission schemes are of three types: back-to-back, two-terminal or point-to-point, and multi-terminal dc links [8]. A two-terminal dc link consists of a rectifier and an inverter (commonly called a converter) along with the associated control, commutating transformers, harmonic filters, shunt capacitors, smoothing reactors, and dc transmission lines [1-5]. It can be one of monopolar, bipolar or homopolar [2]. The back-to-back hvdc link consists of all the above components except the dc transmission line. From an operational point of view the back-to-back scheme is very similar to the two-terminal type with a few small exceptions. A multi-terminal link, in addition to all the above components, consists of more than one rectifier and/or inverter terminal. Detailed information regarding the components of dc links can be obtained from [2]. The relationships between ac and dc quantities can be obtained from [1-5].

Hvdc Modelling

During the past decade, interest by utilities has increased in the use of high voltage direct current transmission. An underlying reason for such interest is that the fast response of the hvdc system adds a degree of controllability to a power system which is not available with the ac system alone [9]. There has been a corresponding development in modelling and simulation of hvdc systems to evaluate the performance of ac/dc systems using transient and dynamic stability programs. The initial trend in the hvdc modelling was towards simple models which are now being found to be inadequate for modelling of a dc system connected to a weak ac system and for more complex multi-terminal systems [10]. Thus models having various levels of details have been developed and used in power system stability studies [10]. In hierarchical order they are classified under the following headings: simple model, response or performance model, detailed model, and electromagnetic transient program (EMTP) simulation model.

A simple model of hvdc transmission is algebraic in nature and represents the dc link by constant real power (P) and reactive power (Q) injection at its ac terminal. A response model is more involved and realistic and represents the dc link using ac/dc interface equations. A response model also includes the functional action of the hvdc controls and pro-

tection plus the dynamics of the modulation control. The detailed model on the other hand includes the full hvdc controller including the RL/RLC dynamics of the dc line and the firing angle control at the pole. The highest level of detail is represented in EMTP models where a 3-phase representation of the ac system, controlled converter action of the dc pole, and distributed model of the dc line are used.

Hvdc Control

The complete hvdc control system is realized at four levels, designated respectively as overall controls, master controls, pole controls, and bridge controls [4]. The overall controls provide the interface between the ac and dc system and generate the current orders for the master controls in response to required functions such as control of transmitted power, ac system damping, ac system frequency or combinations of them. The master controller provides coordinated current orders for the pole control. The pole control provides current margin, current limits, tap changer control and signals needed for the bridge control. The bridge control, also known as valve control, generates the firing angle for all the valves in the bridge to obtain the desired level of voltage and current in the system.

The pole controller at both rectifier and inverter of a two-terminal hvdc link consists of a direct current control loop including a current measuring device, a current regulator, and associated valve firing angle control equipment. In addition, the inverter pole control is also provided with a constant extinction angle (CEA) control to prevent inverter commutation failure and to minimize the reactive power consumption. The rectifier pole control on the other hand consists of inherent minimum firing angle control, also known as natural voltage characteristic, obtained by limiting the firing angle to some minimum value (normally about 5 degrees) so as to ensure appreciable positive voltage across the valves for safe operation under any circumstances. Unlike minimum firing angle control, the constant extinction angle control is not a "natural" characteristic and has to be maintained artificially.

The assignment of current control to the rectifier or to the inverter station is made after considering the investment cost for reactive power consumption, the availability of reactive power, the minimization of losses and the total running cost. Normally the total reactive power consumption becomes minimum and the utilization of the dc line the best when the rectifier is assigned current control. Thus, under normal operation the converters are coordinated in such a way that the rectifier controls current while the inverter remains on

constant extinction angle control. This coordination is achieved by reducing the current reference (current order) at the inverter end by an amount called the current margin which is 10 to 15% of the rectifier current order. A reduction in the rectifier-end dc voltage or an increase in the inverter-end ac voltage could result in the loss of current control at the rectifier end causing the rectifier to go into a minimum firing angle control mode. If the reduction in the current is more than the current margin, then the inverter will pick up the current control, or else it will continue to operate in the constant extinction angle control mode. Thus the basic control strategy referred to as the 'conventional control strategy' allows the following three modes of operation.

1. Mode CE, rectifier in constant current and inverter in constant extinction angle control.
2. Mode IC, rectifier in minimum firing angle control and inverter in constant current control.
3. Mode IE, transition mode between the above two modes where the rectifier is in minimum firing angle control and the inverter is in constant extinction angle control.

Advantages of this conventional current controller, which keeps the inverter on constant extinction angle during normal operation, are minimum reactive power consumption and minimum harmonic generation as well as optimal utilization of the dc

line. However, the inverter in this mode exhibits a negative impedance characteristic that may cause voltage and power instability [11]. If the negative source resistance of the inverter exceeds the positive resistance of the circuit, a relaxation oscillation can build up in which the inverter, the line and the converter control take part. The inverter periodically goes into the current control mode even if it is scheduled to stay in the extinction angle control mode. Also, during ac system faults at the inverter end, there is a big risk of commutation failure. If the fault is electrically close to the inverter, the inverter may not be able to recover. In such cases one way to reduce the stress on the inverter valve is by providing a Voltage Dependent Current Order Limit (VDCOL) for the rectifier control characteristic. The function of the VDCOL is to reduce the current order linearly from its normal value to some minimum value when dc bus voltage falls considerably below its rated value, thereby reducing the stress on the inverter valve.

Another problem with the basic characteristic arises when the rectifier voltage ceiling gets very close to that of the inverter. In this case the rectifier and inverter characteristics intersect in the region of current margin which leads to three point instability. This can be avoided by providing

a positive resistance slope characteristic for the inverter in the current margin region which amounts to changing its modes of operation.

One way of improving the voltage/power stability of the basic conventional control scheme is to provide compensation equipment at the inverter terminal. This equipment may consist of static capacitors, synchronous condensers or static var compensators (thyristor switched capacitors or thyristor controlled reactors or a combination of both). Therefore, the principle of minimizing the reactive power consumption by operating the inverter at constant extinction angle is partially ineffective due to the need for more reactive support equipment. The other economical solution is to use the high speed control capability of the hvdc converter. It has been shown that by changing the inverter mode of operation it is possible to improve system stability. Various nonconventional modes of operation have been suggested in the literature for this purpose [11-20]. These control modes are: constant ac voltage control, constant dc voltage control, constant reactive current control, constant power factor control, constant active power control, and constant reactive power control.

In addition to the above conventional and nonconventional modes of control, modification is also possible to maintain constant power on the dc line under abnormal conditions. Such

modifications include the addition of a voltage dependent current order limit (VDCOL) and a margin switching unit (MSU) as described in [21]. The VDCOL is used to maximize the power transfer capability of the dc line under adverse conditions and to reduce the dc tie power and consequently the volt-ampere-reactive (VAR) demand from the ac system during periods of depressed ac system voltage. VDCOL is introduced in the current order determination logic of the dc control system and its function is to reduce the current order linearly from its normal value down to some specified minimum value of the current when dc bus voltage drops below some specified percentage of its rated value. The MSU is used to prevent any sustained decrease in the scheduled power of the dc line when the inverter takes control of the current at a value which is less than the desired value by the amount equal to the current margin. Essentially, the margin switching unit raises the current order at both rectifier and inverter ends when the rectifier has lost current control.

The pole controller of the multi-terminal system is merely an extension of the two-terminal pole controller. There are basically two types of multi-terminal hvdc systems in existence: namely, constant voltage parallel systems with all converters connected in parallel, and constant-current series systems with all converters connected in series. Both of them could

be either monopolar or bipolar and when bipolar, each pole may serve different stations [2]. The disadvantages of the constant current series system are full I^2R losses even at light load and the possibility that at certain times certain converters may be lightly loaded which requires their operation at voltage levels well below the rated value. To compensate for this, either a tap changer transformer with wide tap range is needed or the converter has to be operated at higher control angle thereby increasing the consumption of reactive power, losses in the valve damping circuit, and probability of converter faults [2]. Thus most of the existing multi-terminal systems are of constant voltage parallel type.

In the case of constant voltage multi-terminal systems, all the converters operate at constant current except the one having the lowest ceiling voltage. This converter controls the line voltage, and is normally one of the inverters operating at constant extinction angle. The remaining converters operate at voltages lower than their respective ceilings. The current command at the voltage controlling converter is made equal to the negative of the algebraic sum of the current commands of the current controlling converters and the current margin. In taking the algebraic sum, the rectifier currents are taken as positive and inverter currents as negative.

Hvdc Modulation Control

In an ac interconnected system, the power flow is determined by the conditions existing in the connected subsystems [22]. So if one of the subsystems suffers a disturbance then it directly affects the other subsystems, and in some cases disturbances can result in cascade tripping of many generators. This cascade tripping may be avoided if the infeed tie line to the disturbed subsystem is tripped. However, this results in further aggravating the disturbed system and may cause its complete shutdown. An hvdc link, on the other hand can provide buffering of one system from the other. Even with the simplest of control strategies, the power flow may be continued almost unchanged. It is possible to provide additional controls which enable the hvdc link to vary power flow within the rating of the link, to assist the subsystem in trouble, to the extent which the healthy system can allow without putting itself in difficulty [22]. In essence if the power being transmitted by the dc line is modulated properly in response to a signal from the ac network, then a disturbance originating in any of the ac subsystems can be shared, and the oscillations occurring in the system often can be damped. As a result various forms of modulation have been successfully utilized by a number of dc projects to dampen system oscillations and to enhance stability.

There are two types of modulation control: small-signal and large-signal modulation [9]. Small-signal modulation is generally continuous and is used for modulation of current, power, or voltage set points. Large-signal modulation is initiated in response to discrete events such as the occurrence of faults, or the loss of generation or transmission.

Adaptive Control

An adaptive controller is a regulator that modifies its behavior according to the changes in the dynamics of the process it is controlling [23]. There are mainly two types of adaptive controllers: 1) the direct type in which the regulator parameters are directly changed as the dynamics of the system change; and 2) the indirect type in which the regulator parameters are modified indirectly. Direct adaptive controllers are also called model-reference adaptive controllers (MRAC) because they strive to make the closed-loop plant behave like a model system. Indirect adaptive controllers are also called self-tuning adaptive controllers, since they automatically tune the controller to the desired performance specified by the design procedure.

Practical power systems are high order, nonlinear, and time-varying systems. These characteristics make power systems suitable candidates for application of adaptive control. The

time varying nature of the power system makes it extremely difficult and sometimes impossible to obtain an accurate model of the system. Also, it is difficult to present the problem of damping of low frequency oscillations in the power system into an idealized model. This rules out the possibility of direct adaptive control of power systems. Thus an indirect adaptive control strategy will be used in this thesis for control of ac/dc power systems.

Literature Review

Because there are a large number of publications in the area of hvdc modelling, hvdc control, and hvdc modulation control, it is not possible to review them all here. Only the available relevant literature which has more bearing on the problem at hand is covered in this section. However, in the case of adaptive control of hvdc systems there are only two known papers, both of which are reviewed. For the sake of organization and simplicity, this section is subdivided into the following subsections: hvdc modelling, hvdc control, hvdc modulation control and hvdc adaptive control.

Hvdc Modelling

A general and a sufficiently flexible model structure for functional modelling of the existing hvdc links, and for use in planning studies, was issued by an IEEE working group [9].

This model which is in common use is referred to as a pseudo steady-state dynamic hvdc model because it represents dynamic conditions, using relationships, which are technically valid only for a steady-state condition. However, acceptably accurate results are obtained from the model when dynamic conditions are changing slowly, i.e., when a pseudo steady-state condition exists. The hierarchical structure proposed in [9] has 3 major components: the ac system controller, the hvdc system controller, and the ac/dc network interface.

The hvdc system controller develops the schedule current/power order. A current regulator forms a part of this controller and includes rate and amplitude limiters as well as inherent regulator dynamics. Closed loop regulator response is employed to obtain functional results rather than detailed simulations. The dc line dynamics, if required, can be included in the overall controller transfer function. Available control modes at each terminal include constant current/power control at the rectifier and inverter end, minimum firing angle control at the rectifier, and constant extinction angle control at the inverter. Other nonconventional control modes [11-20] can also be made available at the inverter end. Special limits on controls such as VDCOL, MSU and low voltage restraints, are included in the hvdc controller.

The ac system controller deals with the intended response of the hvdc system to events that occur in the ac part of the system. It utilizes the general ac system conditions as inputs and provides control information to the hvdc controller. The hvdc response includes both small and large signal modulation and reaction to abnormal events, which may cause dc blocking and/or bypass or similar action. The generalized modulation representation is capable of representing both small signal and large signal modulation control.

The ac/dc network interface is intended to reconcile ac system conditions with the dc system conditions. Quantities calculated within the interface logic for the dc system can include converter control angles, dc voltages and currents and, for the ac system, active and reactive power at the converter terminals. The interface solutions can be subjected to constraints as determined by network calculations performed elsewhere in the stability program.

This flexible model, proposed in [9] allows the tailoring of the hvdc system model to the special conditions of the ac system and does not require small and different integration time steps for ac and dc system calculations. Yet for most applications this kind of model is too general and does not provide the degree of details required for the particular application. Also it is not able to directly represent a non

steady-state mode of operation which occurs during startup or for a cycle or two following a disturbance, where the rectifier firing angle and the inverter margin angle are neither at the limit nor are controllable by the respective regulators [24].

B. K. Johnson [24] has proposed a variation of the pseudo steady-state model which does not represent the high speed hvdc controller dynamics and line dynamics. It is therefore similar to the pseudo steady-state model and can therefore use the normal integration time step. The temporary non-steady-state (dynamic) condition mentioned above is modelled using certain basic assumptions. It uses the desired current set points of the converters to calculate their respective firing angles and currents. This then allows the explicit representation of the VDCOL and other auxiliary controls which affect the current set points [24].

The level of detail in digital models is an important consideration, and concerns regarding this have been expressed lately [9,24]. Detailed hvdc models have been in use since 1966 [25,26]. In the detailed model given in [25] differential equations are used to represent the relationship between direct voltage and current. Also, complete representation of the control system is obtained using a transfer function for each of its units (the current regulator, the voltage dependent current order limit, the margin switching unit, etc.). Since

the time constant associated with the firing angle control and the RLC dynamics of the dc transmission line are very small (less than few tens of ms) the integration time step required in this model is very small (less than 0.01 s). However, a detailed model is necessary if one wants to evaluate the performance of various hvdc link controls or if new special control modes are to be studied. Also, a detailed model allows the representation of VDCOL, MSU, etc., which are important in determining the dc voltage and current recovery rate during startup and immediately following a disturbance [24].

The feasibility and viability of dc power interchange between more than 2 terminals has been under active consideration since the introduction of the modern hvdc system more than 30 years ago. Favorable operating experience with back-to-back and two-terminal dc systems provided the necessary interest and motivation for the prospective use of multi-terminal dc system. Before actual application and implementation, there were few publications [27,28] on possible multi-terminal design strategies. Also, as early as 1977, an IEEE panel session [29] had reviewed the developments in this field and found that the existing technology was sufficient to provide a viable multi-terminal system. However, only in mid 80's did the application of multi-terminal systems emerge.

Some of the differences that multi-terminal operation introduces are given in [20]. In [31], Reeve reviews papers published before 1980 on the concept of extending two-terminal hvdc transmission to multi-terminal systems and discusses the design and performance expectations. The modelling of a multi-terminal hvdc system in a transient stability program of the Bonneville Power Administration (BPA) is given in [32]. This model is a direct extension of the method used for a two-terminal dc system except for two refinements. The first modification involves the removal of the inverter-current-compensation signal given to the delay-angle determinator when the converter is operating in the constant current mode. It is replaced by a logic block which selects the greater of the current regulator signal and the inverter-current-compensation signal. The second modification involves the operation of the inverter in the constant advance angle (β) mode which provides positive slope and stable operation. In [33] a new control method using two automatic current regulators and an hvdc circuit breaker is proposed. The method does not require a fast communication system even under contingencies which coordinate each terminal current order. Some more considerations for implementing multi-terminal systems are presented in [34,35] which includes operation of the rectifier as a voltage controlling converter, use of current balancing to

avoid reliance on high-speed communication, and use of an hvdc circuit breaker to minimize the effects of converter and controller faults. Finally application aspects of four available multi-terminal systems; Nelson River, Pacific hvdc intertie, Sardinia-Corsica-Italy (SACOI), and Hydro-Quebec/New England systems are presented in [30].

Hvdc Control

The basic conventional pole control modes of hvdc converters have been discussed in a number of publications [36-38] and have been the most favored modes of control. As already mentioned the inverter in the conventional pole control mode exhibits a negative impedance characteristic which can cause voltage and power instability. To overcome this problem various alternative modes of operation of an inverter have been proposed which are referred to as nonconventional modes of operation. Nishimure et al. [16] proposed a constant power factor control system where voltage of the transformer valve winding is kept constant by tap changing control and dc voltage of the inverter or rectifier is maintained constant by controlling the advance angle or delay angle. During full load operation the extinction angle is the same as that under CEA control but is increased as the load decreases keeping the power factor the same. Hammad et al. [12] prescribe the use of static systems for controlling the ac voltage of an hvdc terminal connected to a weak ac

system. Various possibilities like the use of static var compensators and synchronous condensers along with hvdc control are investigated. The main principle for controlling the ac voltage is based upon changing the firing angle according to dc voltage under steady-state operation and ac voltage under transient conditions. J. P. Bowles [14] proposes a constant reactive power control to improve the stability of the system. Here the inverter is controlled such that the reactive component of current fed to the ac system is kept constant as the dc current is changed; hence in essence it is a reactive current control scheme. However, as conventional current control is maintained at the rectifier the power flow across the system is constant, and as a result the reactive power consumed at both terminals is constant. The implementation of the above scheme is presented in [11] where it is shown that the studied system behaves unstable with the conventional control, and by changing the control to constant reactive control (CRC) the system performance improves significantly. The above reference has also shown that with the CRC control, a current modulation scheme can be used without causing ac voltage instability.

The ideal bridge control system of an hvdc converter requires symmetrical firing of valves under steady-state conditions, with the instant of firing based on permissible values of commutation voltage in the case of the rectifier,

and on commutation margin in the case of inverter [8]. Earlier techniques for timing of firing pulses were called voltage dependent control or individual phase-control (IPC) techniques [4,8]. Here the firing instant is determined individually for each valve, so that a constant delay (or extinction) angle is maintained for all the valves in steady-state with respect to the earliest firing instant (i.e. the voltage crossing) [4]. The various pole control modes only differed in the type of feedback control loop (constant current or constant extinction angle) which provides the control voltage V_c to be used for timing the firing pulses. Some of the more important firing schemes include constant alpha control and inverse cosine control [8].

In the constant alpha scheme the firing pulse for each valve is generated at nominally identical delay time subsequent to the respective voltage zero crossing [8]. The delay is adjustable from 0° to 70° and is controlled by a direct control voltage V_c. This type of control is susceptible to ac sine wave distortions.

In the inverse-cosine scheme the delay is nominally proportional to the inverse cosine of the ratio of the control voltage (V_c), and peak ac line voltage (Vp) [8]. Thus, here the delay depends on ac system voltage amplitude and shape

[39]. Though inverse cosine is a popular control method because of the simplicity of the control system, it is inherently less accurate as is evident from its characteristic [8].

Inverter valve operations involve special requirements such as maintaining the commutation margin at a constant value independent of load variations, voltage variations, and asymmetric disturbance of the ac system. For this a system called a consecutive control scheme has been developed [40]. Since the dc current and the commutating voltage can vary within a wide range, the consecutive control scheme senses these two parameters for each valve to calculate the firing angle needed to maintain a set margin of commutation under steady-state conditions. Also using suitable differentiations of the commutating voltage and direct current, the system generally can be made to operate satisfactorily under transient conditions in both the ac system and the dc link. Most circuits for CEA control of an inverter valve using the consecutive control scheme, operate by prediction and therefore have limitations that they can only operate on smooth waveforms. Any deviations from the ideal voltage waveforms break the 120° symmetry of the current waveform and cause irregular firing pulse spacing. However they have the advantage of being able to achieve the highest direct voltage possible under asymmetrical or distorted supply waveforms.

One way to obtain a smooth waveform is to place filters between the ac system and the control system, so as to attenuate the harmonics [8]. However the use of filters will cause the control system to ignore the harmonics whereas the valves will respond to the actual voltage reaching them which also includes harmonics [8]. Also, filters introduce inherent frequency dependent phase error in the signal and are unable to attenuate negative sequence fundamental voltage which is the main cause of irregular firing [4]. These difficulties spurred the development of alternative schemes commonly known as Equi-distant Firing Control for timing of firing pulses.

The first such control scheme to appear in late 1960 was a phased-locked oscillator control scheme by English Electric [41]. It consists of a voltage-controlled oscillator which delivers a train of pulses at a frequency directly proportional to a dc control voltage V_c. The train of pulses is fed to a ring-counter which consists of a number of stages. The Start and Stop pulses for each stage are obtained cyclically at successive intervals of time and are used to fire the valve. Another scheme by ASEA [42] entitled "equidistant firing predictive-type control". It involves an element of prediction of the extinction angle, similar to the consecutive control scheme of individual phase-control. In this scheme the prediction is effective for the incoming firing, and a feedback

loop is used to update the predictive model for the subsequent firings. Both of the above schemes are referred to as Pulse Frequency Control (PFC) schemes as a change in the control voltage directly changes the frequency of the oscillator.

The Trans 5 control scheme [43] developed by the HVDCT working group (AEG Telefunken+Brown Boveri+Siemens) also uses a voltage controlled oscillator and is designed along similar principles of equidistant firing. However, in this scheme the change in control voltage V_c causes a proportional change in the control (delay) angle and hence is called Pulse Phase Control (PPC). Here the constant extinction angle control at the inverter normally operates as a feedback type depending on the measurement and corrections of the extinction angle. Other features which are dependent on rate of change of current (rise only), rate of change of ac system voltage (drop only), instantaneous voltage level at the ac bus, action against asymmetry [8], etc. are also included in the closed loop control. A catching device is used which forces the inverter into rectifier operation very smoothly by skipping the next valve firing in sequence upon commutation failure.

Hvdc Modulation Control

The stability problem associated with conventional control has become increasingly complex and pronounced as power systems grow and interconnections increase. From a dynamic study,

based on Edison Electric Institute's (EEI) 700 KW model, it was found that the response time over an ac transmission line having a typical length of 300 miles for a disturbance on an ac bus is of the order of several hundred milliseconds [44]. From a preliminary test of dc control on the same model, it was found that the response time for per unit step change in rated current is approximately 10 milliseconds [44]. From this it was concluded that under certain circumstances, a dc line can be used to mitigate severe system disturbances if it can be made to change its power flow at proper time. The above motivation was used by Cresap and Mittelstadt in [45] to simulate the first power flow modulation scheme using rate of change of the power angle of the machine rotors. It was suggested in [45] that the power flow on a dc link could be modulated by various signals from the ac system during system disturbances, including the current or power level of the ac lines, the total power flow between buses, the magnitude of power angle between buses, frequency and rate of change of frequency. It was also shown that for small signal modulation of the Pacific hvdc intertie, use of rate of change of ac intertie power would increase the damping of the low-frequency swing modes of the system. However, the operating experience with this modulation has shown that the modulation system provides better damping of large disturbances than had been

anticipated [46]. It was suggested in [46] that the ac intertie current instead of power should be used as a modulating signal. This is because the changes in ac power (near the steady-state stability limit) are insensitive to the changes in the relative angle between the two systems connected by the intertie. As a result the time derivative of ac power does not provide a good indication of the frequency difference. The Square Butte project uses frequency deviation at the sending end as the modulating signal for damping and the inherent time-overload capability of the solid state valves for modulation is up to 1.3 p.u. current [21,47]. In the Nelson river project the dc power of the two bipoles is modulated from the inverter end to damp the Southern Manitoba ac system power swings [21,47]. The modulation signal used is based on the phase angle measurement of the inverter ac bus. For the dynamic stability of the two ac systems connected back to back in the Eel river hvdc system, the dc power is modulated by a signal derived from the frequencies of both ac systems [47]. The CU hvdc system carrying power between North Dakota and Minnesota utilizes a damping power controller to modulate the dc power in response to rectifier end ac system frequency changes [47]. All the above applications of modulation are on single bipole two-terminal dc systems.

In [47] a power modulation scheme is demonstrated over a proposed Eastwing-Mead-Adelanto multi-terminal system. This project modulation control consists of gamma modulation at the inverter end to damp the ac system voltage rise and large power modulation at the rectifier end to provide voltage support. The gamma modulation involves modulating the inverter extinction angle to a value larger than its minimum limit when the inverter ac bus voltage swings above the normal value. This increases the var consumption of the inverter which in turn reduces system voltage rise. Large power modulation involves modulation of dc power transfer proportional to the ac bus voltage, so that a large reduction in system voltage would cause a reduction in dc power thereby reducing the var consumption which is utilized to support the ac voltage.

The main limitation of most power modulation schemes is that they tend to produce reactive power modulation at each terminal which can cause ac system voltage and powerflow problems, thereby reducing their effectiveness. In addition, modulation of real power without any consideration for adverse effects associated with the coupled reactive power may lead to collapse of the ac voltage at one converter terminal or the other which further contributes to destabilization of the system, or propagation of high ac voltage throughout the network and possible damage to equipment. This phenomenon is observed

most often when the reactive power at hvdc terminals is limited by the capacity of the ac system. In order to assure proper operation of the dc link and to minimize voltage fluctuations throughout the network, attempts can be made to maintain the reactive power constant during the modulation period.

A unified active and reactive power modulation of an hvdc transmission system is demonstrated in [20] where dc voltage is directly modulated, along with the modulation of power, so that reactive power variation can be controlled. For this the converter bus voltage is included in the performance index, and excursions from the desired values are penalized. This type of compounding of the inverter dc voltage controller essentially results in the decoupling of the active and reactive power modulation systems causing significant dynamic performance benefit.

Hvdc Adaptive Control

Adaptive control has been an active area of research for more than two decades, and a substantial amount of literature is available on the application of adaptive control strategies to ac power systems. However, there are only a few papers available on the application of adaptive controllers to hvdc links in ac/dc power systems. An adaptive control scheme for tuning the current regulator using estimates of net commutating resistance of the ac network is presented in [48]. The transient

performance of an hvdc system depends heavily on the current regulators associated with the converter control system. The tuning of the current regulators is a function of converter short-circuit ratio, or equivalents of all the net converter commutation resistance. The net commutation resistance varies with the network operating conditions and the ac system contingencies. The adaptive control in [48] uses estimates of the ac network Thevenin impedance to modify the gains and time constants of the current regulator. The simulation studies carried out on a simple power system show that the dc system dynamic response is improved with the proposed adaptive tuning. However, further work is required to evaluate the algorithm on large power systems.

The development of an adaptive optimal control strategy for a large scale ac/dc power system which uses a nonlinear form of system state equations and real-time system wide measurements is given in [49]. Here simultaneous adaptive optimal control of the synchronous generator exciter and the hvdc converter is used to dampen the electromechanical oscillations. However, implementation of this scheme requires system-wide measurements at remote locations in power systems and their transmission to a control center via fast communication links.

Thesis Organization

In order to give proper attention to each area of the hvdc problem, the remainder of this thesis is subdivided into 12 chapters. Chapter 2 describes the implementation of a two-terminal and a multi-terminal pacific hvdc intertie in a reduced order model of the western North American power system. The details of the hvdc model used are given. A comparison of the constant real and reactive load model, two-terminal model, and multi-terminal model of the dc system is made using time-domain simulation results and Fast Fourier Transform (FFT) analysis. Implementation of the intermountain tie in this reduced order model is also presented along with simulation results. Chapter 3 contains a description of six alternatives to the conventional strategy for controlling hvdc lines - these are classified under the heading of nonconventional modes of hvdc control. Chapter 4 reports on the application of a Prony signal analysis algorithm for obtaining system transfer functions for the ac/dc system studied. Responses of the Prony-based linearized models are used in root-locus studies to show how the feedback of these signals affects system eigenvalues. In Chapter 5, the time domain performance of nonconventional feedback signals is displayed through a series of disturbances applied to the system. The focus shifts in Chapter 6 to the use of small signal modulation schemes in conjunction with a conventional

hvdc controller at the rectifier. Transfer functions that relate the input modulating signal to various system outputs of interest are obtained, and root-locus plots are used to examine how the feedback of these signals affects system eigenvalues. In Chapter 7, a modified Prony signal analysis method is presented to obtain a system transfer-function containing a feedforward term, and root-locus plots are used to examine effects of feeding these signals back through a band-pass compensator. In Chapter 8, the time-domain performance of a particular modulating feedback signal is displayed through a series of disturbances applied to the system, and in Chapter 9 a combined modulation control with Static Var Compensator (SVC) control and its implementation is briefly reported. A supplementary adaptive controller for adaptive modulation of dc current and rectifier firing angle is presented in Chapter 10, and time domain simulation results for the same are presented in Chapter 11. Finally Chapter 12 provides an overall conclusion.

CHAPTER 2

HVDC MODEL

Introduction

The need for a reduced-order model of the western North-American power network resulted in the development of a 42-bus, 17-machine equivalent which retains some of the dynamic characteristics of the detailed model from which it was derived [50]. The actual 2000 bus model from which the above reduced-order model is derived and which is used by the Bonneville Power Administration (BPA) for their simulation studies consists of two embedded high voltage dc lines: the Pacific hvdc intertie going from the Cellilo station in the northwest to Sylmar in Southern California and the Intermountain line going from Intermountain in Utah to Adelanto in Southern California. The 42-bus system given in [50] contains only a two-terminal dc line model to represent the Pacific hvdc intertie while the intermountain intertie is modelled simply by its equivalent real and reactive current injection at its terminal buses.

This chapter describes in detail the development and evaluation of both two-terminal and multi-terminal detailed dc line models for the Pacific hvdc intertie and a two-terminal

detailed dc line model for the Intermountain tie. A comparative study of the two-terminal and multi-terminal models with the simple constant current load model for the hvdc interties is made using generator angle responses to a system disturbance. Fourier analysis is used in this comparative study. Simulation results are presented using the Electric Power Research Institute's (EPRI's) Electric Transient Midterm Stability Program (ETMSP) [51] for operating conditions similar to that of the actual system.

The main reason for including a detailed model for the Pacific hvdc intertie and the Intermountain tie is to provide a reasonable test bed for the initial development and testing of various supplementary control strategies which can be applied to the dc line converters for improvement of the overall system damping. The intended application of the developed models is for study of the dynamic characteristics of the ac-dc system and their interaction, and for testing controllers.

Description of the Reduced-order System

The one-line diagram of the reduced-order system is given in Figure 1. It consists of nine main areas designated as A, C, M, NW1, NW2, P, SC1, SC2, and U. Each area consists of a main bus having the total load in that area lumped directly to it and a number of smaller buses each connected to a generator

with a transformer. Most of the transmission lines have voltage ratings of 500 kV except for few which are rated 230 kV. The electromechanical dynamics of this reduced-order model are established by including two types of generators in each area.

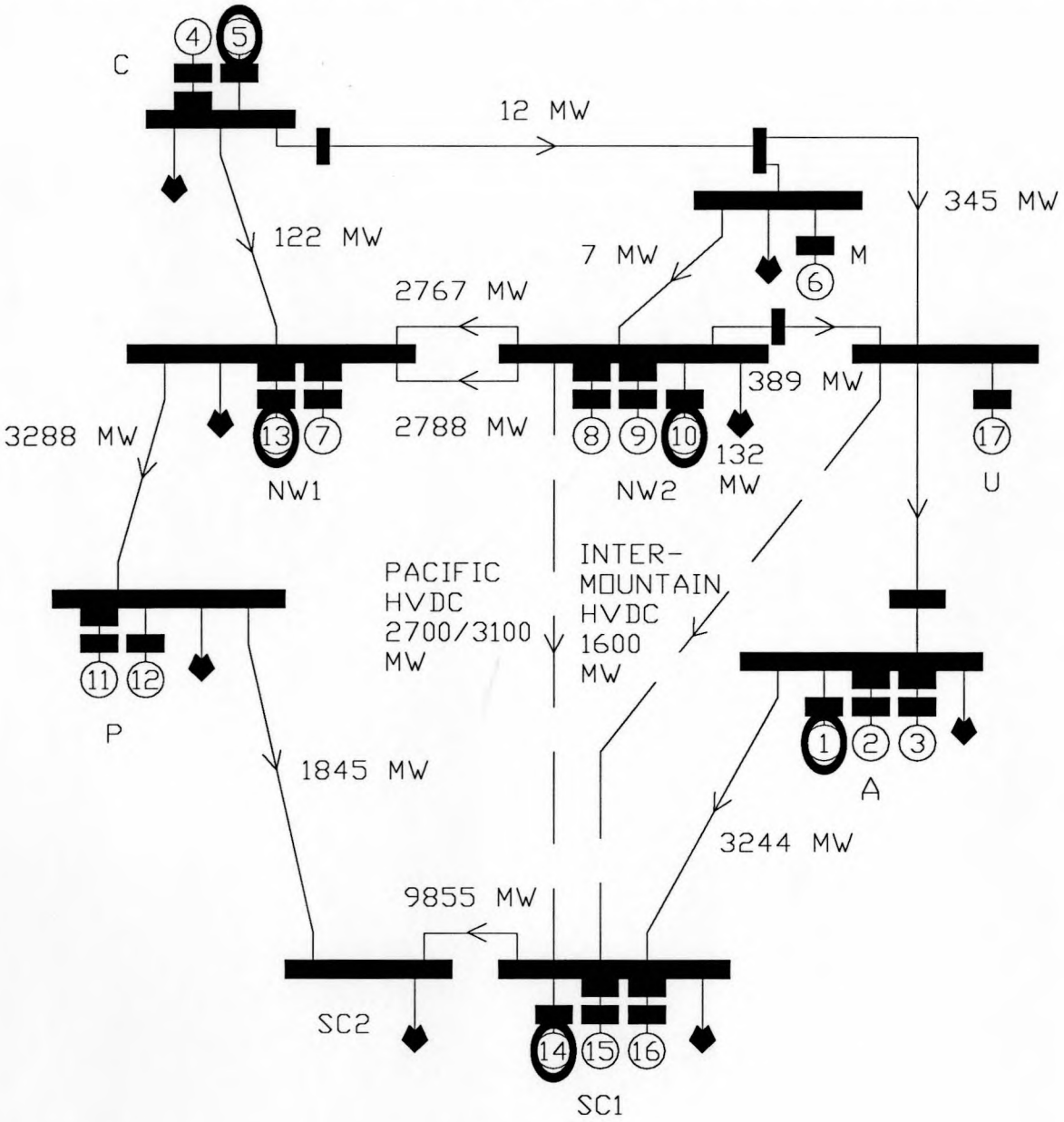

Figure 1. 42-bus, 17-machine test system.

One type of generator is a large inertia machine having large power generation capability and is represented by classical swing equations and a constant voltage behind its reactance. The other type is a smaller machine with actual rating and is modelled using normal d-q axis generator model and IEEE type AC4 [52] exciter model. Both types of generators have governor models included. Table 1 shows the generation and load in each area while generation and kinetic energy data associated with each machine are listed in Table 2. The system in Figure 1 also contains two 500 kV hvdc transmission lines: one between area NW2 and SC1 (representing Pacific hvdc intertie) and the second between area U and SC1 (representing Intermountain tie). Both hvdc lines are shown dotted. This system which is relatively large was considered to be an ideal (realistic) test system to evaluate the performance of the various conventional and nonconventional hvdc control schemes including modulation control and to demonstrate the adaptive control scheme.

Table 1. Generation and load data for each area.

Area	Generation (MW)	Load
A	19,000	15,600
C	11,900	11,750
M	1,250	900
NW1	9,169	11,100
NW2	17,700	9,000
P	11,300	12,600
SC1	14,200	9,800
SC2	0	11,700
U	3,200	3,800

Table 2. Generation and inertia parameters for each generator.
* Total kinetic energy of generators in megawatt seconds.

Generator	Generation (MW)	Energy* (MW.sec)
1	12,500	57,000
2	4,500	18,000
3	2,000	7,680
4	1,600	10,000
5	10,300	13,000
6	1,250	6,000
7	6,700	8,000
8	1,200	5,478
9	2,500	7,856
10	14,000	17,000
11	700	2,206
12	10,600	13,000
13	2,469	10,000
14	12,500	63,000
15	1,000	4,576
16	700	2,539
17	3,200	14,000

Pacific Hvdc Intertie Operating Characteristics

The original two-terminal Pacific hvdc intertie was constructed using mercury arc valve technology in 133 KV six-pulse

groups with a rating of ±400 KV at 1.8 KA, for a total capacity of 1440 MW [30]. However, the dc transmission line had a current carrying capability in excess of 3 KA. Later, the dc intertie was upgraded to include a series connected 100 KV thyristor group to increase the system rating to ±500 KV at 2 KA for a total power capability of 2000 MW. Figure 2 shows the two-terminal dc intertie with the thyristor groups (in solid) showing the original system, and the thyristors (dashed) showing the upgrade.

The final expansion of the Pacific intertie makes use of the previously installed line current capability and increases the line current from 2 KA to 3.1 KA. One 500 KV 12-pulse converter is added at each station rated at ±500 KV at 1.1 KA continuous, for a power rating of 1100 MW. These units are connected in parallel with the original six-pulse series group using the same North to South dc line , thus making the system multi-terminal with a total power rating of 3100 MW. Figure 3 shows the expanded dc intertie with the new 12-pulse converter units shown (cross-hatched). The control of this multi-terminal dc system is basically the same as that of the two-terminal system and will be discussed in the next section.

In this study the Pacific hvdc intertie is represented in two ways: 1) as a bipolar two-terminal system carrying 2700 MW of power; and 2) as a bipolar multi-terminal system carrying 3100 MW of power.

Pacific Hvdc System Control Units

The available control modes at each converter of the dc intertie include constant current or power control, minimum angle control and constant extinction angle control [45]. The rectifier and inverter controllers are coordinated to give constant current or power control at the rectifier and constant extinction angle control at the inverter during normal operation. To accomplish this the current order at the inverter is set 10 to 15% less than the current order at the rectifier (the difference between the two current orders is called the current margin). These conditions are used in the simulation study of the Pacific intertie with the northern station (Cellilo) operating as a rectifier and the southern station (Sylmar) operating as an inverter at constant extinction angle.

In addition to the above normal controls, the following features are available in the Pacific hvdc intertie to maintain constant power on the dc line under abnormal conditions and to enhance its overall performance [21]:

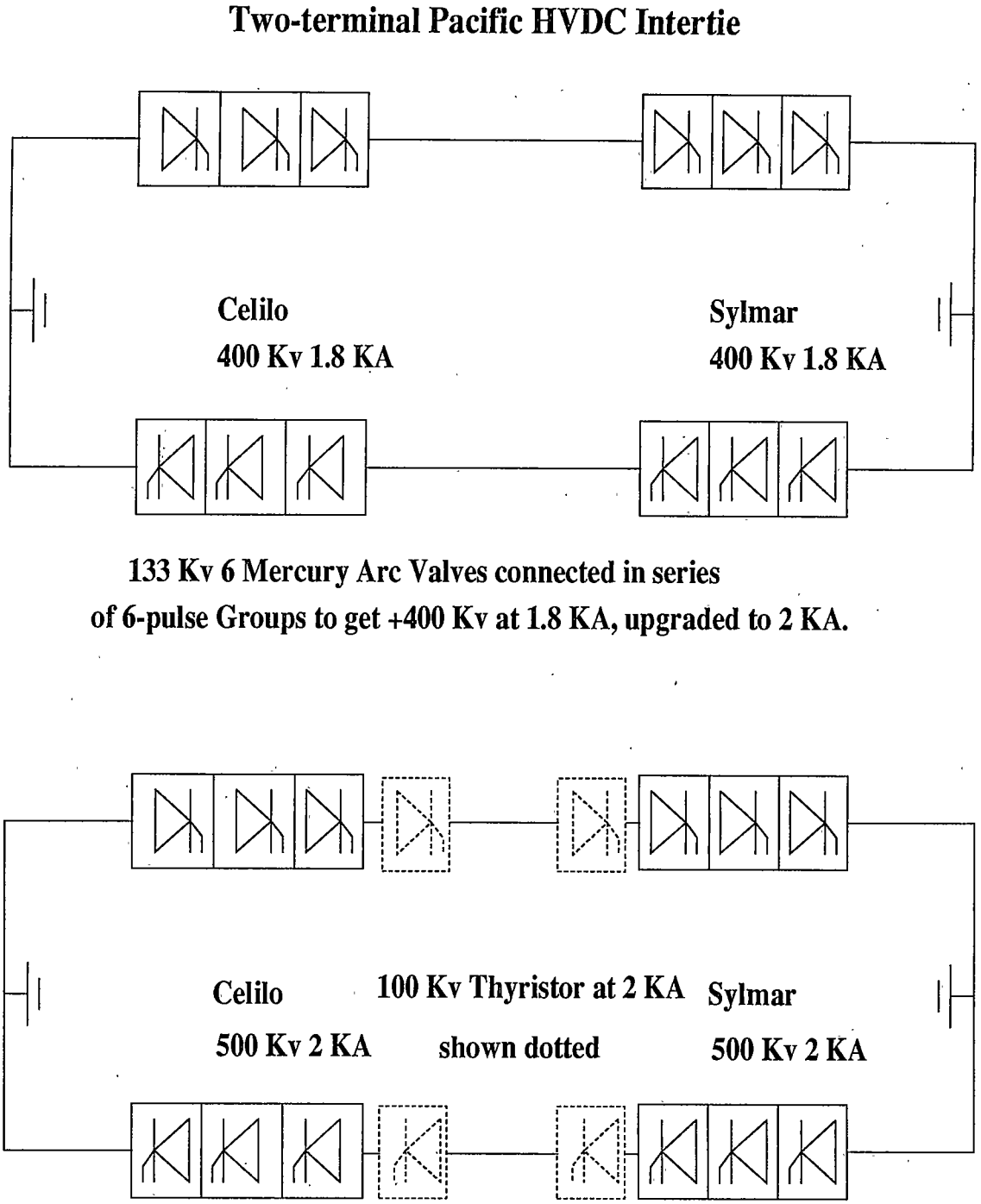

Figure 2. Pacific hvdc intertie.

Multi-terminal Pacific HVDC Intertie Expansion Project

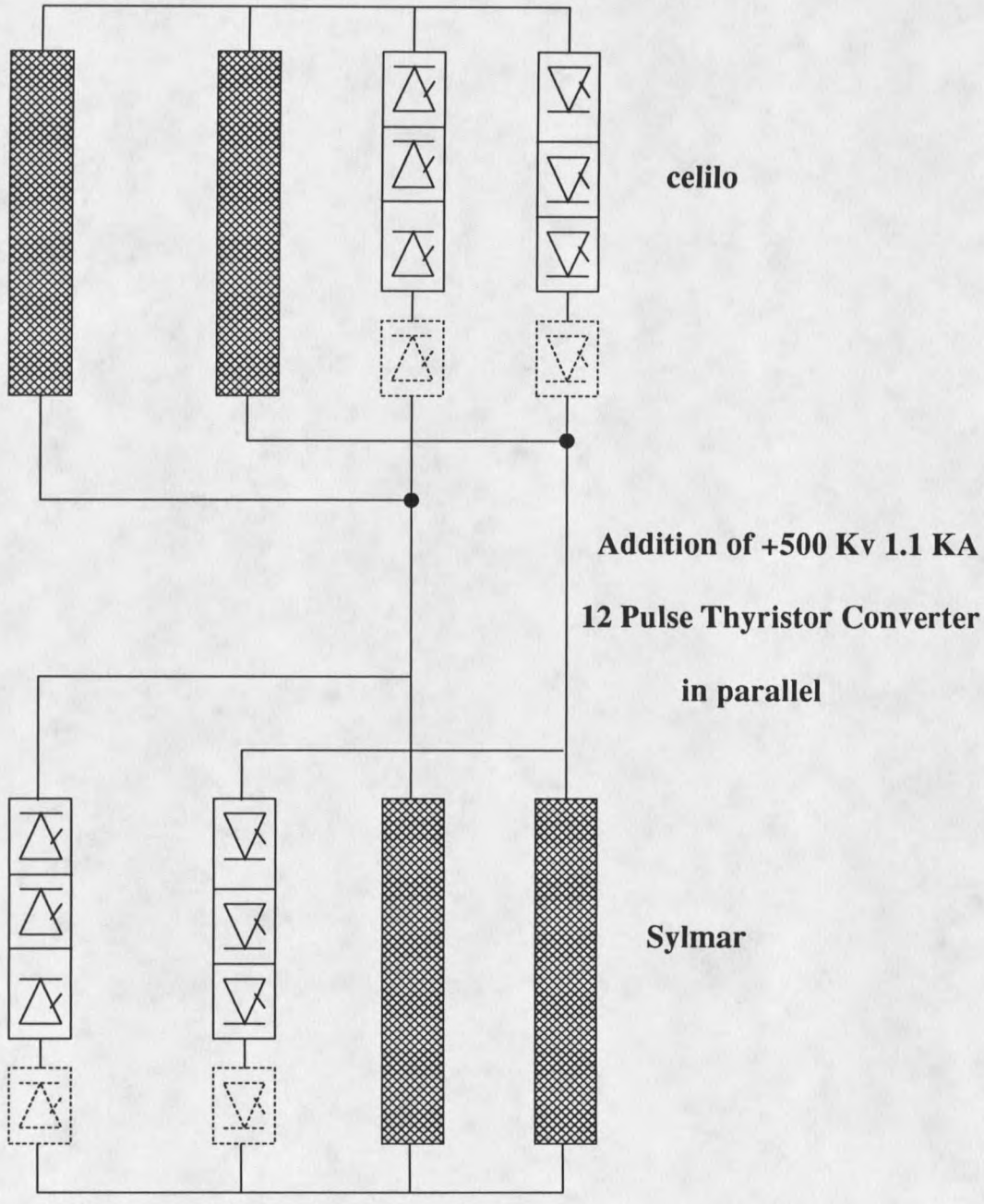

Figure 3. Multi-terminal Pacific hvdc intertie.

Power modulation of the dc line for enhancement of the ac system stability.

Modification of the controllers to maintain constant power on the dc line under abnormal conditions. Such modifications include the addition of a voltage dependent current order limit and a margin switching unit.

These modifications are described below.

Dc Power Modulation

Dc modulation is introduced to improve the system damping of negatively damped oscillations [21]. Dc power modulation is based on the rate of change of power on the parallel Pacific ac intertie. In the present study the ac intertie is modelled as a single line carrying about 2100 MW of power from north to south. Dc power modulation is however not used in this chapter.

Voltage Dependent Current Order Limit

In terms of the ac commutating voltage E_{ac}, direct current I_d and the dc line inductance L, the dc line power is given as follows [21]:

$$P_d = \frac{3\sqrt{2}}{\pi} E_{ac} I_d \cos(\alpha) - \frac{3}{\pi} \omega L I_d^2 \qquad (2.1)$$

For any given ac voltage there is a value of direct current beyond which any increase in the line current decreases the dc power. However, the introduction of a voltage dependent current order limit (VDCOL), as shown in Figure 4, maximizes the power transfer capability of the dc line under adverse conditions. The other function of the VDCOL is to reduce the dc tie power, and consequently the VAR demand from the ac system during a period of depressed ac system voltage. VDCOL is introduced in the current order determination of the dc control system. For the Pacific intertie this modification in current order limit becomes operable when the dc bus voltage drops below 0.6 p.u. (D_v in Figure 4) [21]. Below this voltage, maximum current order limit (I'_{MAX}) decreases linearly from its normal value (I_{MAX}) down to some specified minimum value of current (I_{MIN}) as shown in Figure 4.

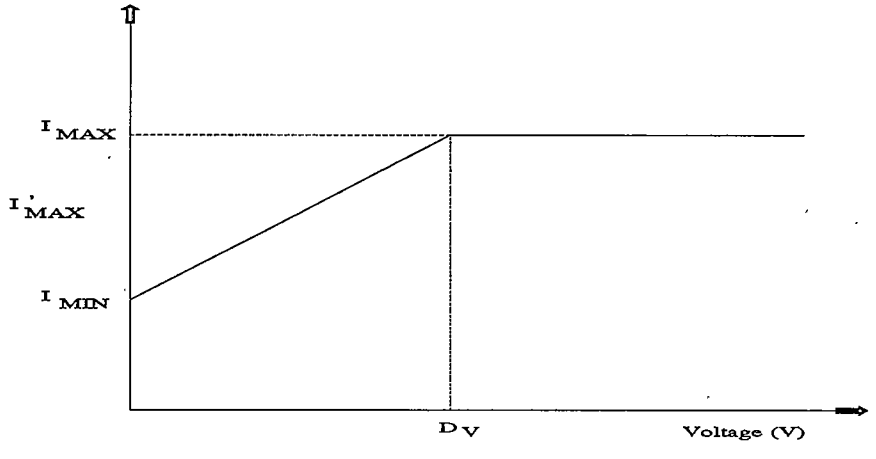

Figure 4. Voltage dependent current order limit.

Margin Switching Unit

The normal operation of a dc line calls for constant current control at the rectifier and constant extinction angle at the inverter. A decrease in the rectifier end ac voltage or an increase in the inverter end ac voltage could result in loss of current control at the rectifier end. This results in a reduction in the dc line current which could be as much as the system current margin (10-15%) before the inverter control prevents further drop in the current. Hence, depending on the ac system voltage, the dc line power could decrease from its scheduled value by as much as 15% depending on the magnitude of the current margin [21]. This sustained decrease in the scheduled line power is prevented by providing the dc controls with a margin switching unit (MSU). The characteristic and logic of operation of this unit are shown in Figure 5. Essentially, the MSU raises the current order at both the rectifier and the inverter ends by 75% of the current margin when the rectifier is found to have lost current control. If the current control is still not maintained, the current order is then reduced by the current margin.

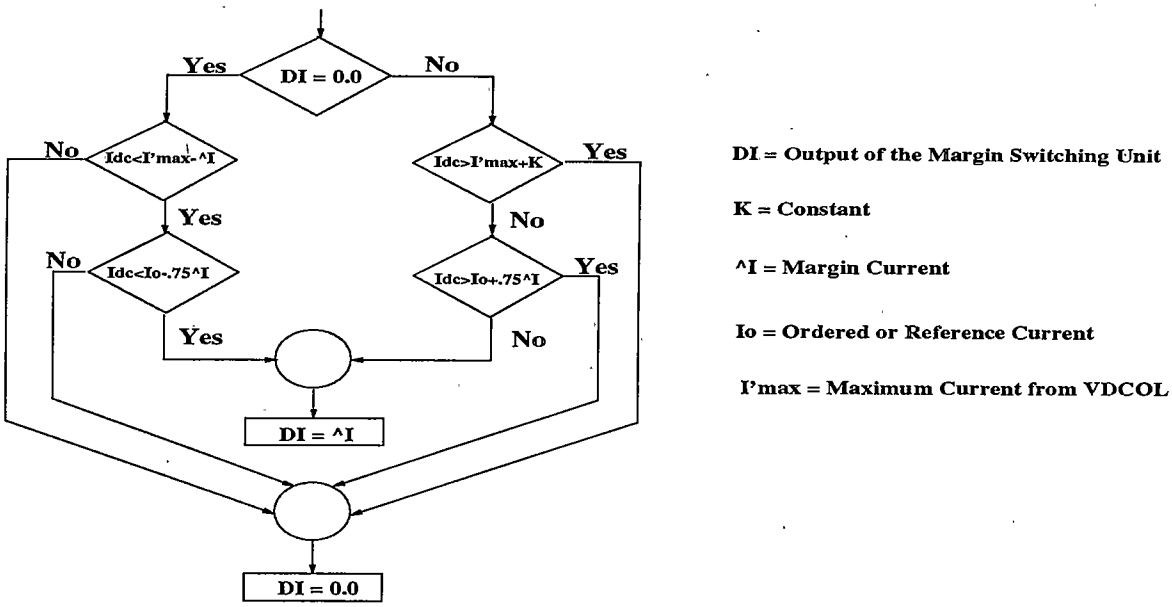

Figure 5. Margin switching unit.

Intermountain Hvdc Intertie Operating Characteristic

The original Intermountain hvdc intertie for the Southern Transmission System (STS) consists of an Intermountain Converter Station (ICS) converting Intermountain 345 kV ac to ±500 kV bipolar hvdc, Adelanto Converter Station (ACS) inverting the ±500 kV back to ac at 500 kV, and a 787 km two bipolar hvdc transmission line from ICS to ACS [53]. Each converter is a 12 pulse type and is designed with two 800 MW valve groups as shown in the Figure 6 for a total capacity of 1600 MW. However, due to reduced Utah load growth, the Intermountain Power Project (IPP - a generation and transmission project in the western United States) was down-sized, and as a result the

STS was reduced to a single bipolar system as shown in Figure 7. The present Intermountain tie consists of a ±500 kV bipolar system with a single hvdc line normally rated at 1600 MW (800 MW per pole) and a continuous overload rating of 1200 MW when one pole is out of service [53].

Intermountain Hvdc System Control Units

The IPP hvdc control system is a microprocessor based system. The hierarchy of the control system consists of four levels: bipole level, pole level, converter level, and valve level. The bipole level consists of two systems: one in active mode and the other in standby mode for complete redundancy. It consists of reactive power compensation, central unit alarm reporting system, bipole control desk, sequence event recorder, master clock and display panel [54]. The pole level controls the pole power, pole sequence, and pole protection. Also, on failure of the bipole level, the pole level controls take command. The converter level controls the firing of the converters, the converter sequence, converter/pole protection, current order memory and the tap changer control. If there is a complete failure at the pole level, converter control takes command. The valve level controls the firing of each thyristor by converting the electrical control pulses to optical pulses and is basically an interface between the control system

and the thyristor.

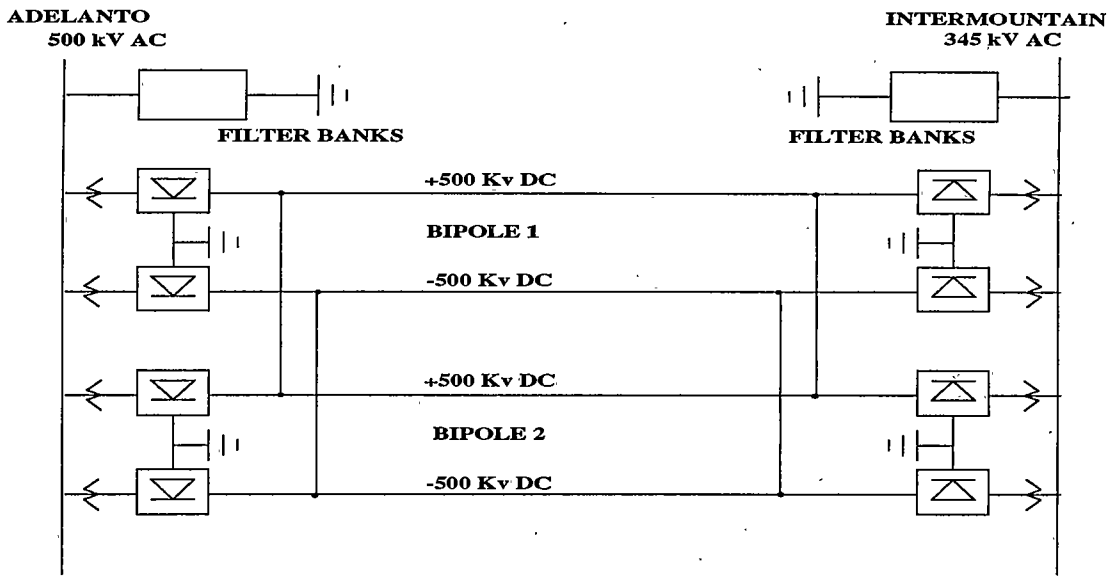

Figure 6. Original Intermountain intertie (Two bipolar system).

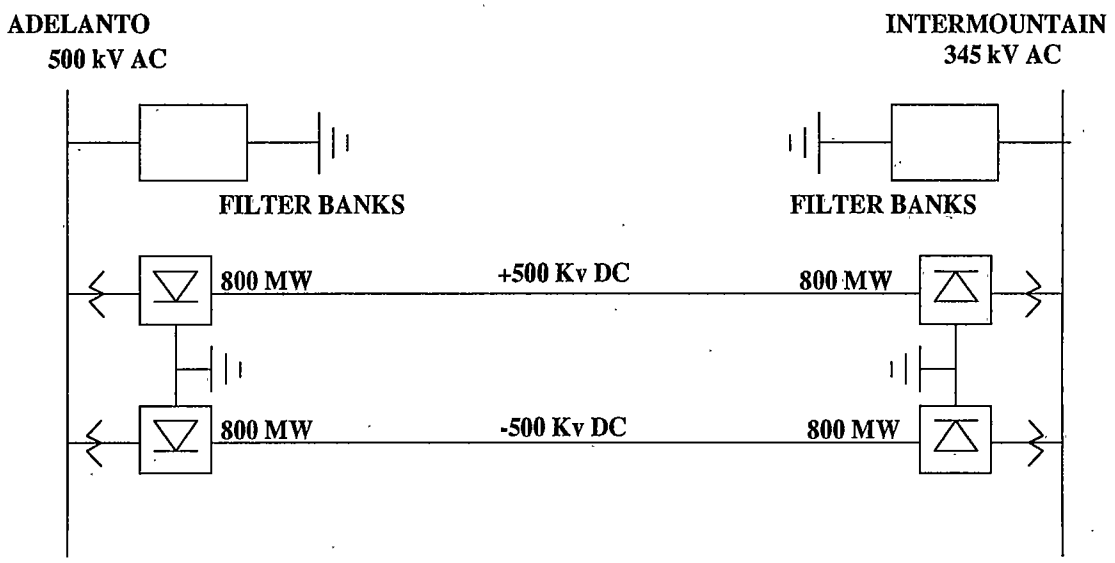

Figure 7. Present Intermountain intertie (Single bipolar system).

The various hvdc control modes available are constant current control, constant power control and constant extinction angle control. The various operating modes include bipolar operation, monopolar operation, and reduced voltage operation. In addition to the above modes, the following stability enhancement techniques were adopted: voltage dependent current order limit, reactive power control, dc power modulation, overload recovery control, isolated startup, electrode current balancing and generator runback control [55].

Model Implementation

The Pacific and the Intermountain dc system model were implemented in the reduced-order equivalent model of the western system shown in Figure 1. In the case of modelling of the Pacific hvdc intertie, most of the characteristics of the actual system described above were retained except for modulation of the dc power. However, in the case of modelling of the Intermountain hvdc intertie only the basic pole level control along with VDCOL were represented. The block diagram of the overall two-terminal hvdc control structure as used in this simulation study for both the interties is given in Figure 8 [51]. The control scheme for the multi-terminal modelling of the Pacific hvdc system is basically the same as that of the two-terminal system. In the multi-terminal dc system

modelling both the rectifiers at Cellilo and one inverter at Sylmar (having current rating of 2 KA) operate in a constant current mode. The other inverter at Sylmar (with lower current rating of 1.1 KA shown crosshatched in Figure 3) operates at constant extinction angle control thereby controlling the line voltage. The current orders at the current controlling converters are set independently. The current order at the voltage controlling station is made equal to the algebraic sum of the current orders of the current controlling station minus the current margin. Current orders can be set from a control station to the respective converter stations via a telecommunication facility, or they can be set manually by varying the converter currents in steps.

Simulation Results

Four configurations for which simulation results were obtained are:

1. The reduced order system with the Pacific and Intermountain hvdc interties represented as equivalent real and reactive constant current loads at their respective terminal buses,
2. The reduced order system with the Pacific hvdc intertie represented by a bipolar two-terminal +500 KV line carrying

2700 MW of power (Figure 2) while the Intermountain tie is represented as equivalent real and reactive constant current loads at their respective terminal buses,

3. The reduced-order system with the Pacific hvdc intertie represented as a bipolar multi-terminal ±500 KV system carrying 3100 MW of power (Figure 3) while the Intermountain tie is represented as equivalent real and reactive constant current loads at their respective terminal buses,

4. The reduced-order system with the Pacific hvdc intertie represented as a bipolar multi-terminal ±500 KV system carrying 3100 MW of power (Figure 3) and the Intermountain tie represented as a bipolar two-terminal ±500 kV system carrying 1600 MW of power (Figure 7).

The dynamic stability simulation for the above four cases was carried out using EPRI's EMTSP package. In each case a 1400 MW braking pulse was applied at bus NW1 in the system shown in Figure 1 for 30 cycles to simulate a braking resistor applied at that bus. This bus represents the Pacific Northwest area where the Bonneville Power Administration generally applies its 1400 MW resistive brake.

In order to compare generator swings in the four different cases under study, the variation of the generator angles (for machines #8 and #15 in Figure 1) were obtained relative to generator #1 which is considered to be a large machine at bus

A. These generator angle variations are shown in Figures 9 through 12 for the four cases discussed above, respectively. It is noticed from these figures that although generator swings are very similar in all the four cases, some frequency components do appear in the generator swings when the dc line is modelled as a multi-terminal or a two-terminal line that do not show up when the dc system is modelled as constant current injections. There is a minor difference in the magnitude of the generator oscillations in the four cases studied.

Figure 13 shows the variation in the converter firing angle and the converter current of the two-terminal Pacific hvdc line. The variation of one of the rectifier firing angles and one of the rectifier currents (converter #1) in the multi-terminal Pacific hvdc system are shown in Figure 14.

The FFT analysis is used to obtain the frequency response of generator angle swings for machines #8 and #15. FFT results are shown in Figures 15 through 18 for the four cases studied. These responses are used to obtain detailed information on the system modes. FFT magnitude information reveals the frequencies of the interarea modes and indicates which machine participates in a given mode. Phase information from the frequency analysis is used to determine which areas swing against one another at a given mode. A thorough comparison of the FFT plots for each machine for the four cases studied shows that the interarea

modes for the four cases are similar. This indicates that the damping of the interarea low frequency oscillations is not possible with conventional converter control modes as used in this simulation study.

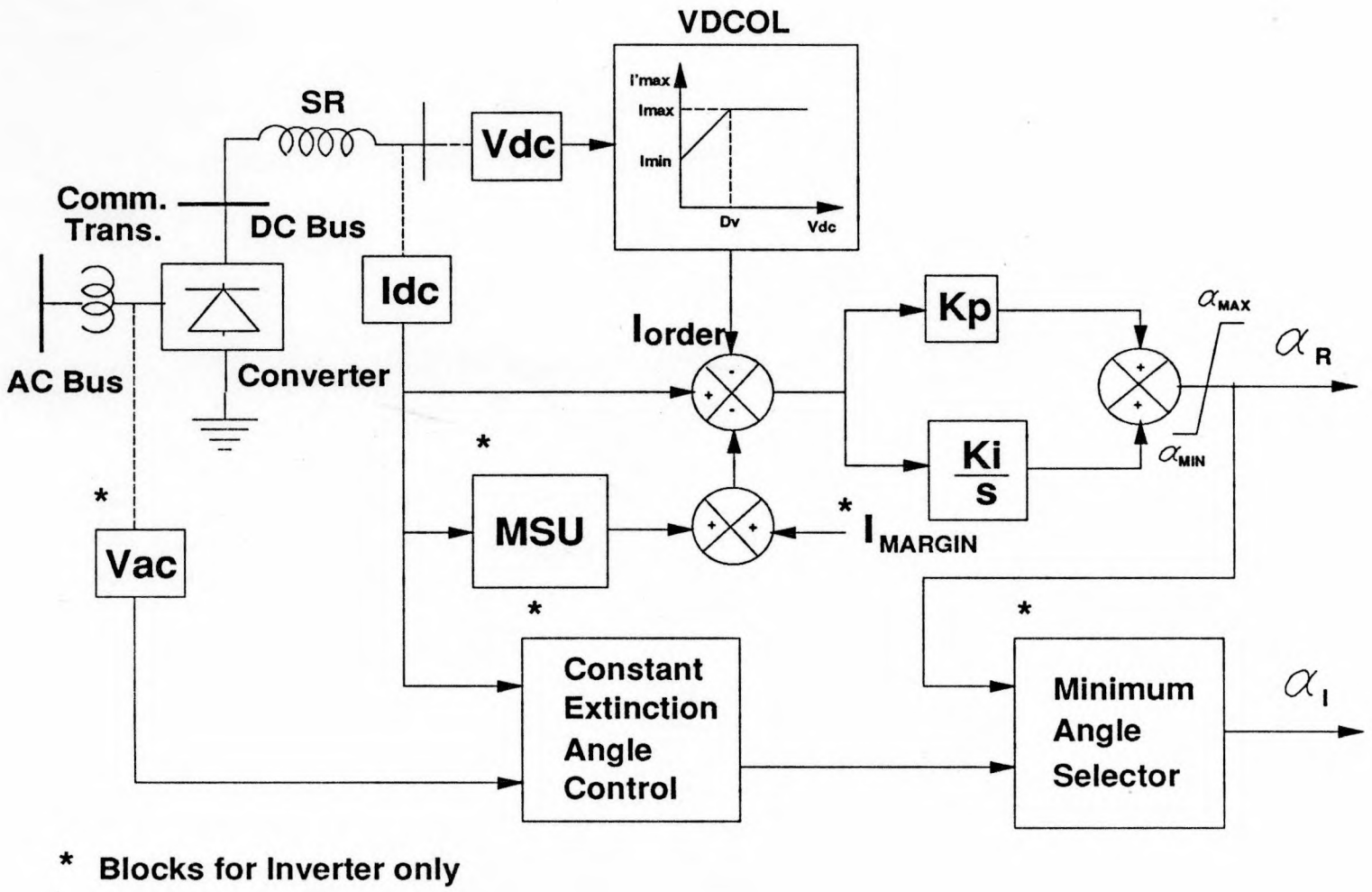

Figure 8. Dc converter control model.

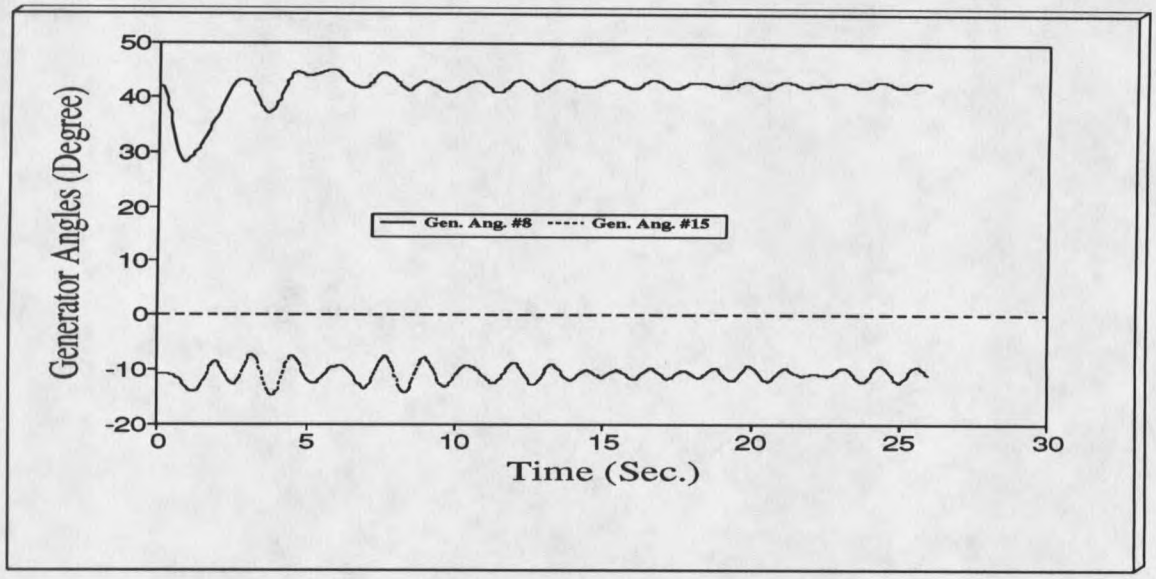

Figure 9. Relative generator angles (machines #8 and #15) for case 1.

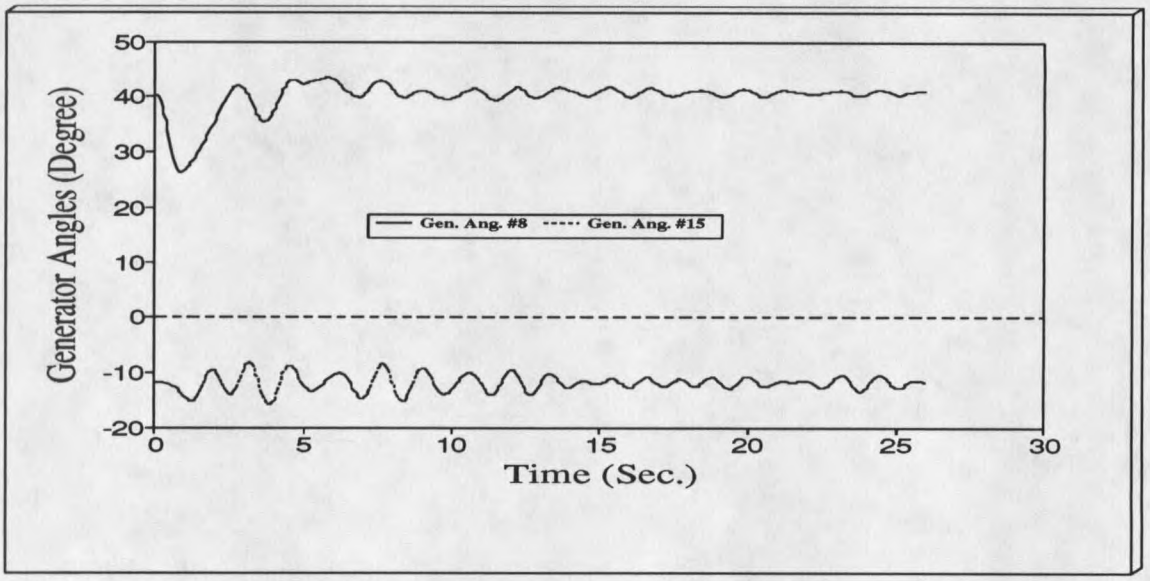

Figure 10. Relative generator angles (machines #8 and #15) for case 2.

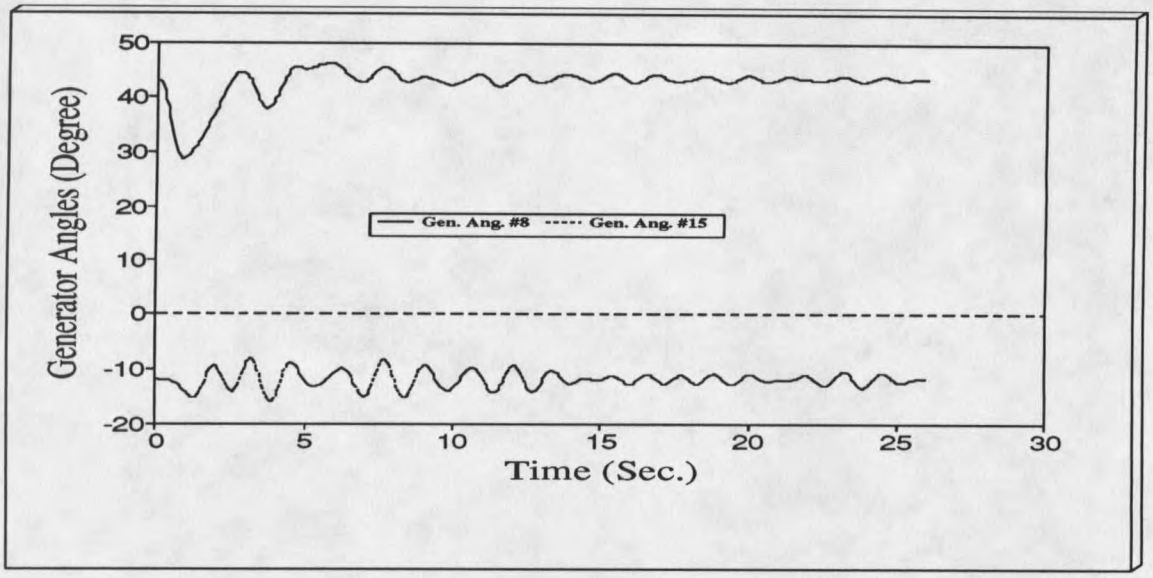

Figure 11. Relative generator angles (machines #8 and #15) for case 3.

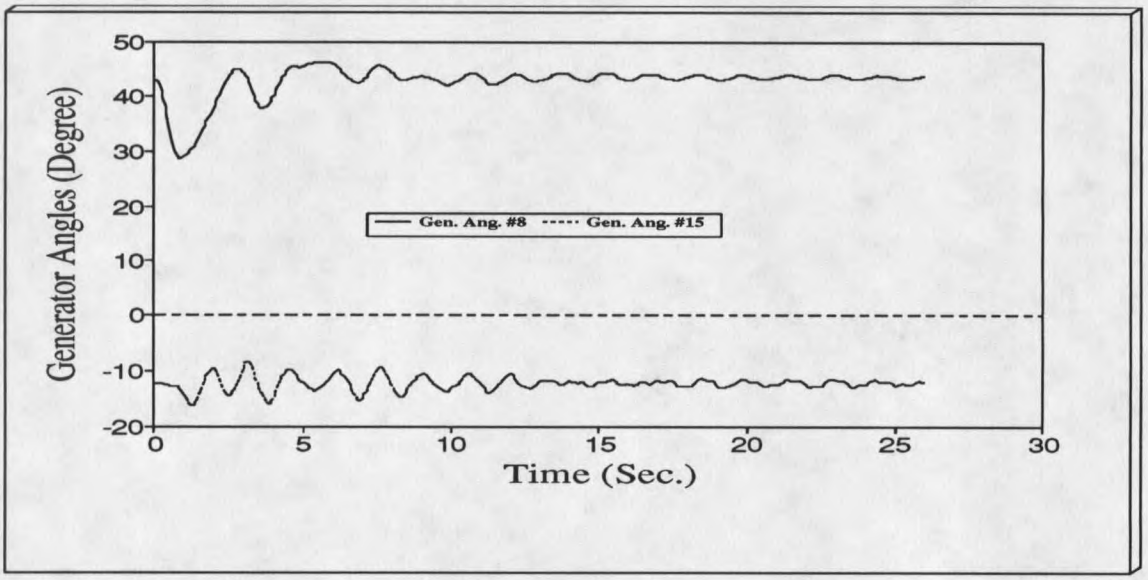

Figure 12. Relative generator angles (machines #8 and #15) for case 4.

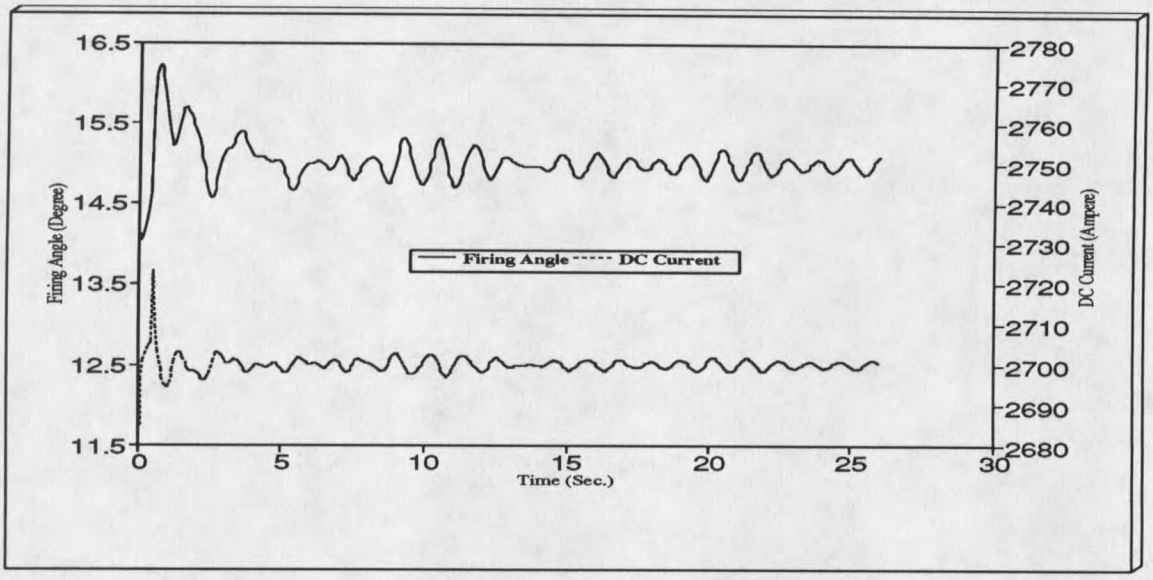

Figure 13. Variation of rectifier firing angle and dc current for case 2.

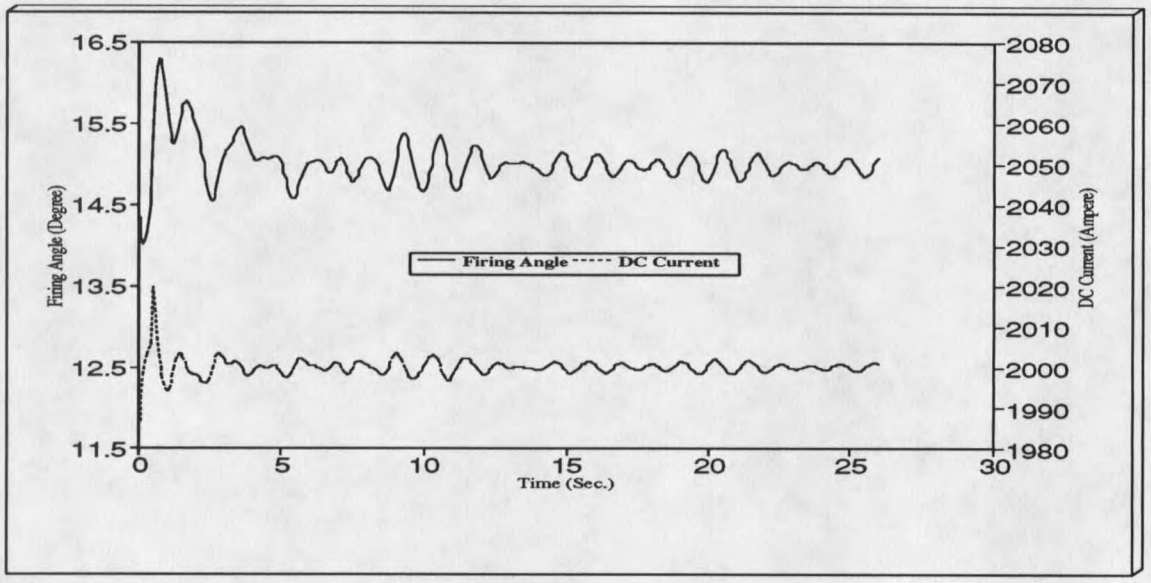

Figure 14. Variation of rectifier (converter #1) firing angle and dc current for case 3.

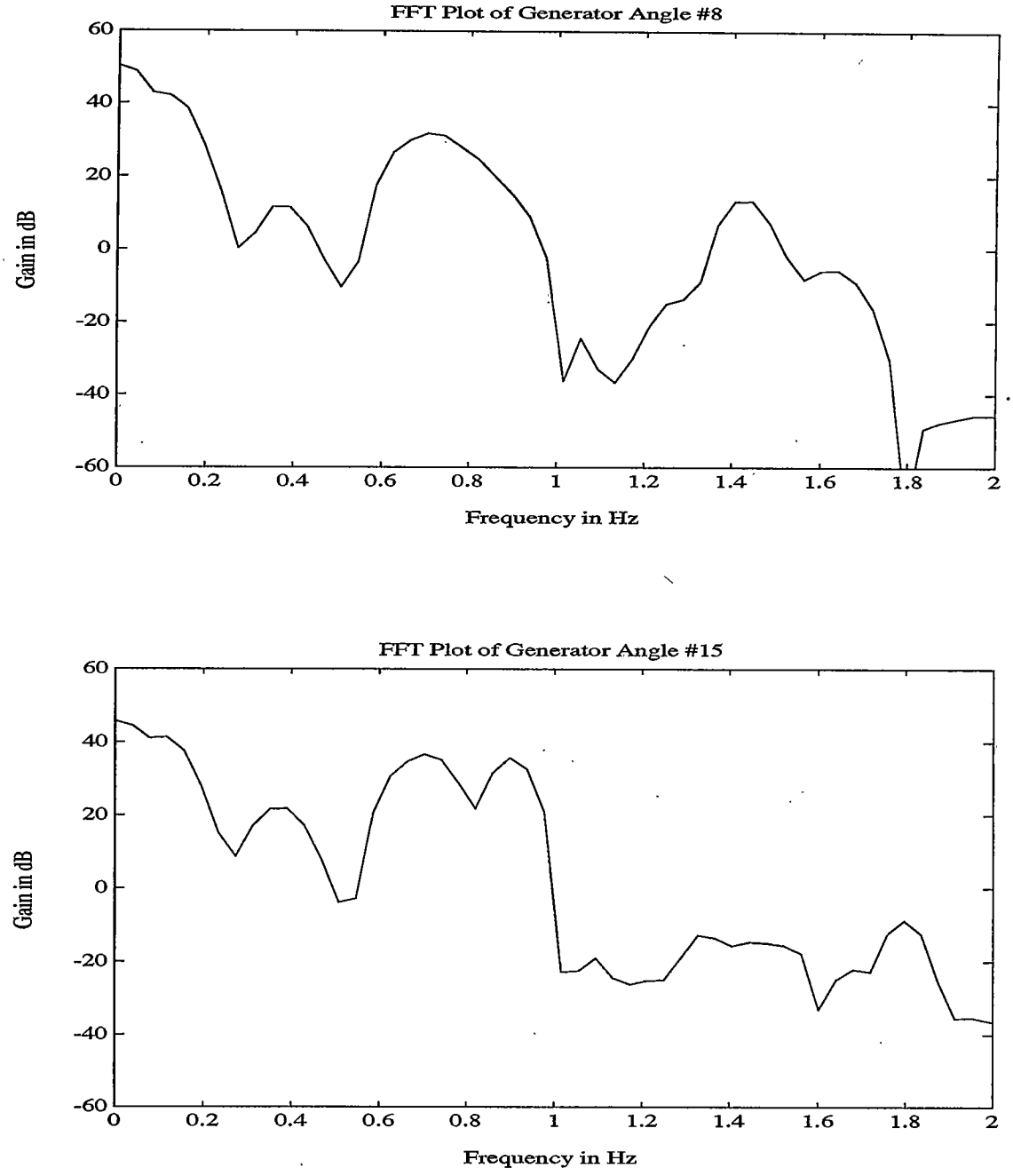

Figure 15. Fourier response of generator angles for case 1.

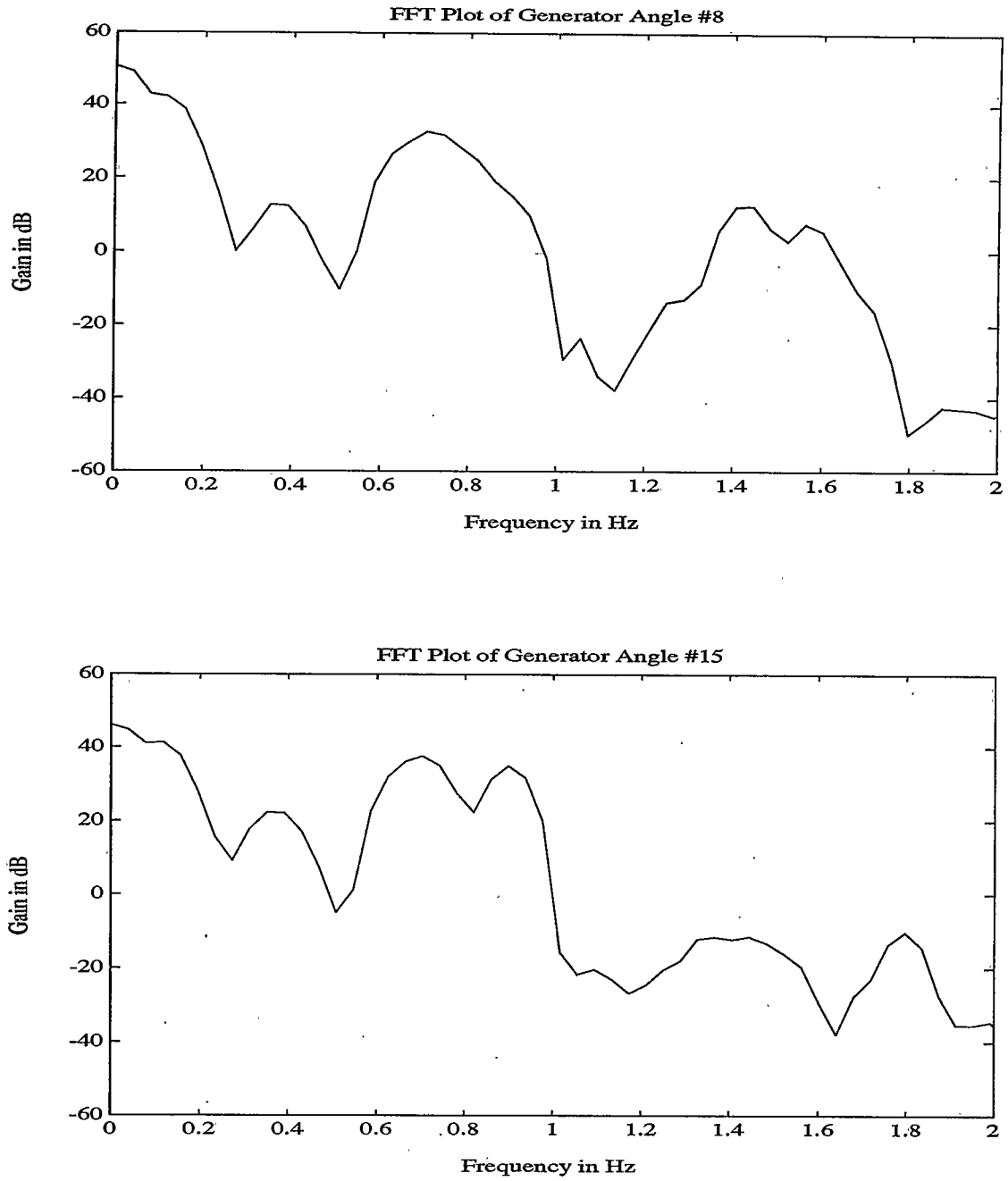

Figure 16. Fourier response of generator angles for case 2.

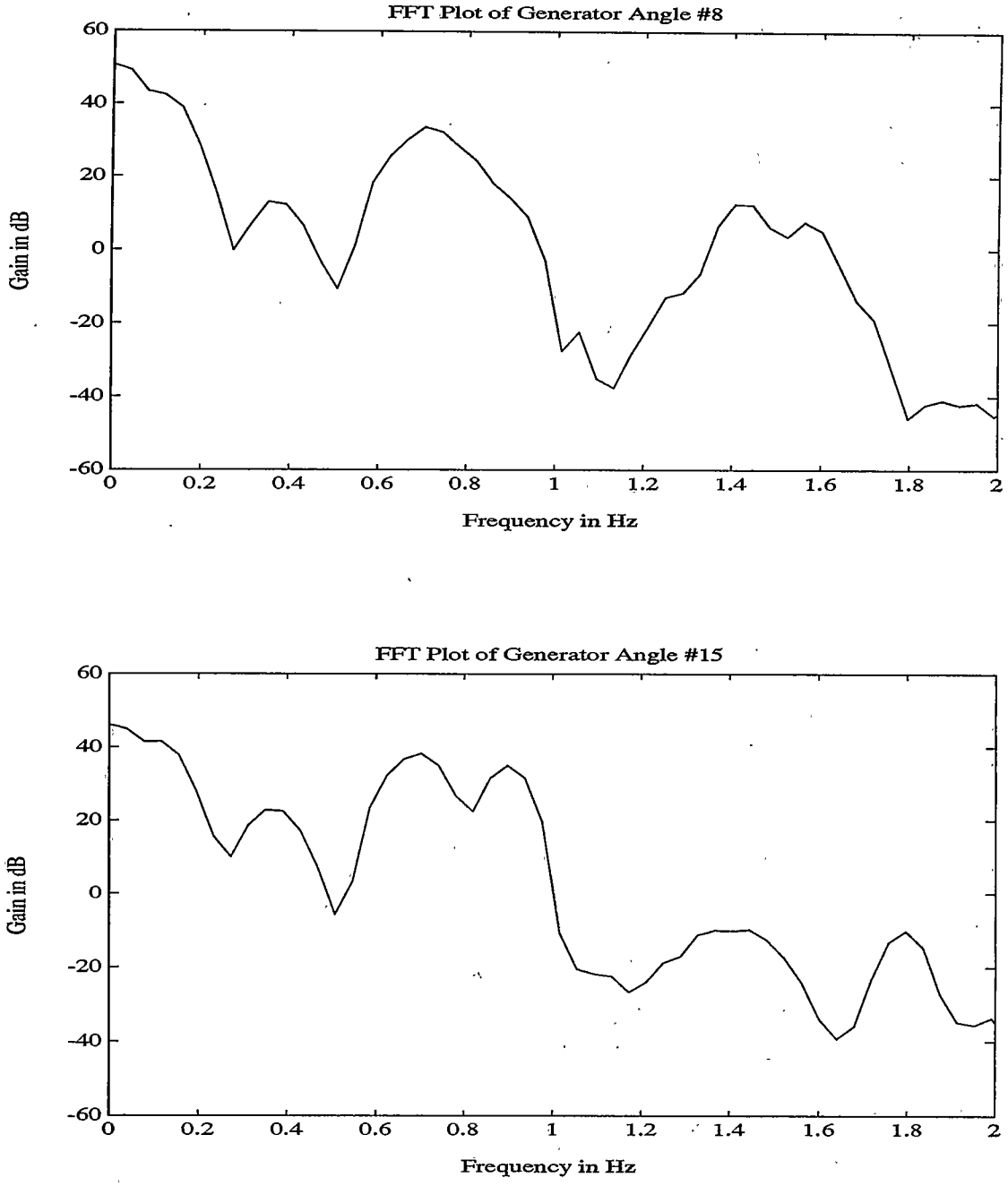

Figure 17. Fourier response of generator angles for case 3.

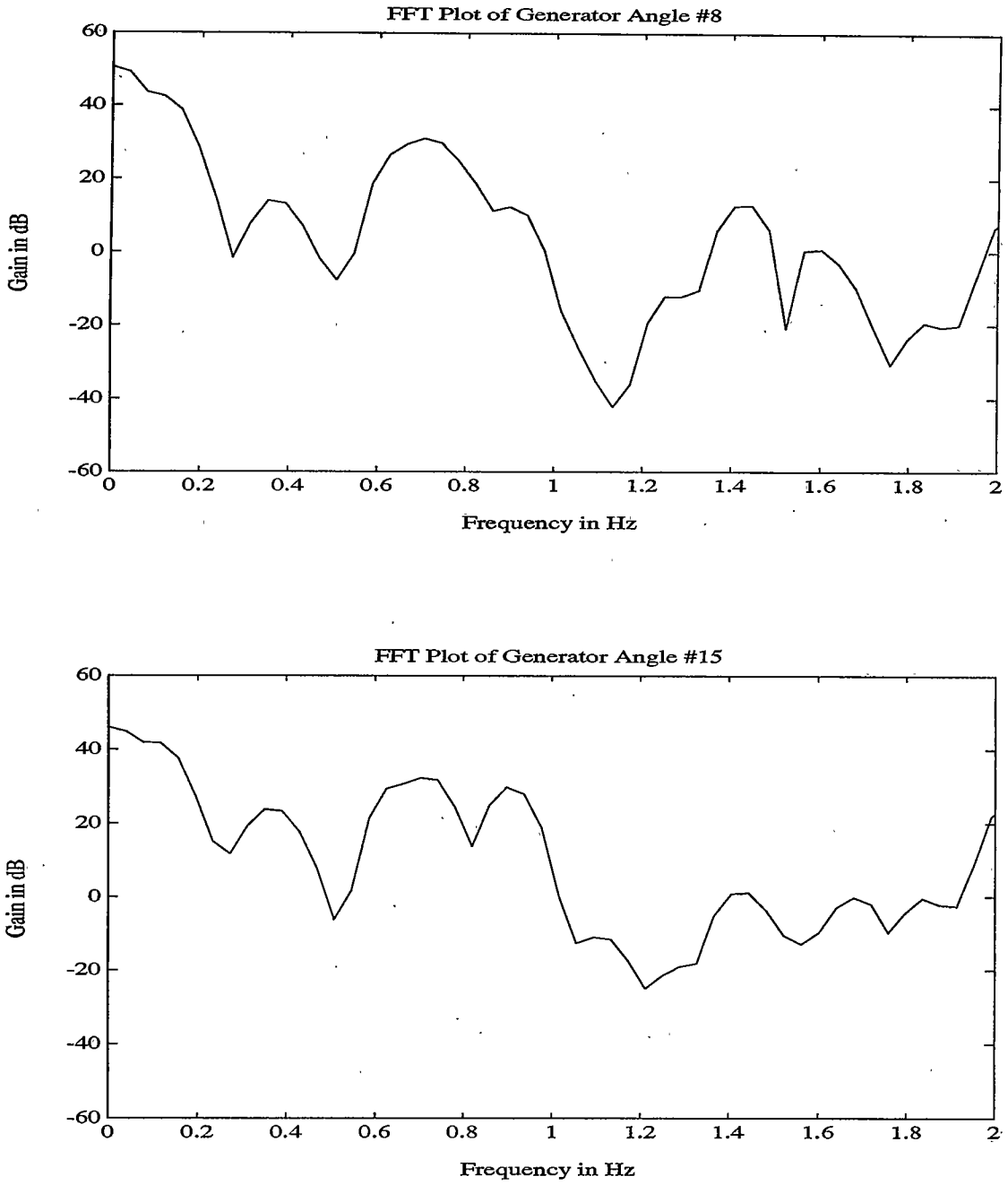

Figure 18. Fourier response of generator angles for case 4.

CHAPTER 3

NONCONVENTIONAL HVDC SYSTEM CONTROL CONFIGURATIONS

Introduction

The conventional way to operate an hvdc system is with the rectifier controlling the current and the inverter operating in the constant extinction angle (CEA) control mode, thereby consuming the minimum quantity of reactive power. However if the dc current or voltage is changed, the reactive power consumption at both terminals changes, and under certain conditions voltage and reactive power instability can result. It is possible to operate the dc system in other modes in which the reactive power or the voltage does not change significantly, thereby reducing the instability effect. The object of this chapter is to describe and compare various control modes referred to as nonconventional control modes at the inverter terminal. It is intended to elucidate the basic theoretical background in order to provide a better understanding of the control functions.

The voltage current (VI) characteristic, also known as operational characteristic, of the conventional control mode at the rectifier and inverter end is shown in Figure 19. In the same figure, operational characteristics of some of the nonconventional control modes of the inverter are also shown.

The functional block diagram for implementation of the non-conventional control schemes at the inverter terminal is shown in Figure 20.

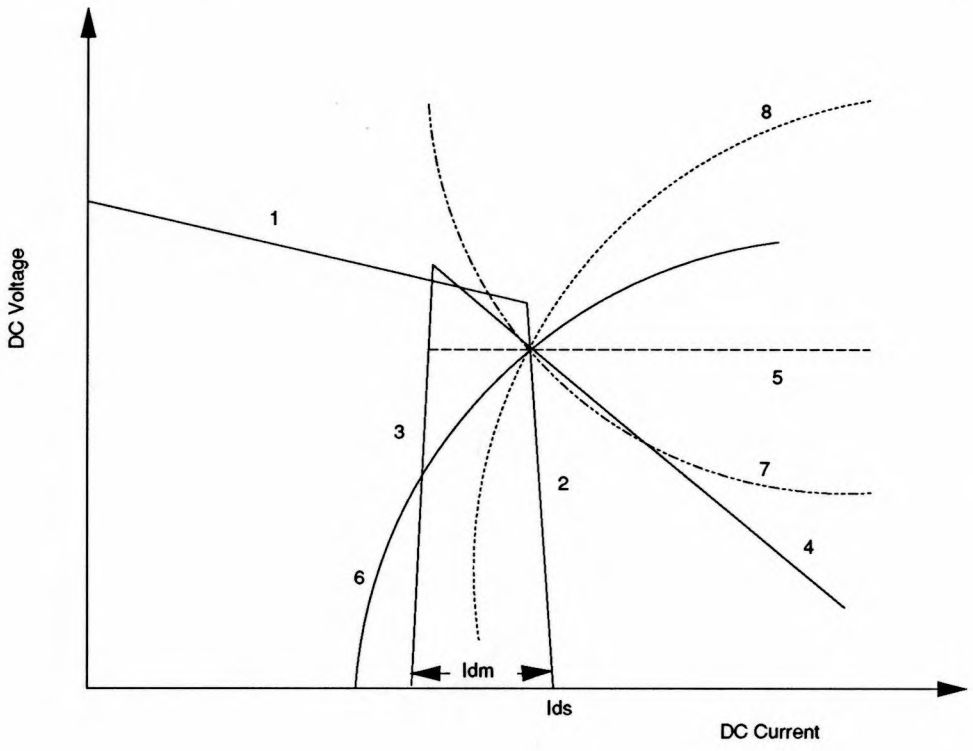

1. Minimum Ignition Angle Control at Rectifier
2. Constant Curretn Control at Rectifier
3. Constant Current Control at Inverter
4. Minimum Extinction Angle Control at Inverter
5. Constant DC Voltage Control at Inverter
6. Constant Reactive Current Control at Inverter
7. Constant Active Power Control at Inverter
8. Constant Reactive Power Control at Inverter

Figure 19. Nonconventional controller characteristics.

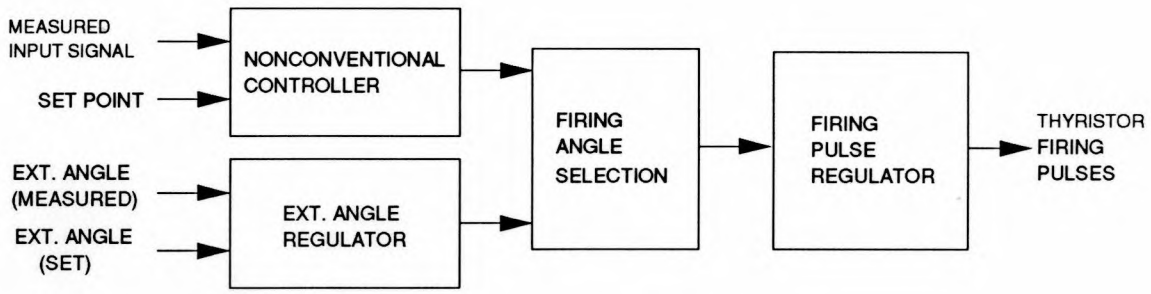

Figure 20. Nonconventional controller scheme.

Constant Ac Voltage Control [12-15]

Large ac voltage fluctuations are considered to be a persistent problem associated with an hvdc system when connected to a relatively weak ac system [12]. Since the fundamental component of the ac current at the hvdc converter terminal lags the commutating voltage, the dc converter terminals absorb reactive power proportional to their real power conversion in both the rectification and inversion modes. If the host ac system has a relatively high source impedance, it cannot supply this reactive power without the ac bus voltage falling to an unacceptable low value. To avoid this, compensating shunt capacitor banks are provided at the hvdc terminal. However, a sudden disturbance in the reactive power balance at the terminal causes high fundamental frequency overvoltages. An economical solution is to regulate the reactive power consumed

by the converter in response to ac voltage variation. Thus, the inverter can be controlled in such a way that it strives to keep the ac bus voltage constant.

It has been suggested that ac voltage control should operate only when the ac voltage level exceeds a pre-set value [12,13]. This is because if constant ac voltage is administered during undervoltage conditions, the controller will try to reduce the extinction angle gamma. If this angle falls below a minimum value, it will lead to commutation failure. However, in overvoltage conditions an increase in gamma will lead to higher reactive power absorption at the inverter, thereby reducing the voltage level, which is a corrective step. The functional block diagram of the ac voltage control scheme is shown in Figure 20. The conventional current control characteristic is maintained at the rectifier which controls the flow of dc power. At the inverter, a localized ac voltage regulator acting directly on the converter firing control along with the extinction angle regulator is provided. During normal or under voltage conditions the inverter remains in the extinction angle control mode, thereby consuming minimum reactive power. When dynamic overvoltages appear at the ac terminals, the ac voltage controller is actuated. It increases the extinction angle of the inverter and overrides the signal from other regulators,

thereby increasing the reactive power consumption to limit overvoltages. Thus it provides fast, smooth and continuous variation of the converter reactive power.

Ac voltage control offers advantages such as low losses and low probability of commutation failure. However, it has the disadvantage of higher valve stresses due to its operation at higher extinction angles.

Constant Dc Voltage Control [18-20]

This control is designed to control either the midpoint dc line voltage [18], or the inverter terminal dc voltage [19]. As shown in Figure 19, the dc voltage control characteristic at the inverter (curve 5), provides operation with zero slope. As a result, stability is improved compared to the constant extinction angle control mode which has a negative resistance characteristic. Furthermore, this control has the advantage of utilizing the insulation most effectively. During steady-state operation it is also possible to maintain the extinction angle near its minimum value by coordinating the tap changer control.

Constant Reactive Current Control [11]

If the inverter is controlled such that the reactive component of the current supplied to the ac system is kept

constant as the dc side current is changed, then the dc side voltage follows the characteristic as shown in Figure 19 (curve 6). Since this characteristic has a positive slope, the incidence of commutation failure and the recovery time of the valves reduces considerably. Figure 20 shows the functional block diagram used in the implementation of constant reactive current control. The conventional current control characteristic along with its natural minimum ignition angle control characteristic is maintained at the rectifier so that power flow across the system can be regulated. The reactive power consumption (at both terminals) is then defined by the inverter constant reactive current characteristic. A minimum gamma control mode is also provided at the inverter end so as to limit the gamma to its minimum value and thereby avoid commutation failure. Here both the inverter and rectifier operate with positive resistance characteristics resulting in extremely stable operation. Also, as the inverter operates with a value of extinction angle (γ) in excess of the minimum extinction angle (γ_{min}), the incidences of commutation failure would be few. Hence, rapid recoveries from faults could be expected. However, since this scheme operates at extinction angles larger than γ_{min}, the steady-state reactive power consumption is large and requires that the converter valves (including cooling and

damping circuits), the ac filters and the dc transmission line be designed to enable operation with higher than conventional extinction angles (2 to 3 degrees higher in steady state) [11].

Constant Power Factor Control [16,17]

To maintain constant power factor at the inverter terminal, the dc voltage at that terminal is controlled by controlling its firing angle, while the ac voltage variations are compensated by the commutating transformer tap changer. In this mode the inverter operates at a higher extinction angle during partial load conditions. Furthermore, at full load, its operating characteristic is exactly the same as that of extinction angle control. This scheme has a serious drawback of slow response, as the time needed to change the transformer tap during and soon after the disturbance is quite large. This makes the control operate as a dc voltage controller during transient operation. A power factor controller which does not need a tap changer control is suggested in [17]. In this thesis a power factor controller is implemented in the simulation without a tap changer. Also, a minimum extinction angle control is superimposed to avoid commutation failure. The advantage of power factor control is that the extinction angle is increased as the direct current reduces, and hence the possibility of commutation failure is minimized. Also as the

power factor remains constant, the real power transferred and the reactive power consumed are directly proportional to the direct current, and this minimizes the possibility of high reactive power consumption.

Constant Active Power Control

In constant current control mode, the inverter strives to maintain a constant dc current even if there are large changes in dc voltage. These changes can be caused by changes in the ac bus voltage or by loss of one valve group in a pole consisting of two or more groups. Such a voltage change would of course cause a proportional change in the power flow over the dc link because of the constant current control. A link with this type of control would obviously not make an ideal interconnection. It would not respond to the needs of a system in distress, and indeed loss of a valve group on such a system would cause a disturbance in the form of a sudden change in power flow.

Thus for many applications a constant power control mode would be an improvement over the constant current control. Such a system is designed by merely deriving the dc current order from a power signal divided by the dc voltage. For application in an interconnected system this control is better compared to constant current control because it strives to

hold its power constant. Constant power control will not cause the system to suffer unduly by transferring more power under adverse conditions. However, it will still not respond to the needs of the system in distress in the way that an ac tie does. Another disadvantage is that it leads to two operating points in the steady state as shown in the Figure 19 (curve 7), hence causing two point instability.

Constant Reactive Power Control [19,20]

In the past, a reactive power signal has been used as a modulating signal to produce a secondary signal such as dc voltage at the inverter for pole control [19]. However, a reactive power control strategy can also be implemented as a primary control strategy at the inverter. The characteristic of this control scheme is as shown in Figure 19 (curve 8). This control has additional capability, over that available with reactive current control, to suppress variations in the ac bus voltages.

CHAPTER 4

APPLICATION OF PRONY-BASED ANALYSIS FOR EVALUATION OF NONCONVENTIONAL CONVERTER CONTROLLERS

Introduction

This chapter presents an approach to obtain reduced-order linearized models of power systems which are actually nonlinear, time varying, and extremely large order. An off-line system identification method based on Prony signal analysis is used to obtain the system transfer function for the ac/dc test system used in this study. Responses of the Prony-based linearized models are then used in root-locus studies to see how the feedback of these signals affects system eigenvalues.

Prony analysis is an off-line technique of analyzing signals to determine modal, damping, phase, and magnitude information contained in the signal. It is an extension of Fourier analysis in that damping information as well as frequency information is obtained. Here a known input of a given class is applied to the system and the output is analyzed using Prony signal analysis. Though standard Prony analysis does not directly give estimates of transfer functions, it can be extended to obtain the transfer functions for inputs of a given class. Some aspects of Prony analysis of power system response signals are given in [60]. A detailed description of the Prony based

system identification technique can be obtained from [7].

Application

In this section a reduced-order linear model of the ac/dc system is obtained for each dc control scheme used, by applying Prony signal analysis. To carry out the analysis, system transfer functions for particular output signals were first identified using the method described in [7]. The linear models obtained show the local and interarea modes of interest, and are used to analyze the nonconventional dc system control schemes with reference to damping of both the local and interarea modes. The transfer functions obtained from this Prony based method are then analyzed using the root locus technique. Root locus, through a graphical representation, provides information about the amount of damping that a particular controller can contribute to each of the modes present in the system.

The test system used is the 42-bus, 17-machine system described in Chapter 2 with the Pacific hvdc intertie represented by a two-terminal, bipolar ±500 Kv dc line model and the Intermountain intertie by equivalent real and reactive constant current loads at their respective terminal buses. The rectifier is provided with a proportional-plus-integral (PI) type of constant current controller along with minimum firing angle control. At the inverter a constant firing angle

is maintained. The output signals used are ac voltage, dc voltage, reactive current, power factor, active and reactive power at the inverter bus, each corresponding to a particular nonconventional dc controller mode. In each case a low amplitude rectangular pulse disturbance of 1 s width is added to the inverter firing angle signal as input to the system, as shown in Figure 21. The input is shown in the Figure 22 and is a special case of the general signal used in [7] which has the following form in the Laplace domain:

$$I(s) = \frac{\left(c_0 + c_1 e^{-sD_1} + c_2 e^{-sD_2} + \ \ldots \ + c_k e^{-sD_k}\right)}{s - \lambda_{n+1}} \tag{4.1}$$

where $D_i < D_{i+1}$, the c_i's are arbitrary real constants, and n is the order of the model. In our case the following parameters are used to describe the input I(s) to the system.

$$k = 1, \quad c_0 = 3, \quad c_1 = -3, \quad D_1 = 1 \quad \text{and} \quad \lambda_{n+1} = 0 \tag{4.2}$$

Prony analysis and results from [7] were used to fit a suitable transfer function for each of the above mentioned output signals. For each case the transfer function is described by its eigenvalues and residues as given in Tables 3 through 8.

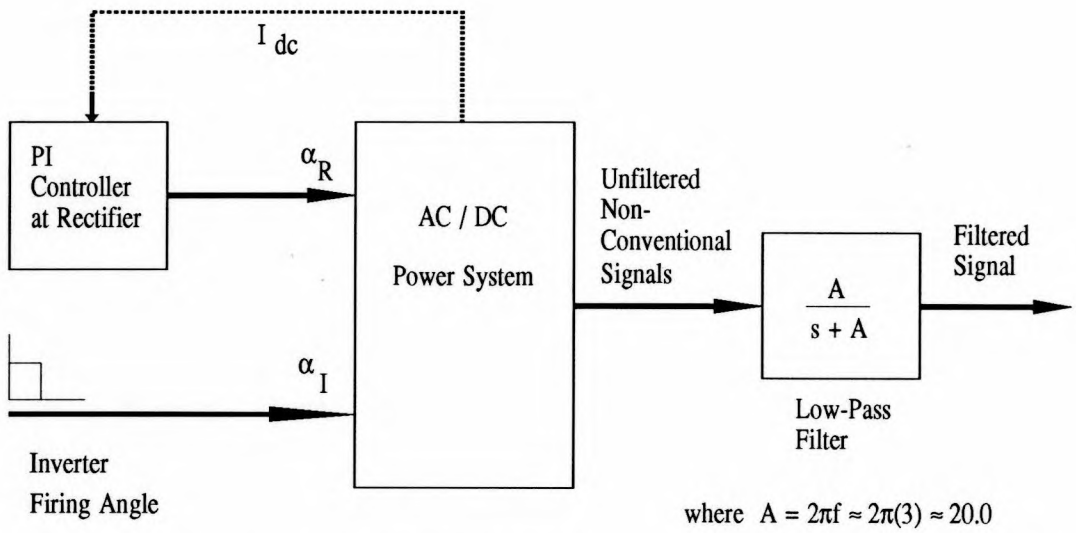

Figure 21. Implementation of a general nonconventional control scheme for Prony based analysis.

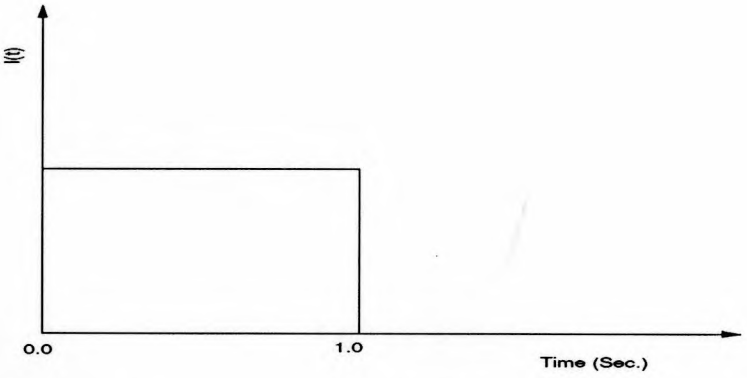

Figure 22. Input signal used to obtain system transfer function.

The pulse input of Figure 22 was also applied to the transfer function for each of the outputs to show the validity of the low-order transfer-function fit as compared to the actual system response for the same input. The transfer-

function responses and the actual responses are shown in Figures 23 through 28. In every case the linear low-order model output fits the actual system response quite well except during the application of the input signal.

The associated root-locus plots are shown in Figures 29 through 34. These plots are obtained for the transfer-function gain variation from 0 to 10. It is evident from these figures that the movement of the poles associated with the local and interarea modes is not significant. This can also be noticed from the fact that the residues associated with both the interarea and local modes for each case of the nonconventional dc controller schemes studied are relatively small. The magnitudes of these residues give a good measure of the amount of damping that can be achieved for corresponding modes (eigenvalues) through feedback. From the root-locus plots of ac voltage and dc voltage controller schemes it is noticed that one pair of eigenvalues corresponding to 0.91 Hz local mode is in the right half plane (see also Table 3 and 4) signifying that these two controllers are unstable for this mode. It can also be noticed from the root-locus plots for each of the nonconventional dc controller schemes that for all residues which are relatively small the corresponding pole-zero pairs are very close to each other. Hence, little damping of such modes is possible through feedback.

Table 3. Identified reduced-order transfer-function model for ac voltage as output signal.

Mode	Freq. (Hz)	Eigenvalue	Residue
1	1.71	-0.1710d+02±j0.1074d+02	+0.1773d+01±j0.1974d+02
2	0.91	+0.2988d-01±j0.5742d+01	+0.6172d-01±j0.1110d+00
3	0.71	-0.5575d-01±j0.4484d+01	+0.2541d-01±j0.4492d-01
4	2.08	-0.6141d+00±j0.1307d+02	+0.2766d-01±j0.1306d-01
5	4.70	-0.8541d+00±j0.2948d+02	-0.3078d-01±j0.2269d-01

Table 4. Identified reduced-order transfer-function model for dc voltage as output signal.

Mode	Freq. (Hz)	Eigenvalue	Residue
1	5.00	-0.3184d+02±j0.3142d+02	+0.1237d+03±j0.1221d+03
2	1.68	-0.1319d+02±j0.1058d+02	-0.8809d+01±j0.1218d+02
3	0.69	-0.1632d+00±j0.4388d+01	+0.3053d-02±j0.1798d+00
4	0.91	+0.3192d-01±j0.5710d+01	+0.2563d-01±j0.1287d+00
-	-	-0.2501d+01+j0.0000d+00	-0.9447d+00-j0.1080d+00

Table 5. Identified reduced-order transfer-function model for reactive current as output signal.

Mode	Freq. (Hz)	Eigenvalue	Residue
1	2.42	-0.2278d+02±j0.1523d+02	+0.1352d+04±j0.6975d+04
2	0.36	-0.3175d+00±j0.2271d+01	+0.2278d+01±j0.3996d+01
3	0.92	-0.8378d-01±j0.5750d+01	-0.3003d+01±j0.3442d+01
4	2.12	-0.8531d+00±j0.1333d+02	-0.9537d+00±j0.1480d+01
5	4.57	-0.6664d+00±j0.2871d+02	-0.1195d+01±j0.1637d-01

Table 6. Identified reduced-order transfer-function model for power factor as output signal.

Mode	Freq. (Hz)	Eigenvalue	Residue
1	1.66	-0.3257d+02±j0.1044d+02	-0.1010d+01±j0.2453d+01
2	0.37	-0.3314d+00±j0.2337d+01	-0.3377d-03±j0.3617d-03
3	0.91	-0.2354d-01±j0.5695d+01	+0.1564d-03±j0.4867d-03
4	3.39	-0.3231d+01±j0.2133d+02	+0.3744d-03±j0.7346d-04
5	1.59	-0.4991d+00±j0.9962d-01	+0.9770d-04±j0.1597d-03

Table 7. Identified reduced-order transfer-function model for active power as output signal.

Mode	Freq. (Hz)	Eigenvalue	Residue
1	0.69	-0.1142d+00±j0.4383d+01	-0.1751d+00±j0.1167d+01
2	0.36	-0.3522d+00±j0.2240d+01	+0.8635d+00±j0.2714d+01
3	0.91	-0.3597d-02±j0.5703d+01	-0.5387d+00±j0.2822d+01
-	-	-0.3046d+02±j0.0000d+00	-0.9009d+03+j0.5213d-14
-	-	-0.2210d+01+j0.0000d+00	-0.3926d+01+j0.5088d-15
-	-	-0.4918d+00+j0.0000d+00	-0.5556d+00+j0.3494d-15

Table 8. Identified reduced-order transfer-function model for reactive power as output signal.

Mode	Freq. (Hz)	Eigenvalue	Residue
1	1.45	-0.3261d+02±j0.9092d+01	-0.8153d+03±j0.5514d+04
2	0.36	-0.3462d+00±j0.2236d+01	-0.4055d+00±j0.9385d+00
3	0.71	-0.1913d+00±j0.4446d+01	-0.1910d+00±j0.8197d+00
4	0.93	-0.3105d+00±j0.5864d+01	+0.5671d+00±j0.7546d-01
-	-	-0.1635d+01+j0.0000d+00	+0.2928d+01+j0.4083d-14

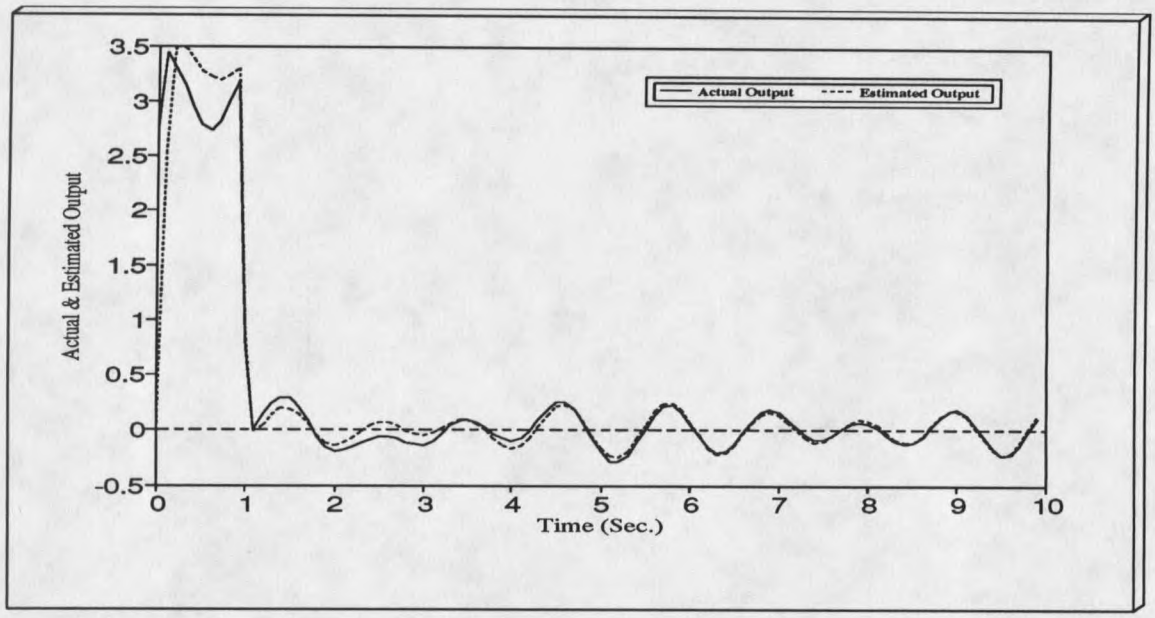

Figure 23. Transfer-function model output data versus actual data for ac voltage signal.

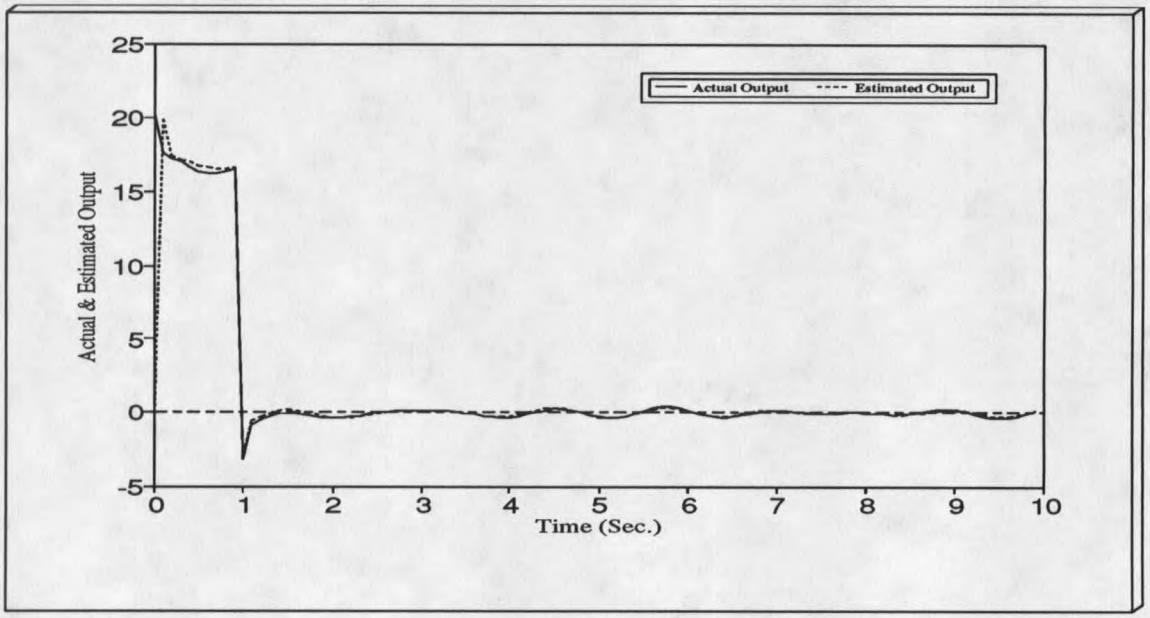

Figure 24. Transfer-function model output data versus actual data for dc voltage signal.

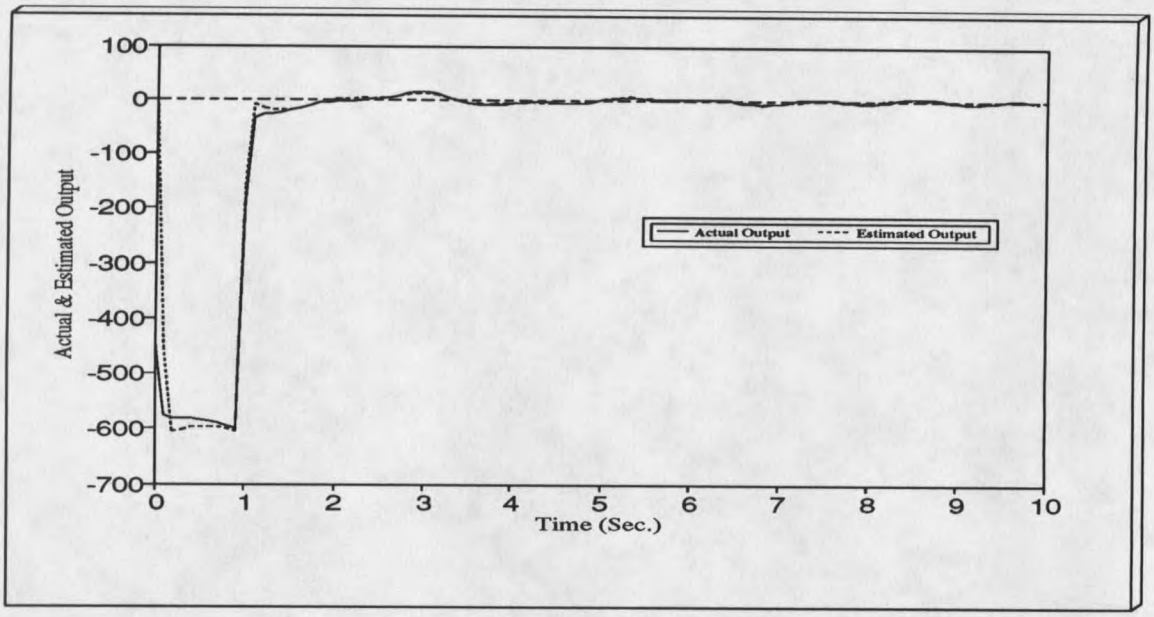

Figure 25. Transfer-function model output data versus actual data for reactive current signal.

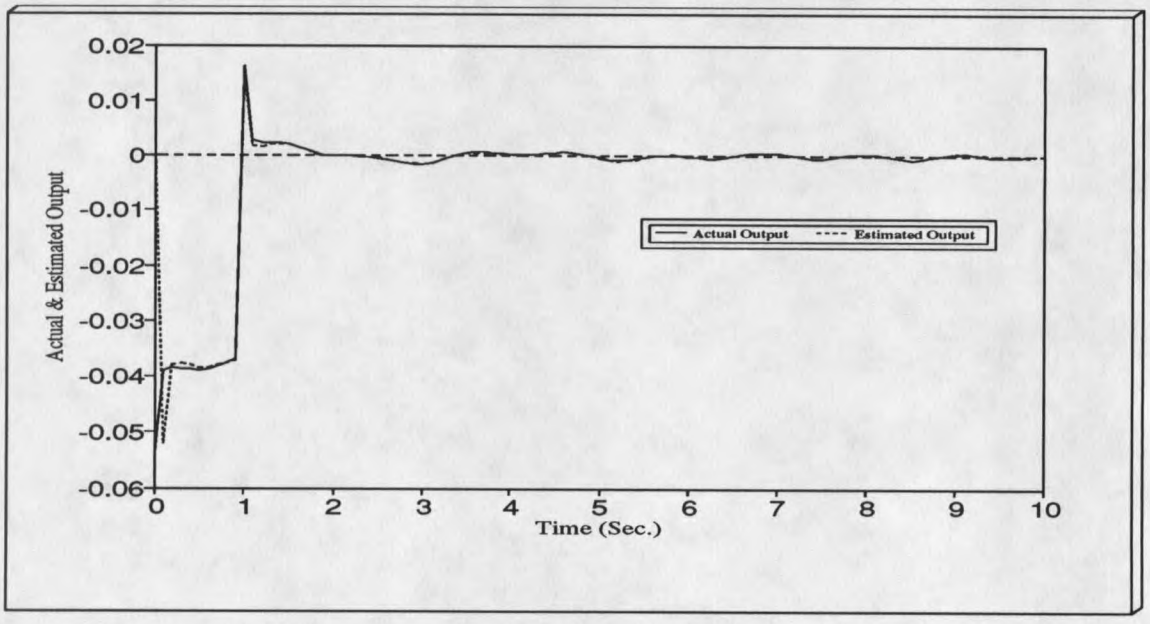

Figure 26. Transfer-function model output data versus actual data for power factor signal.

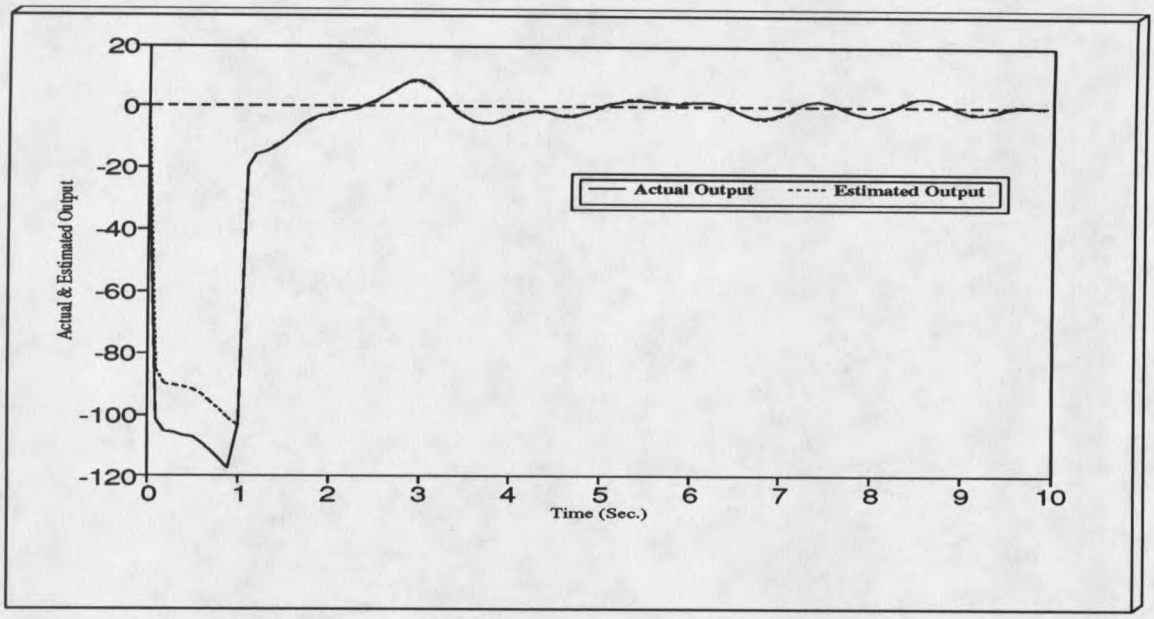

Figure 27. Transfer-function model output data versus actual data for active power signal.

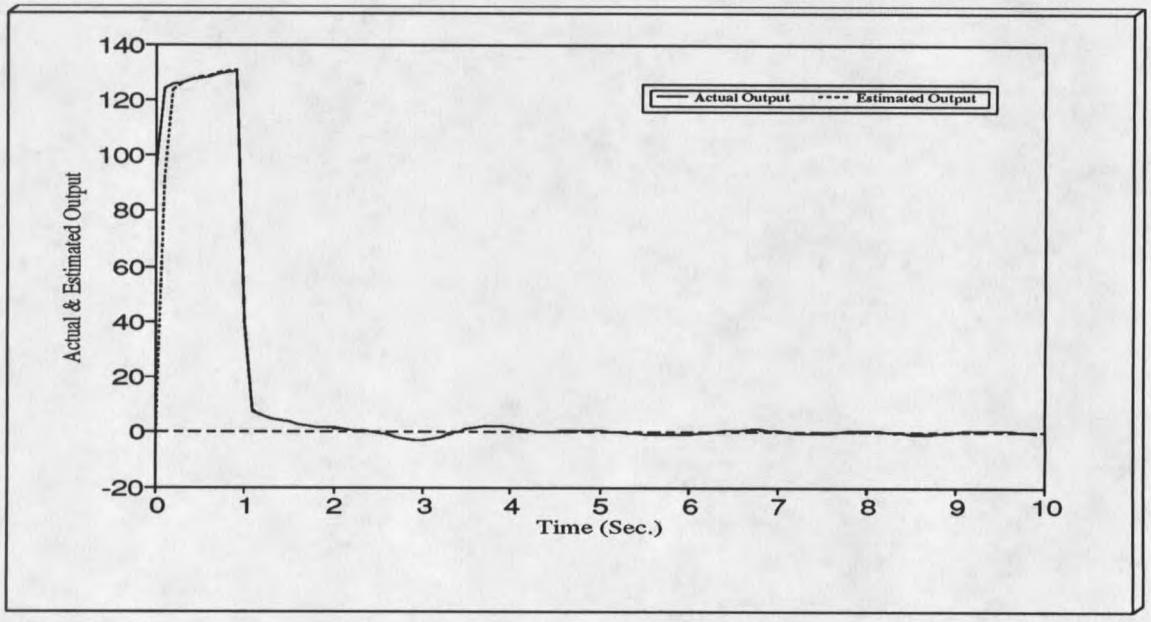

Figure 28. Transfer-function model output data versus actual data for reactive power signal.

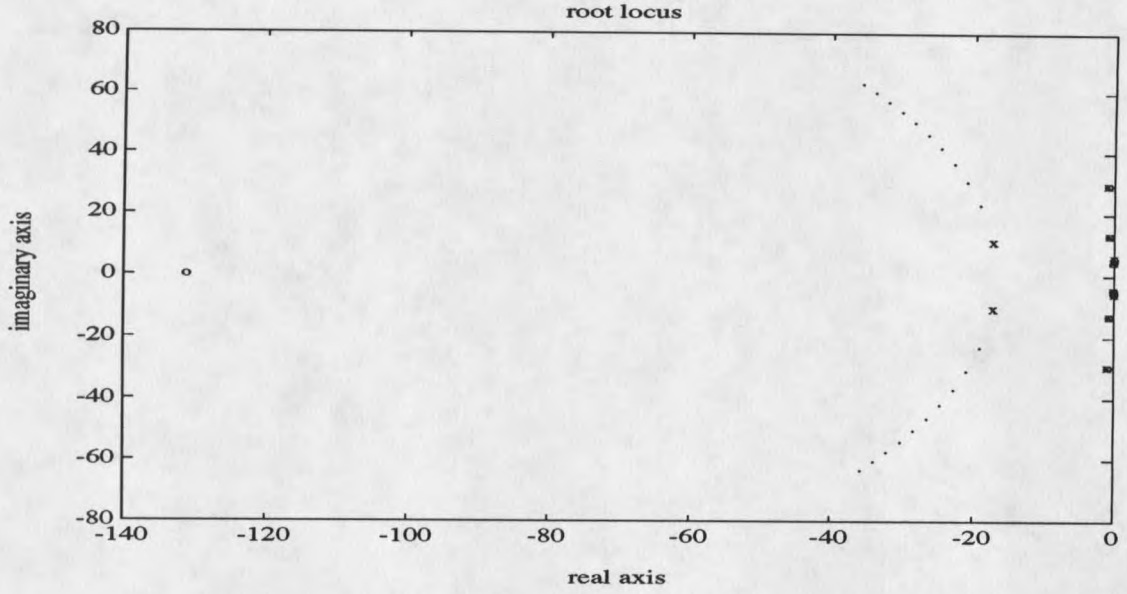

Overall root locus

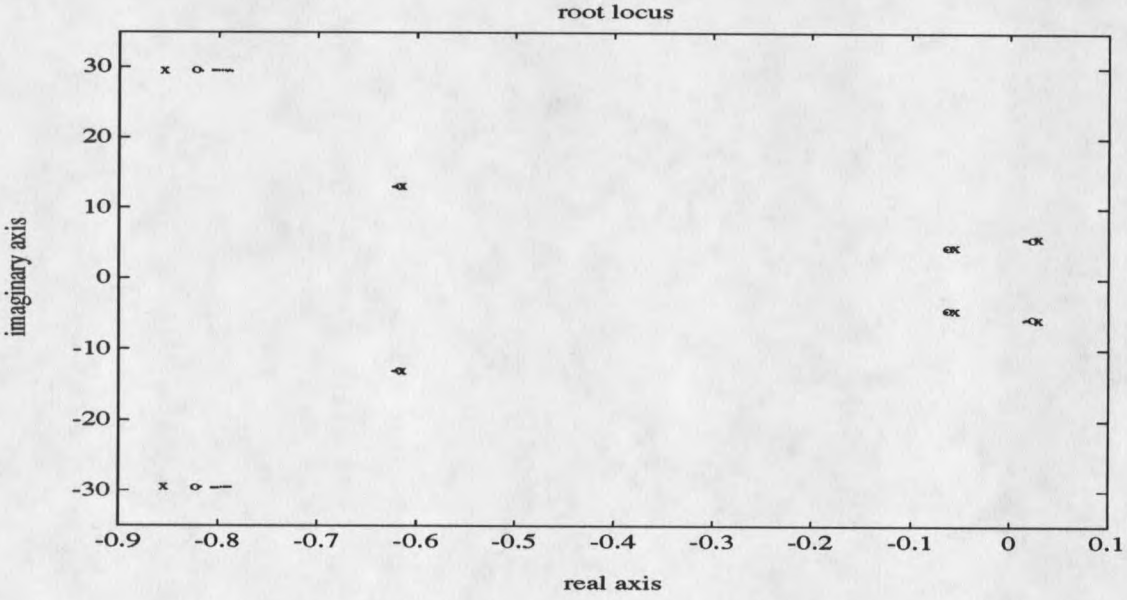

portion of interest expanded

Figure 29. Root-locus plot for ac voltage signal at the inverter.

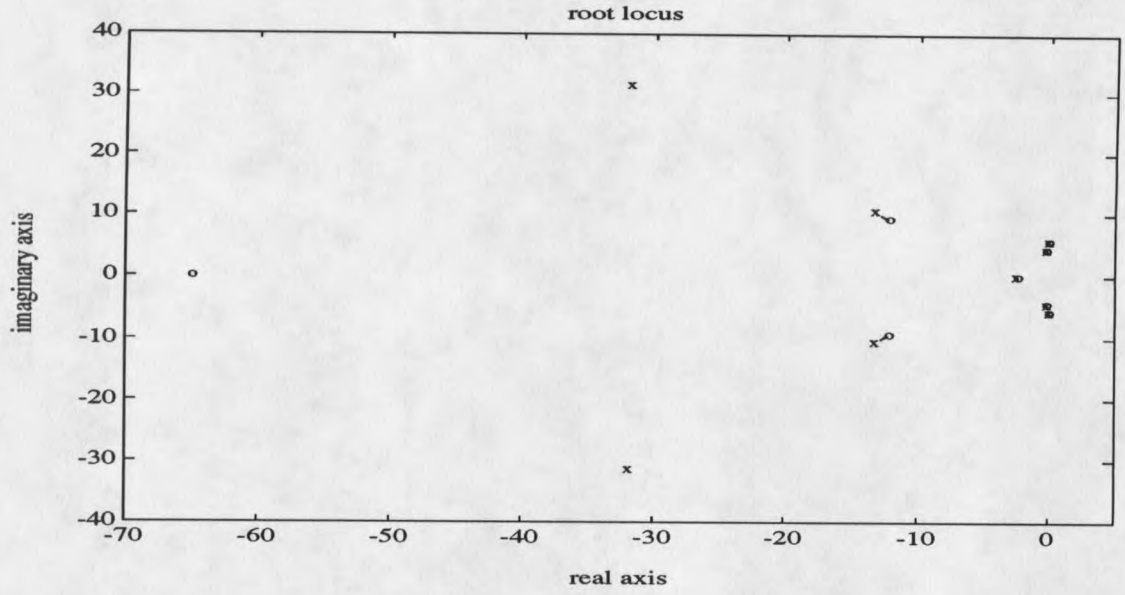

Overall root locus

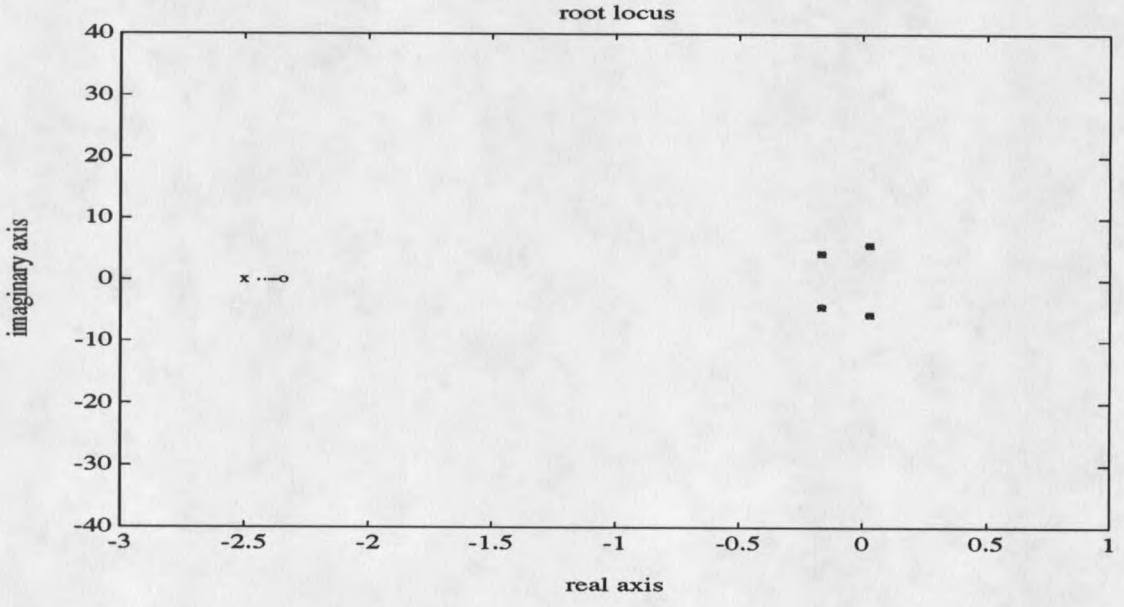

portion of interest expanded

Figure 30. Root-locus plot for dc voltage signal at the inverter.

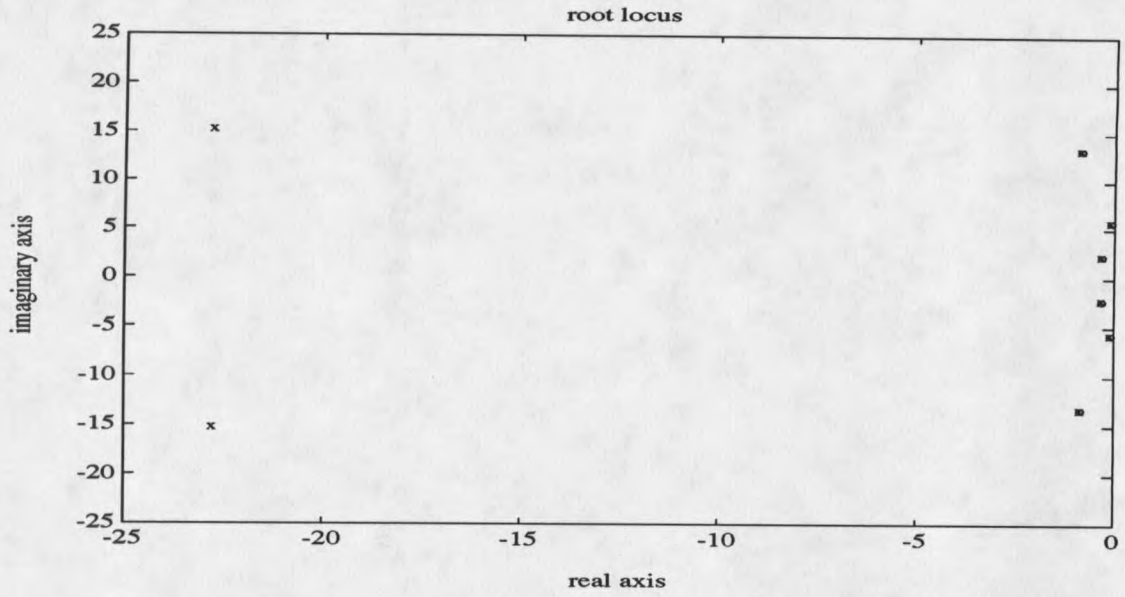

Overall root locus

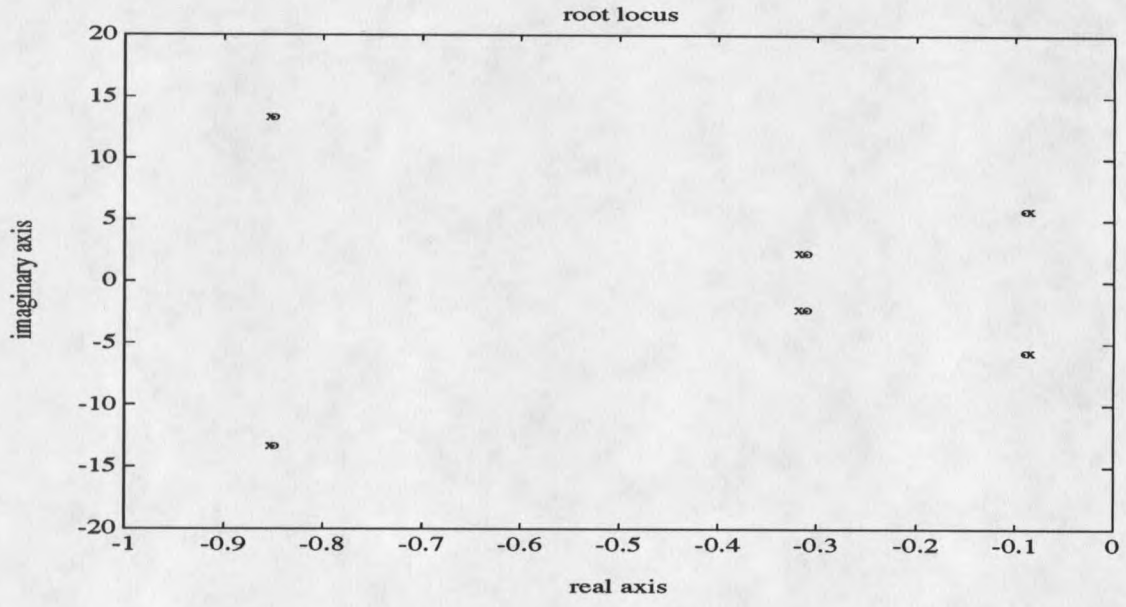

portion of interest expanded

Figure 31. Root-locus plot for reactive current signal at the inverter.

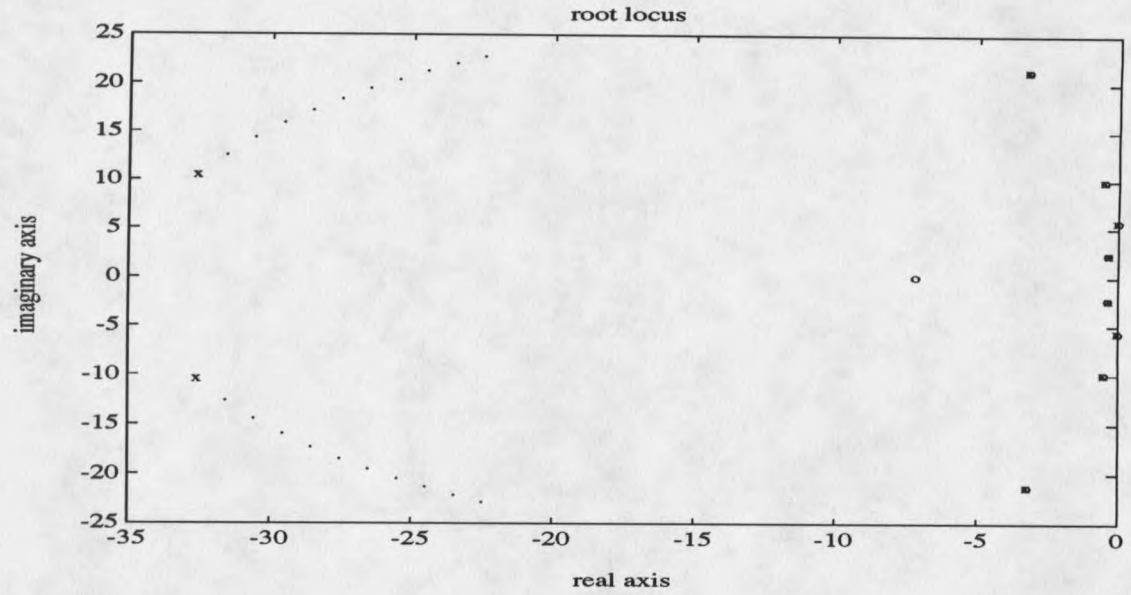

Overall root locus

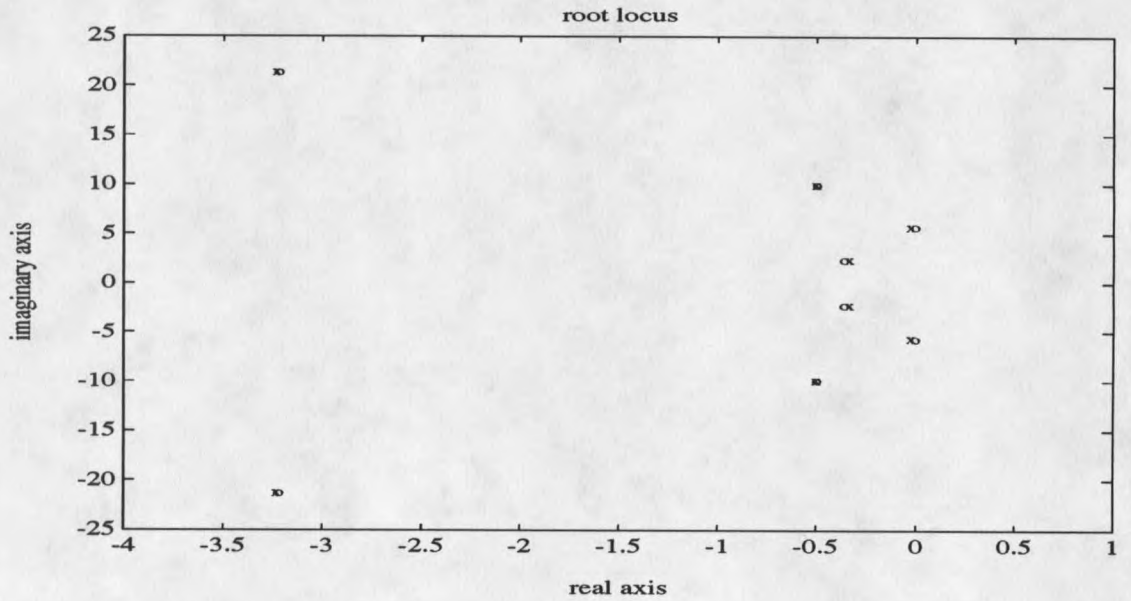

portion of interest expanded

Figure 32. Root-locus plot for power factor signal at the inverter.

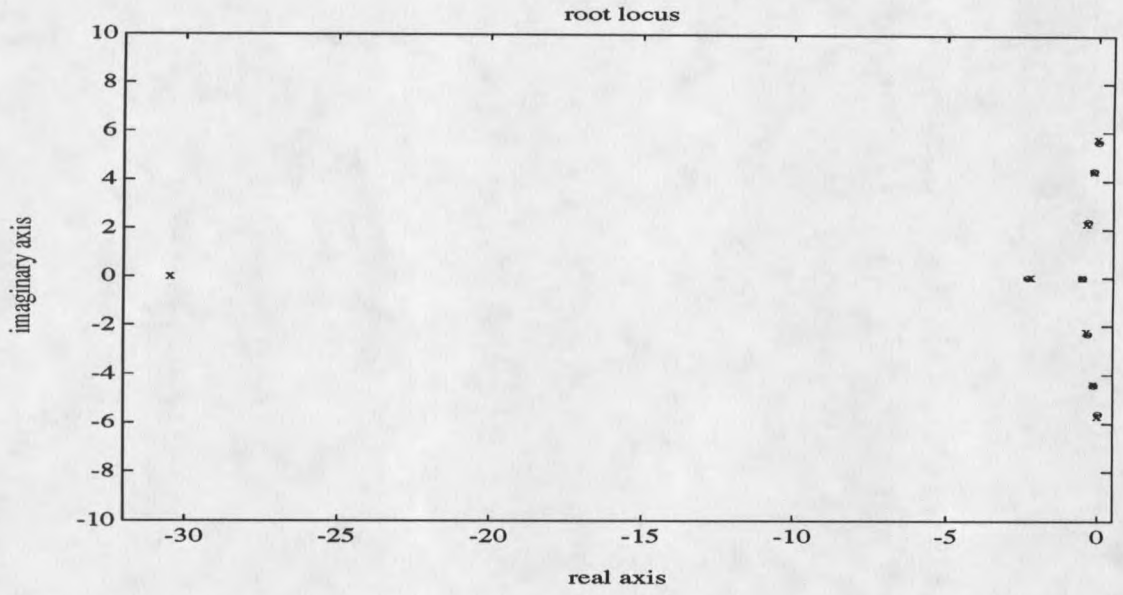

Overall root locus

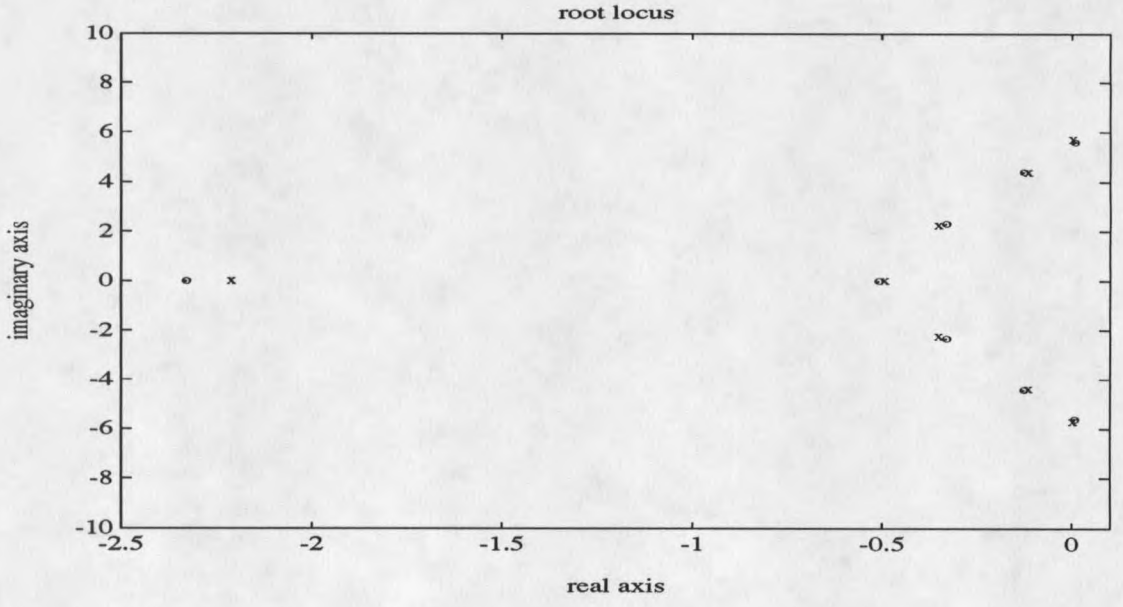

portion of interest expanded

Figure 33. Root-locus plot for active power signal at the inverter.

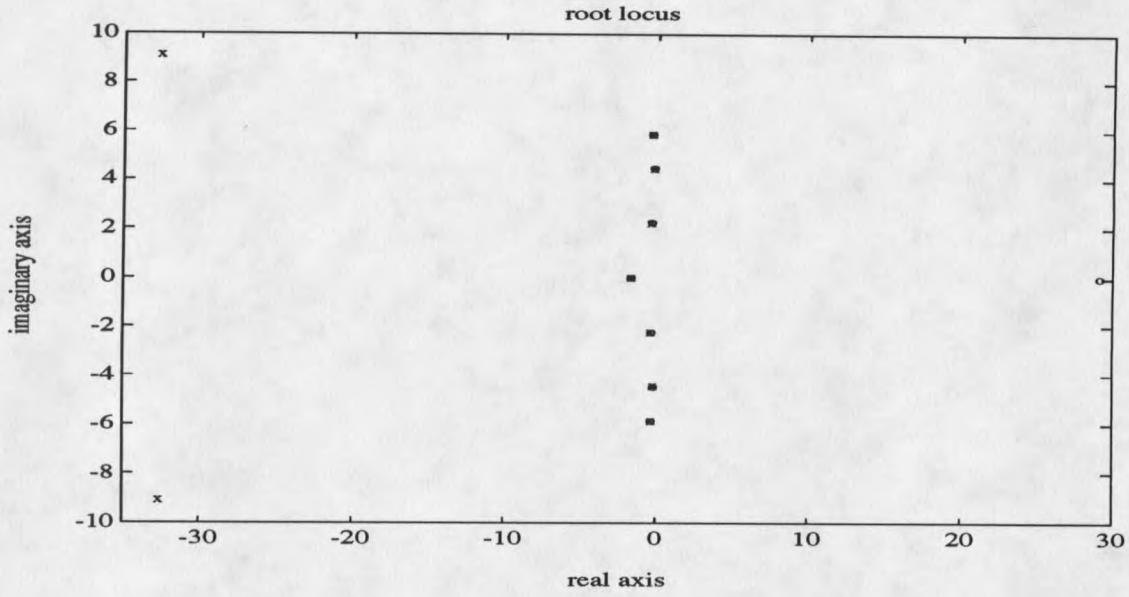

Overall root locus

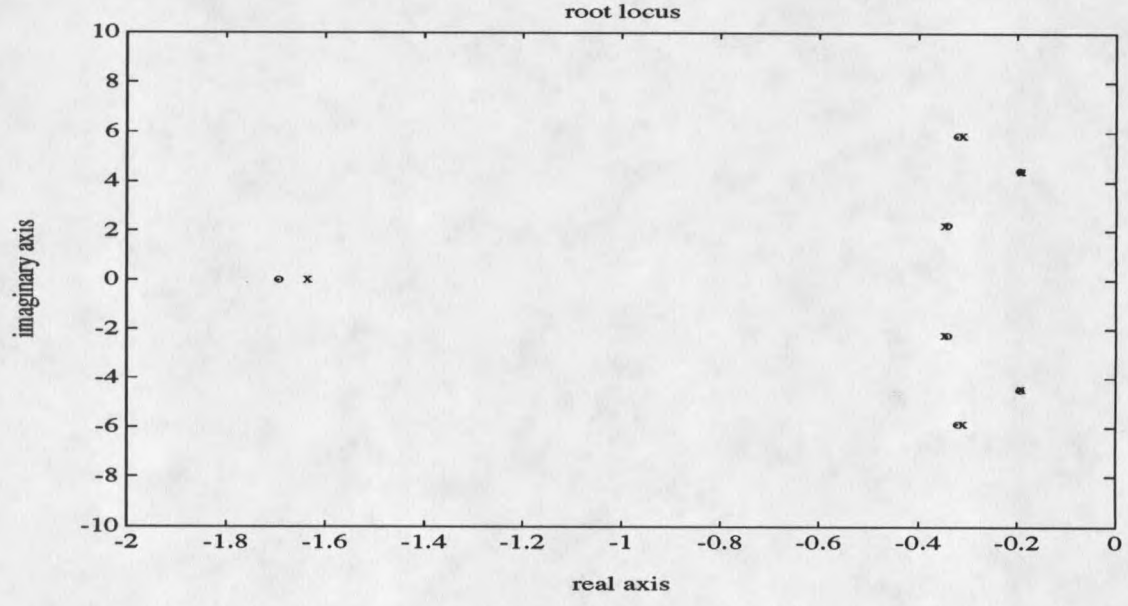

portion of interest expanded

Figure 34. Root-locus plot for reactive power signal at the inverter.

CHAPTER 5

TIME DOMAIN SIMULATION RESULTS FOR NONCONVENTIONAL CONTROL SCHEMES

Introduction

Computer simulation results for the ac/dc test system introduced in Chapter 2 and shown in Figure 1 for various nonconventional hvdc control schemes are presented in this chapter. The performance of the nonconventional control schemes introduced in Chapter 3 are investigated for various system disturbances. Their effectiveness in damping of low frequency oscillations is evaluated and conclusions drawn.

Simulation Results

The nonconventional controllers were applied to the 42-bus, 17-machine test system shown in Figure 1 (Chapter 2). In this simulation the Pacific hvdc intertie is represented by a two-terminal, bipolar ±500 Kv dc line model and the Inter-mountain intertie by equivalent real and reactive constant current loads at their respective terminal buses. The rectifier is provided with a proportional-plus-integral (PI) type of constant current controller along with minimum firing angle control. From the root-locus plots for various nonconventional inverter controllers (given in Figures 29 through 34 of Chapter

4), it is clear that the pole-zero pairs corresponding to the local and the interarea modes of interest are very near each other making it difficult, if not impossible, to design a suitable compensator which can provide damping to these modes. Therefore, a proportional-plus-integral (PI) type of compensator with nominal values of gain was implemented at the inverter. The gain values used for both rectifier and inverter are $K_p = 0.15$ for the proportional controller and $K_I = 5.8$ for the integral controller. The system responses to various disturbances were obtained. Some of the disturbances considered are

1. Fault 1 : A 1400 MW braking pulse is applied at bus NW1 in the system shown in Figure 1 for 30 cycles to simulate a braking resistor.
2. Fault 2 : The line from bus P to bus SC2 (Figure 1) is removed for 0.5 s.
3. Fault 3 : The line from bus A to bus SC1 (Figure 1) is removed for 0.15 s.
4. Fault 4 : The line from local generator bus 16 to bus SC1 is removed for 0.5 s. This represents a local fault near the inverter.

In order to compare generator swings for each nonconventional controller mode with the conventional current-margin control at the inverter, the variation of the generator angles

(for machines #4, #8, #11, #15 of Figure 1) were obtained relative to generator #1 which is considered to be a large machine at bus A. These generator angle variations for fault 1 and fault 2, described above, are depicted in Figures 35 through 46. For all other faults these figures have not been presented as their effects on the local and interarea swing modes were insignificant. Only in the case of the ac voltage controller for fault 2 (Figure 43), there seems to be some enhancement in the damping (compare Figure 43 with Figure 42) while in the case of other control modes like constant dc voltage control (Figure 44), and constant active and reactive power control (not shown in the figures here), the system became more unstable for fault 2. Thus, the degree of the effect of controllers depends on the system under study and type and location of the disturbances. In response to most faults on large systems, the nonconventional controllers examined will not provide consistent damping improvement over that obtainable with the conventional controller.

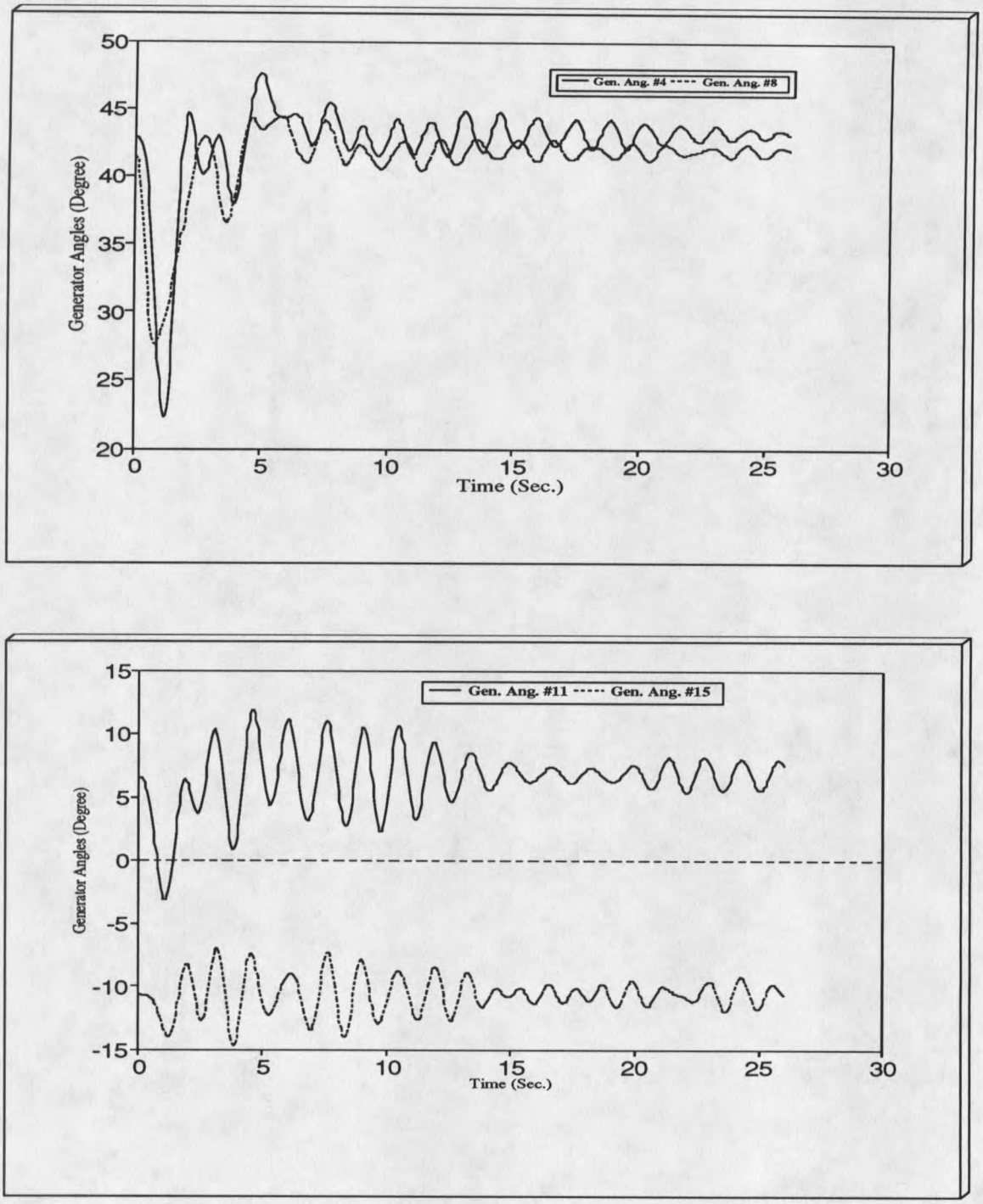

Figure 35. Relative generator angles for fault 1 (machines #4, #8, #11, and #15) with conventional current margin control.

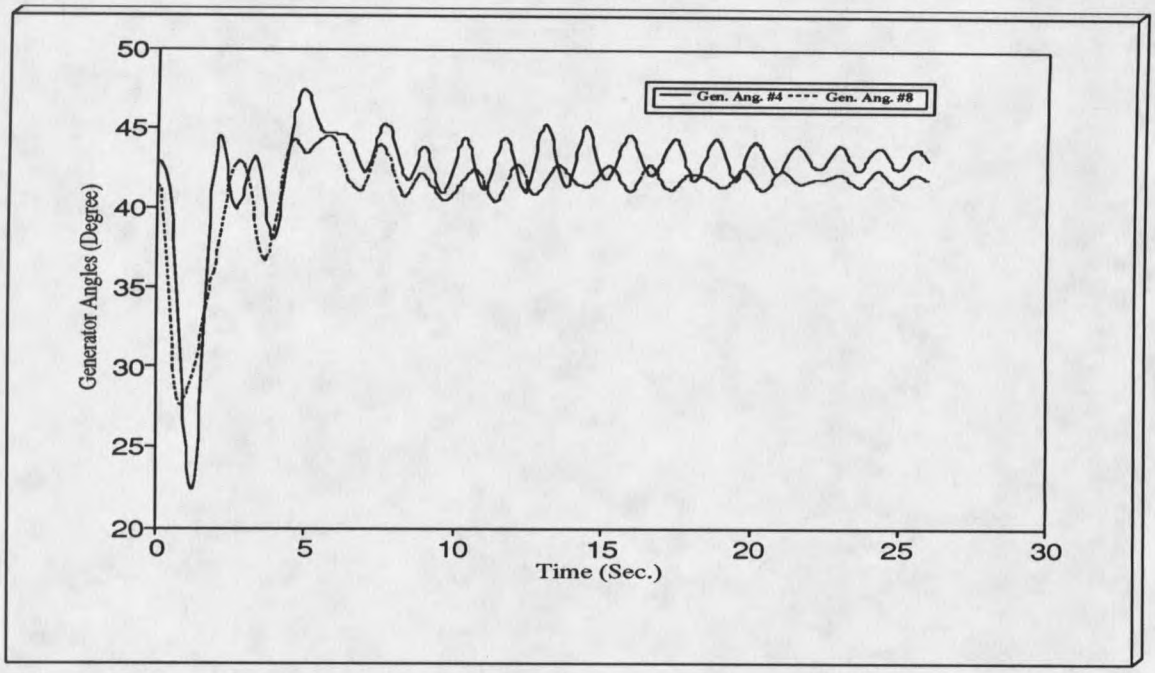

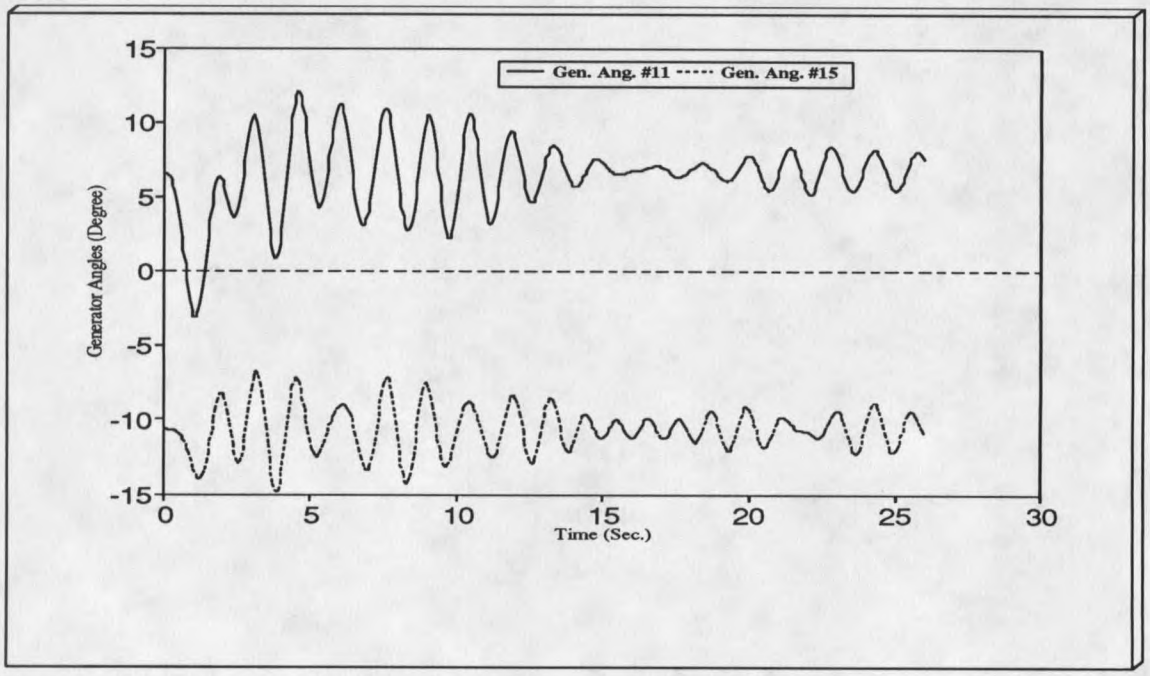

Figure 36. Relative generator angles for fault 1 (machines #4, #8, #11, and #15) with ac voltage control.

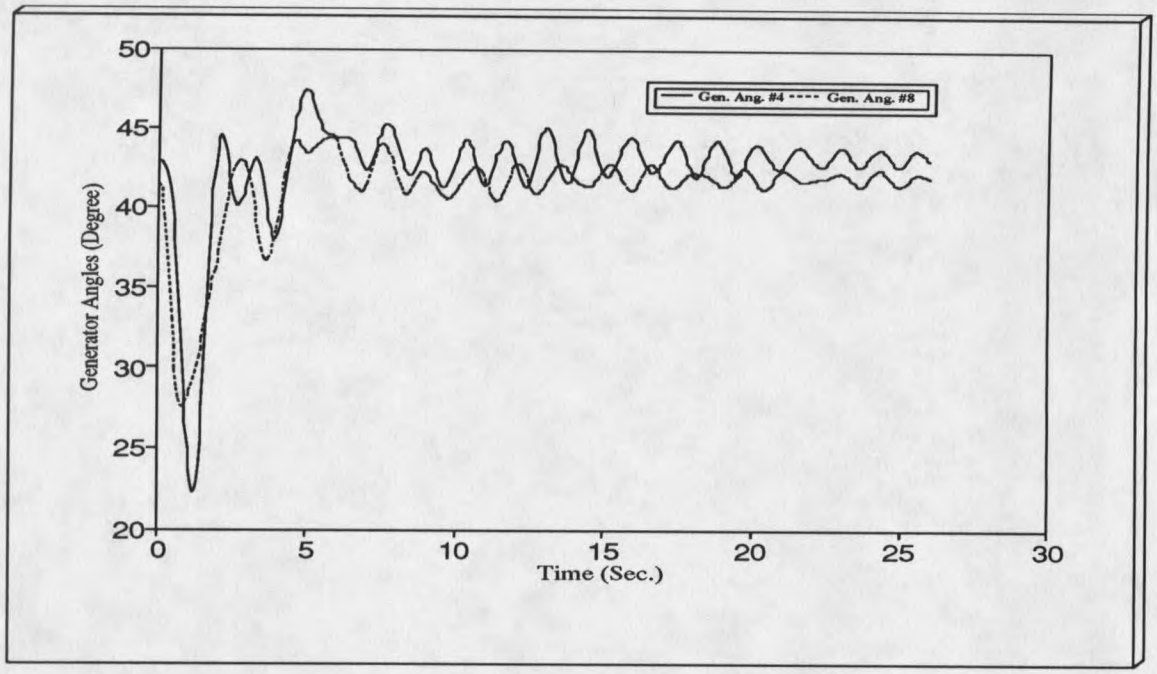

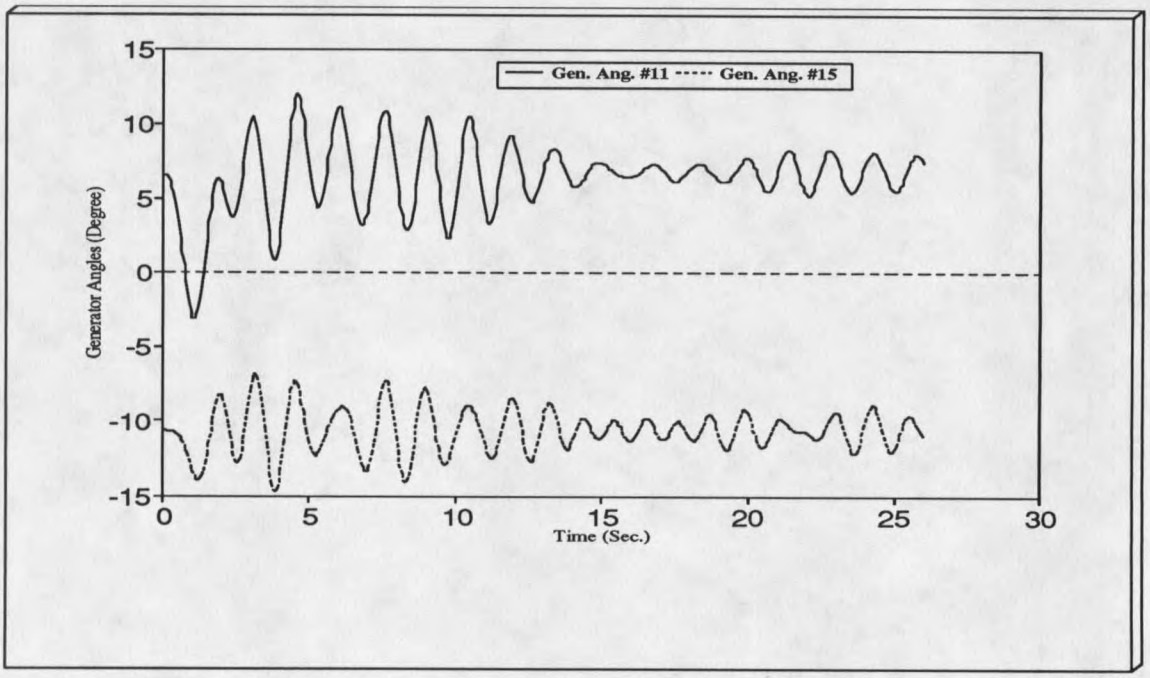

Figure 37. Relative generator angles for fault 1 (machines #4, #8, #11, and #15) with dc voltage control.

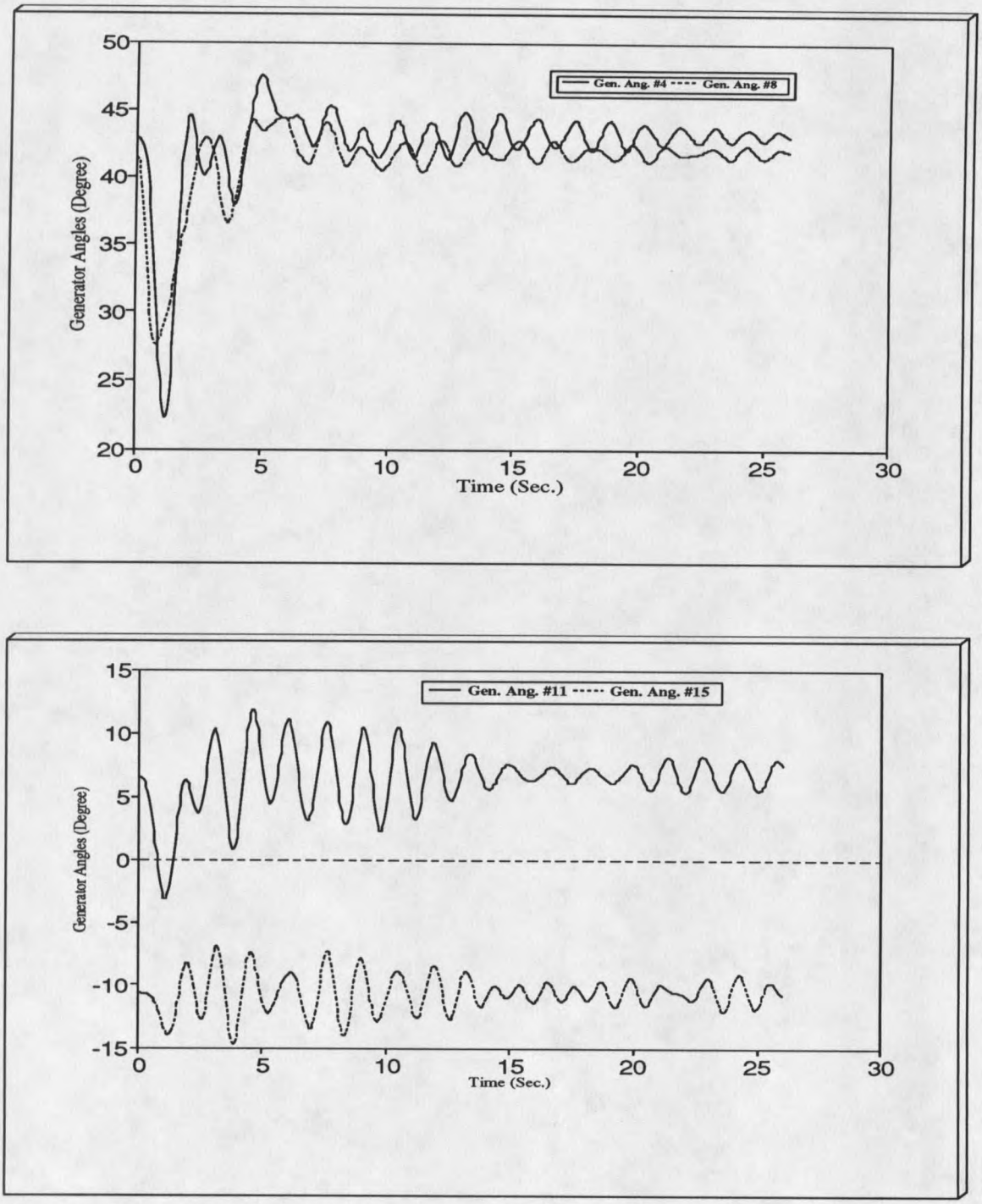

Figure 38. Relative generator angles for fault 1 (machines #4, #8, #11, and #15) with reactive current control.

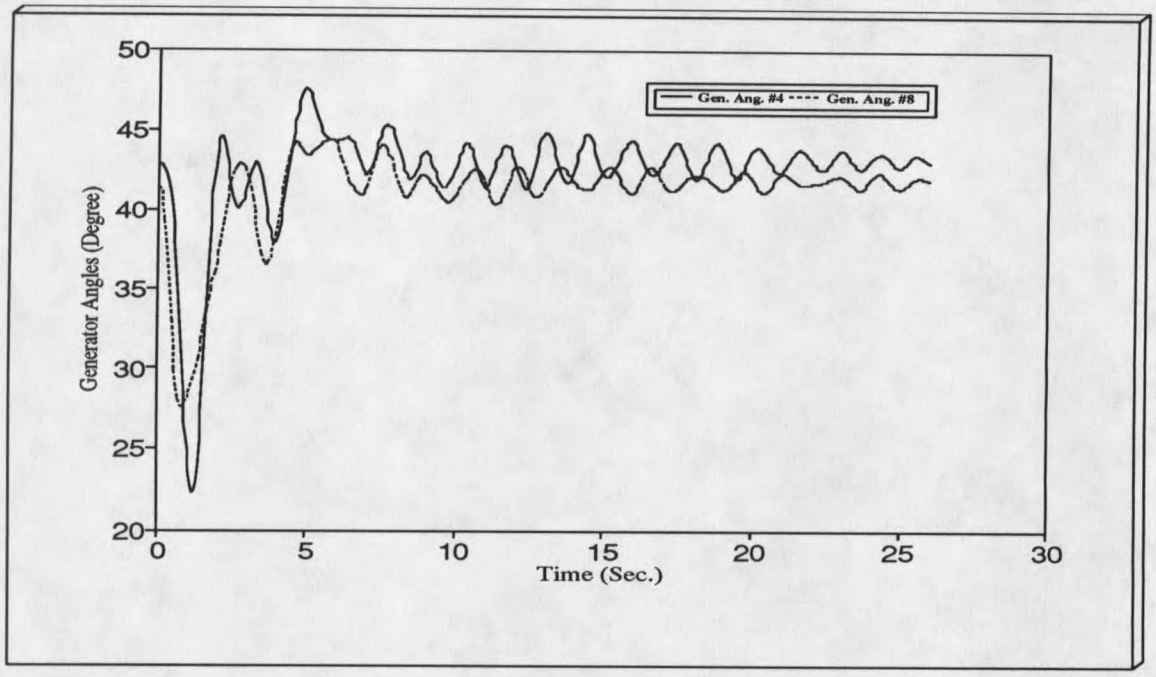

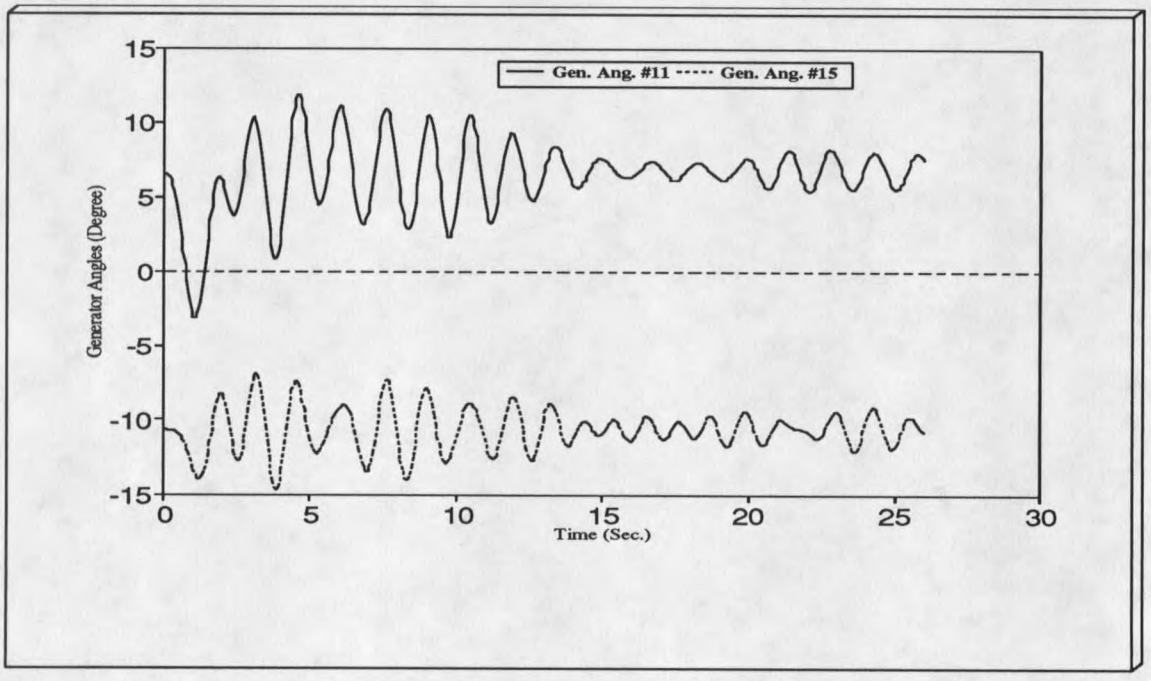

Figure 39. Relative generator angles for fault 1 (machines #4, #8, #11, and #15) with power factor control.

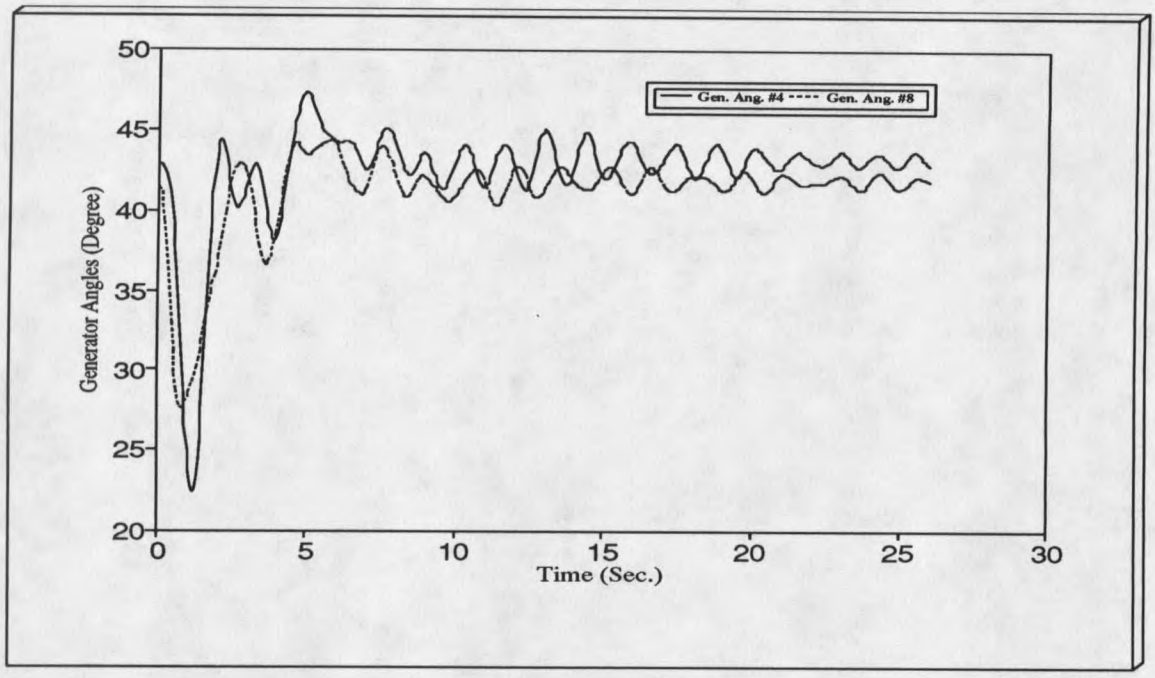

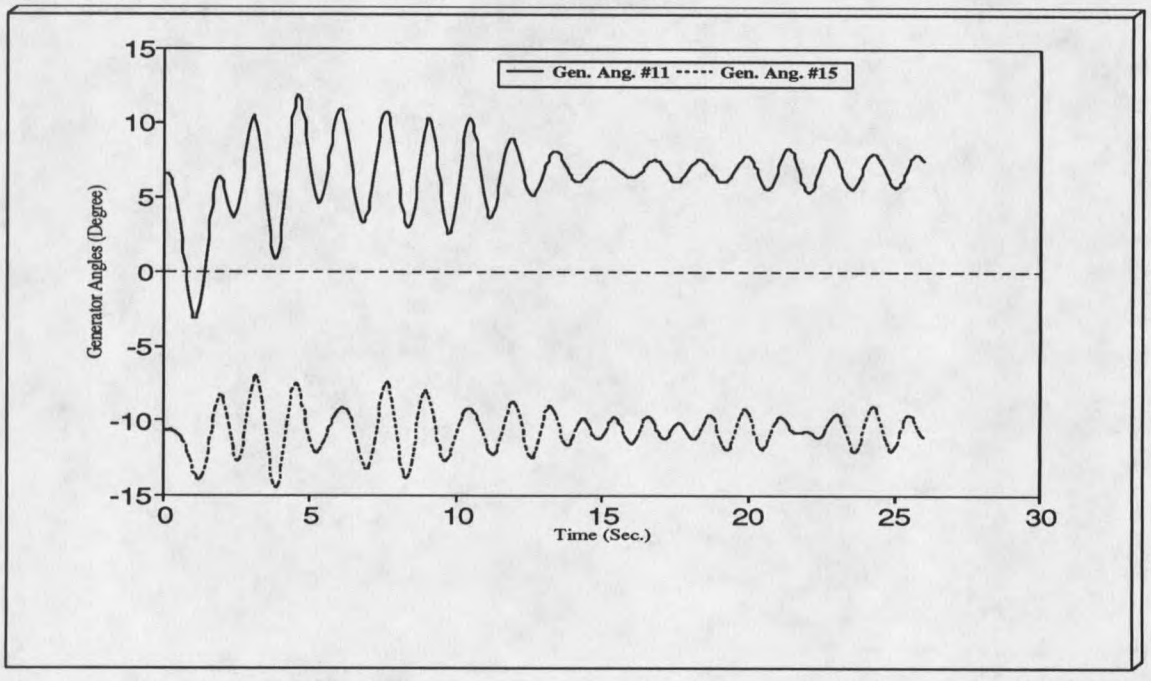

Figure 40. Relative generator angles for fault 1 (machines #4, #8, #11, and #15) with active power control.

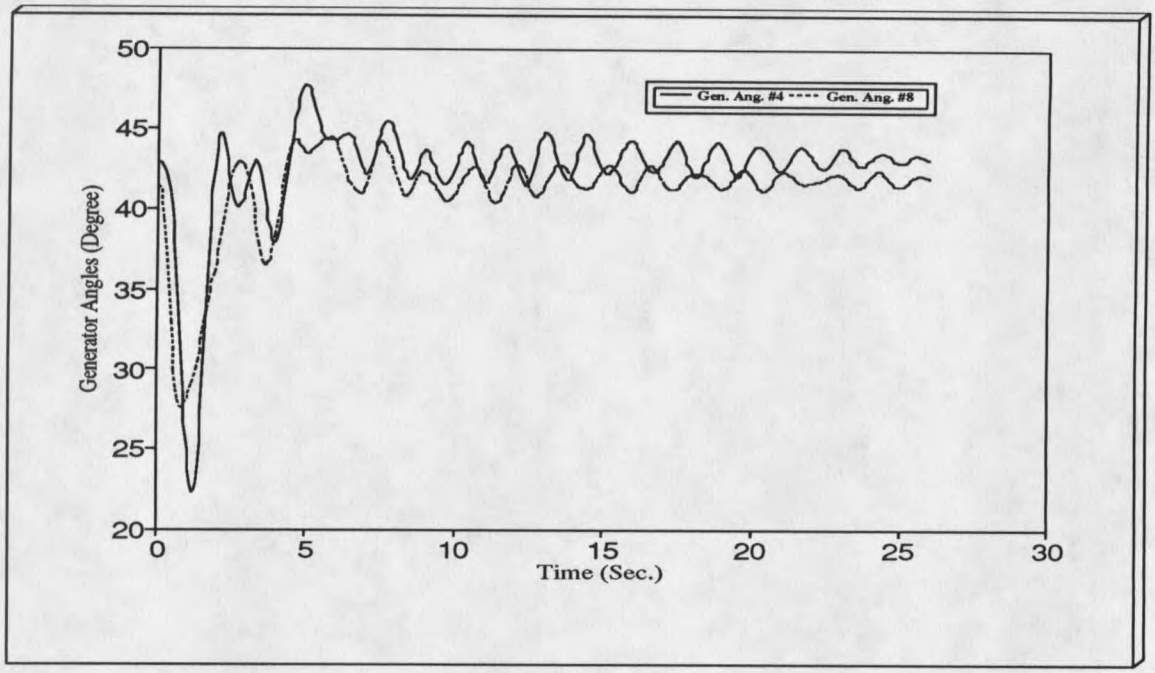

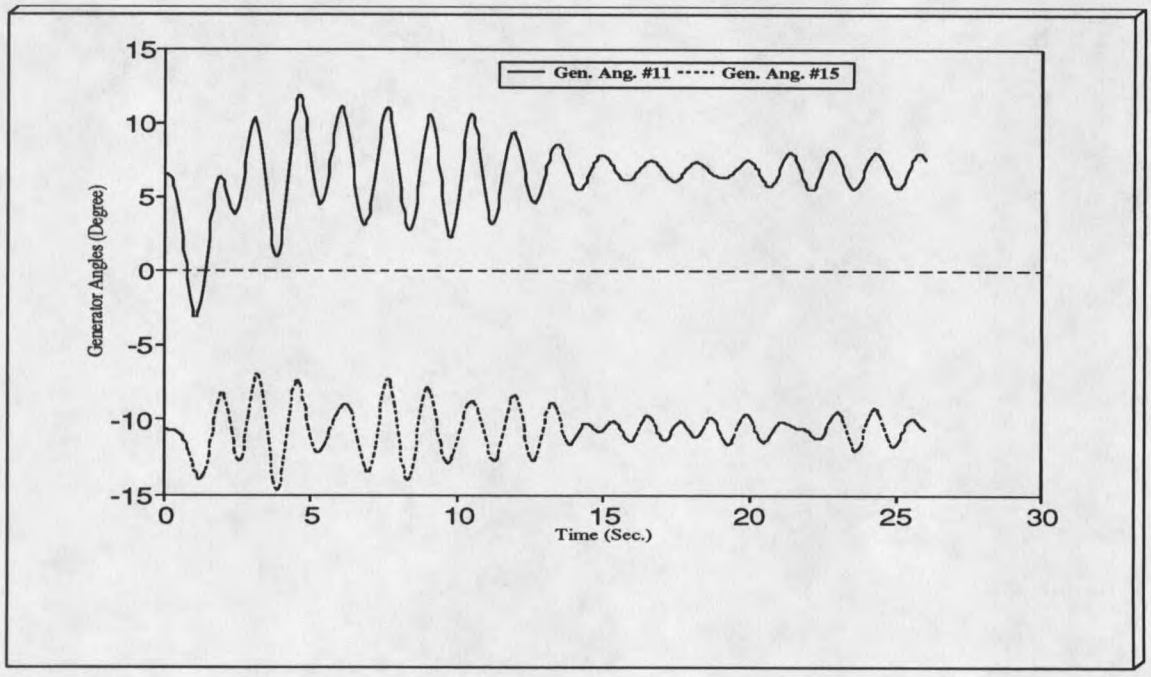

Figure 41. Relative generator angles for fault 1 (machines #4, #8, #11, and #15) with reactive power control.

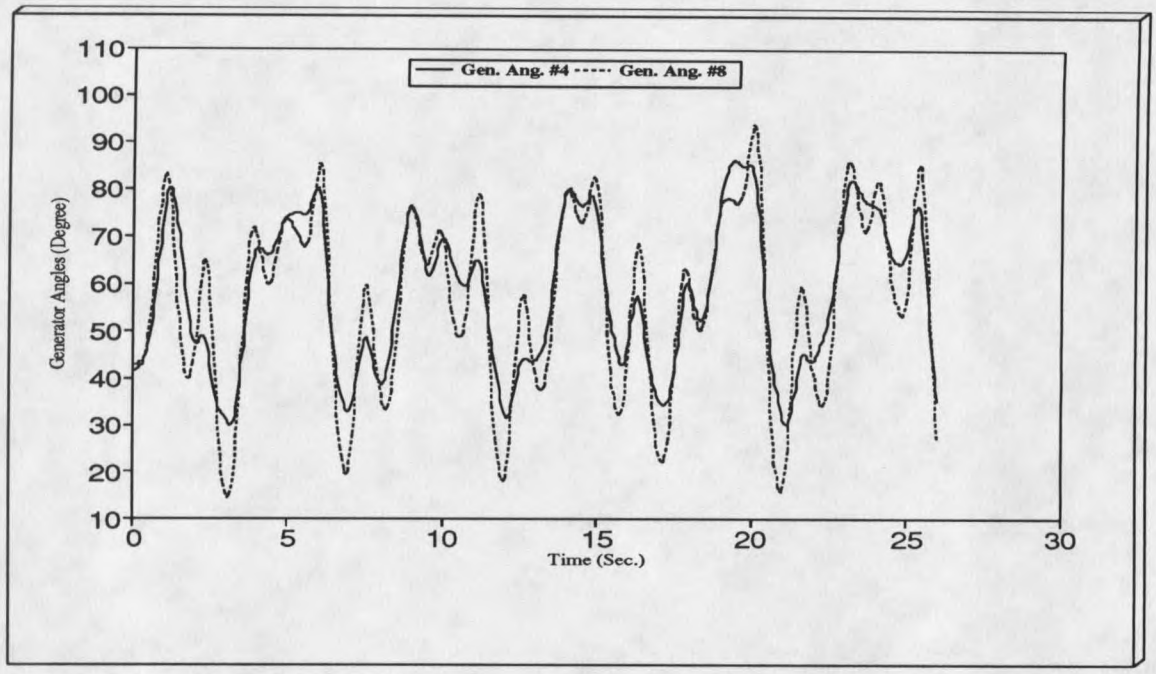

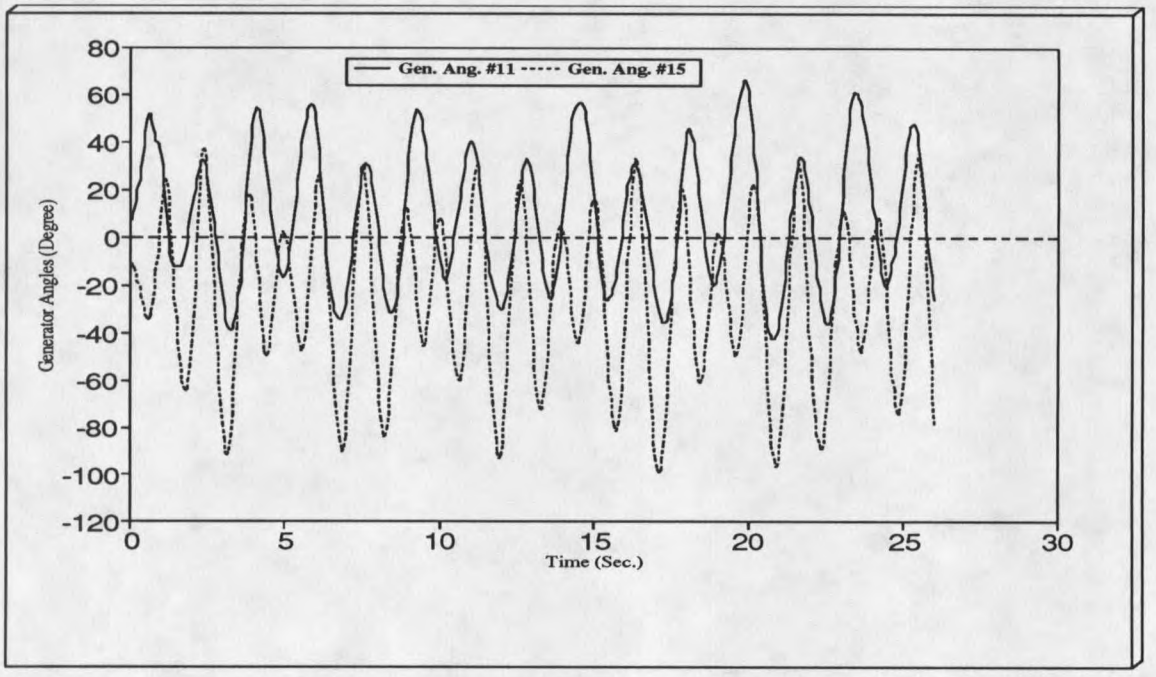

Figure 42. Relative generator angles for fault 2 (machines #4, #8, #11, and #15) with conventional current margin control.

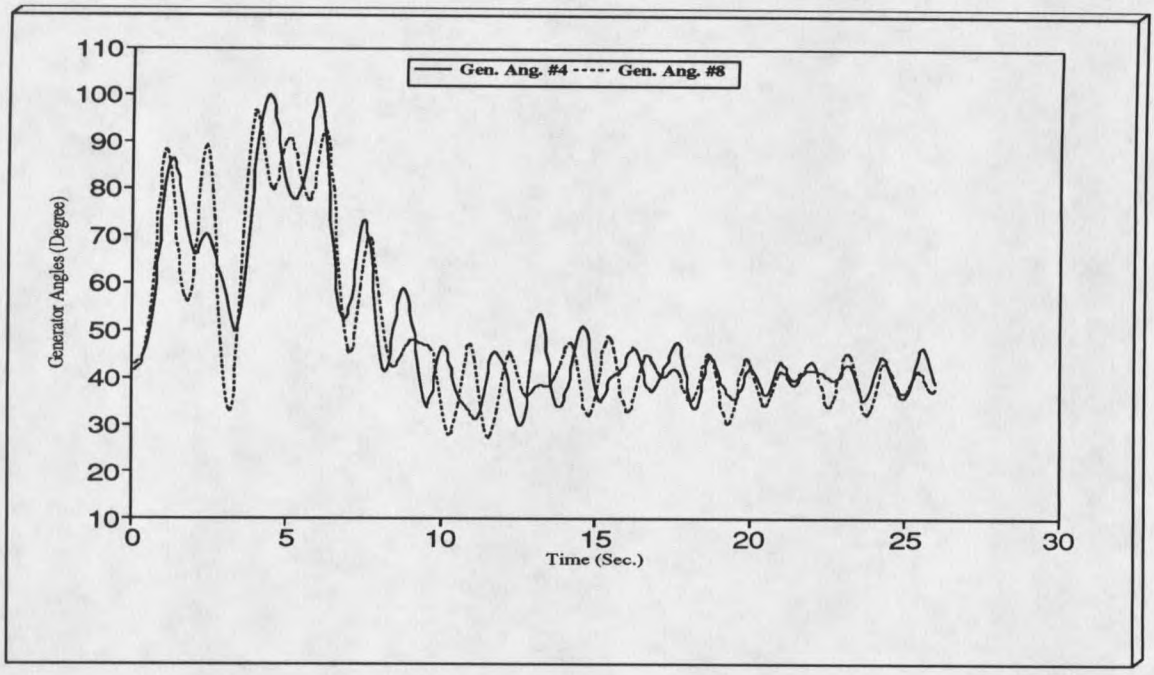

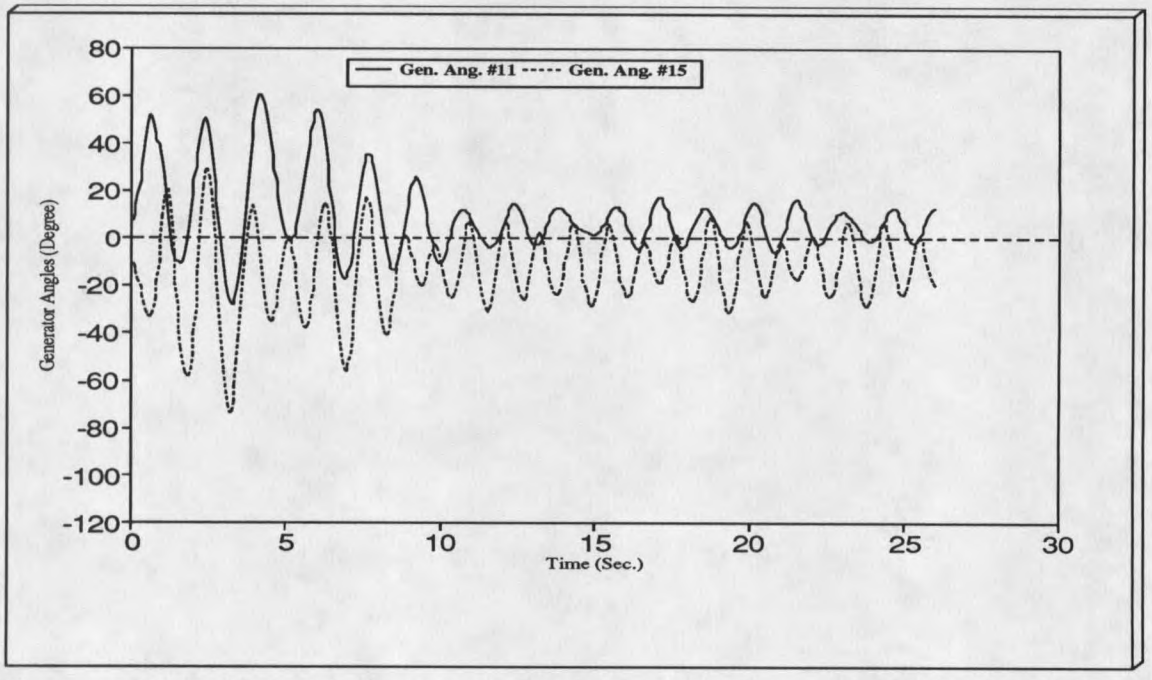

Figure 43. Relative generator angles for fault 2 (machines #4, #8, #11, and #15) with ac voltage control.

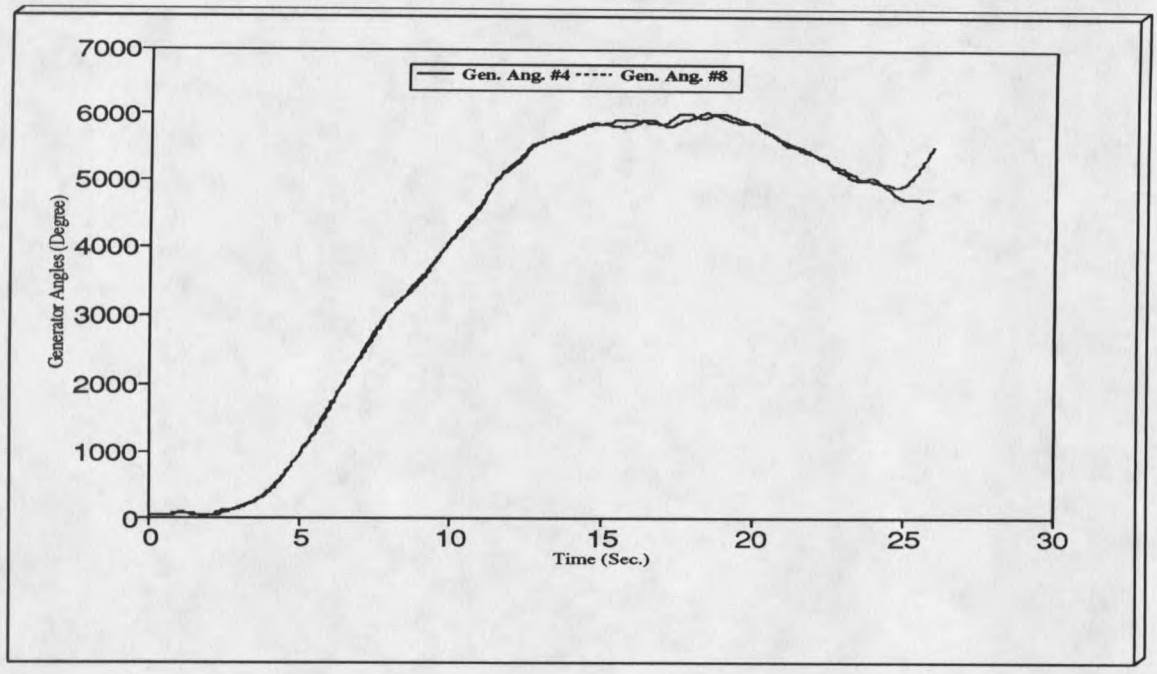

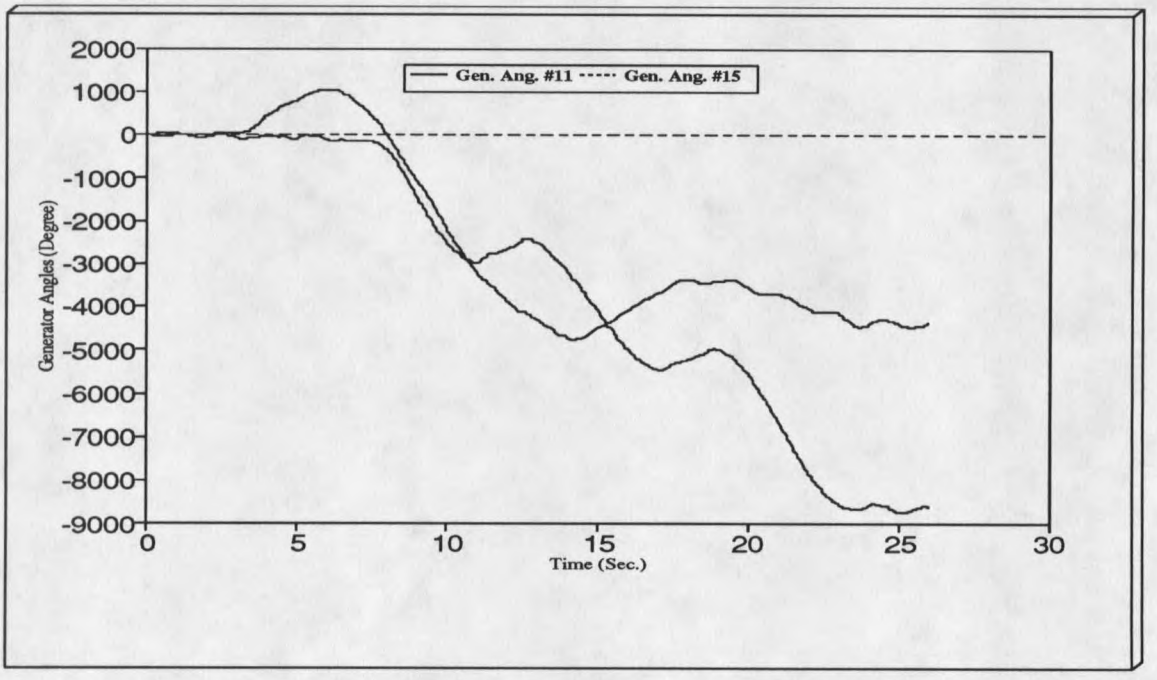

Figure 44. Relative generator angles for fault 2 (machines #4, #8, #11, and #15) with dc voltage control.

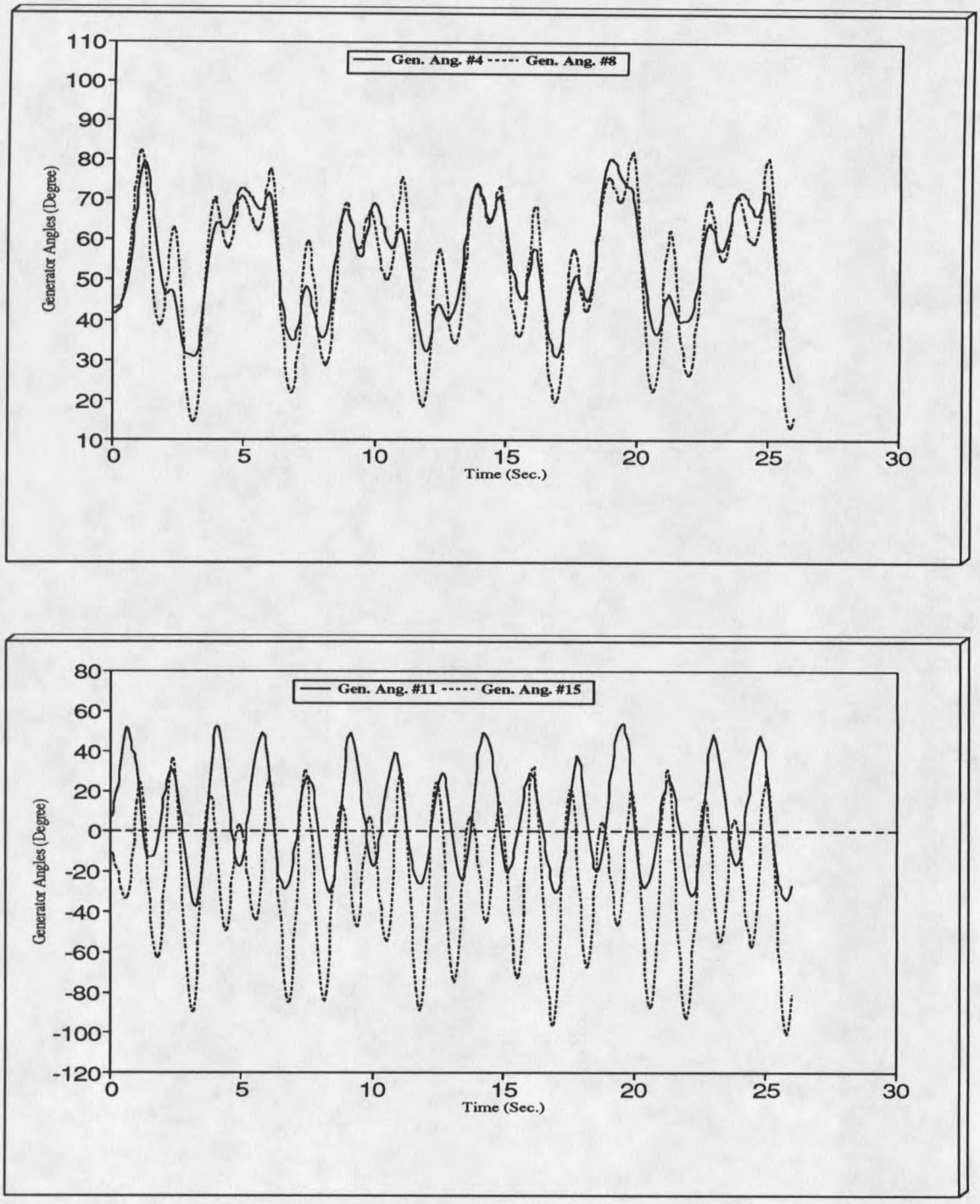

Figure 45. Relative generator angles for fault 2 (machines #4, #8, #11, and #15) with reactive current control.

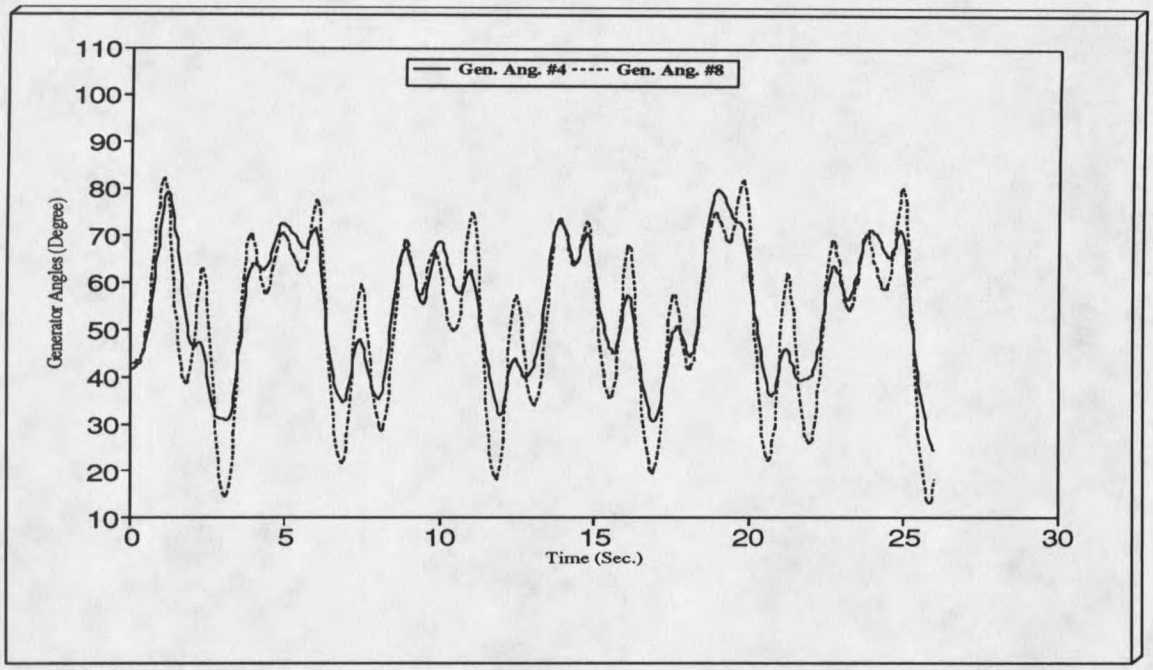

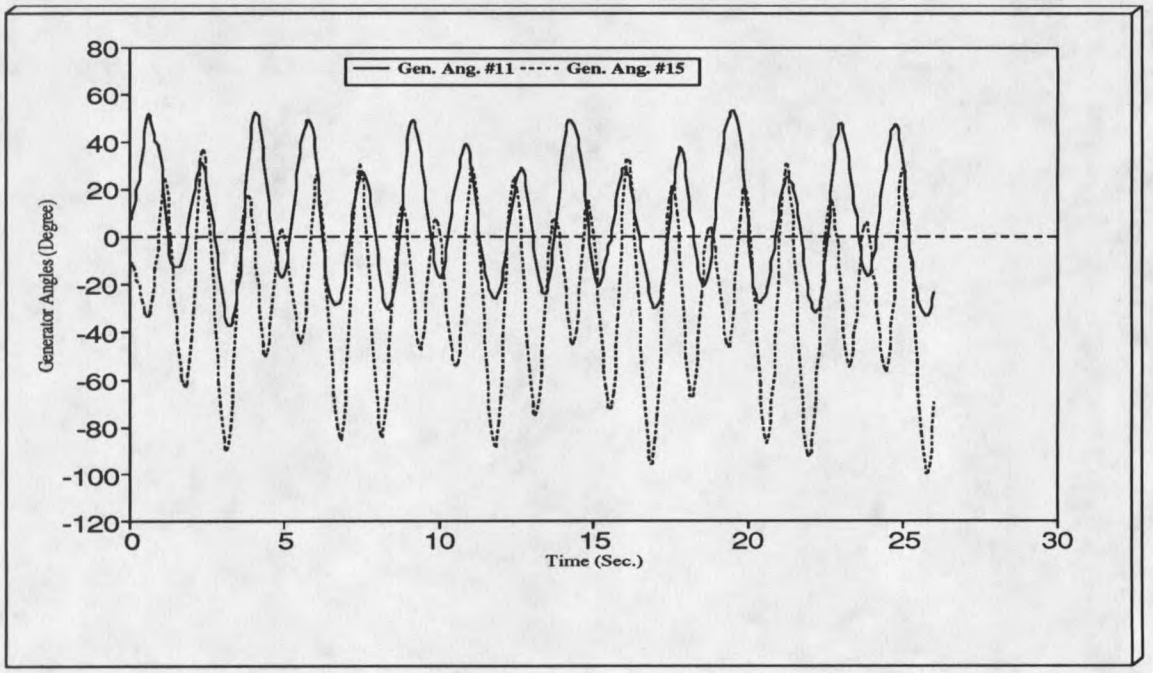

Figure 46. Relative generator angles for fault 2 (machines #4, #8, #11, and #15) with power factor control.

CHAPTER 6

APPLICATION OF PRONY-BASED ANALYSIS FOR EVALUATION OF SMALL SIGNAL MODULATION SCHEMES

Introduction

In the small signal modulation scheme an input signal from the ac side such as power flow, voltage magnitude, voltage angle or frequency is used to modulate the power flow through the dc line. Many studies have also used frequency differences between two interconnected ac systems as the basis for modulation of a dc intertie and have shown that a very powerful damping can be achieved with this type of modulation [45]. However, use of frequency difference as the modulation signal for a system which has a long dc intertie poses a serious problem. It would involve telemetry of the receiving end frequency over a long communication channel which would create a reliability problem and would require equipment coordination between the areas. Also, the frequency signal at any end which is required for obtaining the frequency difference is an inherently noisy signal containing strong high frequency local swing modes (1-2 Hz) in addition to the interarea modes (less than 1 Hz). However, frequency difference does eliminate the common frequencies.

An alternative to using frequency difference would be to use frequency from the rectifier end only which would eliminate the need for a long communication link. However, as already mentioned, this signal would contain the local swing modes in addition to the interarea frequency modes. Other signals which could be used are rate of change of power or current at one end. It has been shown that under certain simplifying assumptions, both of these signals contain information about frequency differences between the areas, and hence a single measurement would be sufficient [45]. However, near the steady state stability limit, changes in ac power are insensitive to changes in the relative angle between the areas and as a result, the time derivative of ac power is not a good indicator of frequency difference. The current on the other hand is strongly related to the relative angle between the areas even at the steady state stability limit. With the advent of new phase measurement techniques it is now possible to use voltage angle as a modulating signal.

In the following sections, a Prony signal analysis algorithm is used to obtain system transfer functions for the ac/dc test system studied for various modulating signals. Responses of the linearized models obtained are then used in root-locus studies to show how the feedback of these signals affects system eigenvalues.

Application

In this section a reduced-order linear model of the ac/dc system is obtained for various modulation signals by applying Prony signal analysis. The primary objective is to select an appropriate ac signal for small-signal modulation of the dc power at the rectifier end in order to dampen the interarea modes, and if possible some of the local modes. The signals considered are change of frequency, voltage angle, rate of change of current, and rate of change of power at an ac bus (NW1 in Figure 1 of Chapter 2) which constitutes a main area near the rectifier end.

As in the case of the nonconventional control schemes of Chapter 4, a system transfer function is first identified for each of the above mentioned signals using the method described in [7]. The test system used is the 42-bus, 17-machine system described in Chapter 2 with the Pacific hvdc intertie represented by a two-terminal, bipolar ±500 Kv dc line model and the Intermountain intertie by equivalent real and reactive constant current loads at their respective terminal buses. The rectifier and inverter are provided with proportional-plus-integral type of constant current controller. In addition, the inverter is also provided with a constant extinction angle (CEA) control. During normal operation the rectifier and inverter current controllers are coordinated to give constant

current control at the rectifier and constant extinction angle control at the inverter. This coordination is achieved by providing the inverter with slightly lower current order than the rectifier, the difference between the two current order being the current margin. The pulse input of Figure 22 (Chapter 4) is applied at the current summing junction of the PI current controller at the rectifier as shown in Figure 47. The input is chosen to be a rectangular current pulse with duration of 1 s and with a magnitude of 30 A, equal to 1% of the rated 3000 A dc line current. The limit of 1% is chosen in order not to overexcite the system. The parameters used for the input signal I(t) to obtain the Prony model are

$$k=1,\quad c_0=30,\quad c_1=-30,\quad D_1=1\quad \text{and}\quad \lambda_{n+1}=0 \tag{6.1}$$

The poles and zeros of the transfer function for each of the outputs are given in Tables 9 through 12. The pulse input of Figure 22 (Chapter 4) is also applied to the transfer functions. The responses of the Prony based transfer-function models were compared with those of the actual simulated system as shown in Figures 48 through 51. It is clear from these figures that the Prony fit matches very closely with the actual response except during the application of the input pulse. The root-locus plots for the modulating signals used are given in Figures 52 through 55. From these figures it is clear that frequency deviation and ac bus voltage angle signal should

provide good modulating signals. This is evident from the root-locus plot, as most of the poles move toward the left when the feedback gain is increased, hence enhancing damping. However, in the case of voltage angle signal one of the eigenvalue is on the positive real axis (Table 10 and Figure 53). Since this eigenvalue is very close to the origin it is assumed that it is the pole contributed by the PI current controller at the rectifier end.

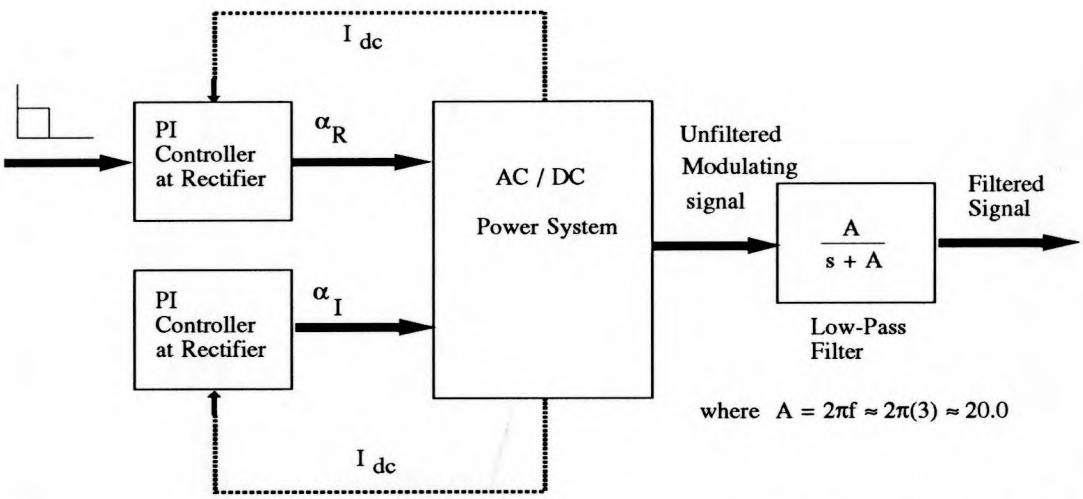

Figure 47. Implementation of a general modulation control scheme for Prony based analysis.

Table 9. Identified reduced-order transfer-function model for frequency deviation as output signal.

Mode	Freq. (Hz)	Eigenvalue	Residue
1	0.37	-0.3458d+00±j0.2333d+01	+0.2495d-03±j0.1104d-03
2	0.71	-0.1153d+00±j0.4467d+01	+0.1922d-03±j0.1573d-04
3	0.05	-0.4800d+00±j0.3237d+00	+0.1617d-03±j0.2733d-03
4	0.86	-0.9045d-01±j0.5418d+01	-0.3964d-04±j0.5660d-04
5	1.38	-0.4866d+00±j0.8686d+01	-0.5432d-05±j0.3246d-04
6	1.64	-0.2321d+00±j0.1032d-02	-0.8841d-05±j0.6942d-05
-	-	-0.2689d+02+j0.0000d+00	-0.3406d-01+j0.1522d-17

Table 10. Identified reduced-order transfer-function model for voltage angle as output signal.

Mode	Freq. (Hz)	Eigenvalue	Residue
1	0.08	-0.4095d+00±j0.5014d+00	+0.8502d-02±j0.8383d-01
2	0.37	-0.3562d+00±j0.2342d+01	+0.2084d-02±j0.3911d-01
3	0.71	-0.8654d-01±j0.4459d+01	+0.1273d-01±j0.1823d-02
4	0.86	-0.1324d+00±j0.5400d+01	-0.3362d-02±j0.4888d-02
5	1.19	-0.2720d+01±j0.7480d+01	+0.8550d-03±j0.6608d-02
6	1.66	-0.1503d-01±j0.1040d+02	-0.2511d-03±j0.6731d-04
7	1.43	-0.2484d+00±j0.8998d+01	-0.3164d-03±j0.6731d-03
-	-	+0.4541d-01+j0.0000d+00	+0.4641d-01-j0.2082d-16

Table 11. Identified reduced-order transfer-function model for rate of change of current as output signal.

Mode	Freq. (Hz)	Eigenvalue	Residue
1	0.37	-0.3209d+00±j0.2339d+01	-0.1911d+00±j0.1396d+00
2	0.71	-0.6277d-01±j0.4473d+01	-0.1017d-01±j0.1082d+00
3	0.91	-0.1004d+00±j0.5737d+01	-0.2762d-03±j0.2863d+00
4	1.72	-0.8308d+00±j0.1078d-02	-0.1783d-01±j0.1200d-02
5	2.00	-0.7579d+00±j0.1252d+02	-0.1004d-01±j0.1183d-01
6	2.40	-0.2223d+00±j0.1502d+02	+0.3001d-02±j0.8128d-03
7	1.45	-0.5958d+00±j0.9085d+01	+0.6475d-02±j0.6978d-02
-	-	-0.8539d+00+j0.0000d+00	+0.4013d+00-j0.9037d-12
-	-	-0.5064d+00+j0.0000d+00	-0.2191d+00+j0.4010d-12

Table 12. Identified reduced-order transfer-function model for rate of change of power as output signal.

Mode	Freq. (Hz)	Eigenvalue	Residue
1	0.71	-0.5166d-01±j0.4463d+01	-0.1339d+01±j0.1813d+02
2	0.37	-0.3269d+00±j0.2338d+01	-0.1164d+02±j0.8035d-01
3	0.90	-0.1716d+00±j0.5676d+01	-0.4256d+01±j0.2952d+02
4	0.89	-0.1701d+01±j0.5616d+01	-0.3565d+01±j0.2072d+02
5	2.47	-0.5222d+01±j0.1554d+02	+0.1211d+02±j0.2226d+02
6	1.45	-0.2389d+00±j0.9123d+01	+0.1142d+01±j0.1209d+00
7	2.34	-0.8999d+00±j0.1470d+02	+0.1189d+00±j0.1696d+01
8	1.81	-0.2518d+00±j0.1138d+02	-0.5806d-01±j0.7343d+00
-	-	-0.2071d+00+j0.0000d+00	+0.1231d+00-j0.2634d-11

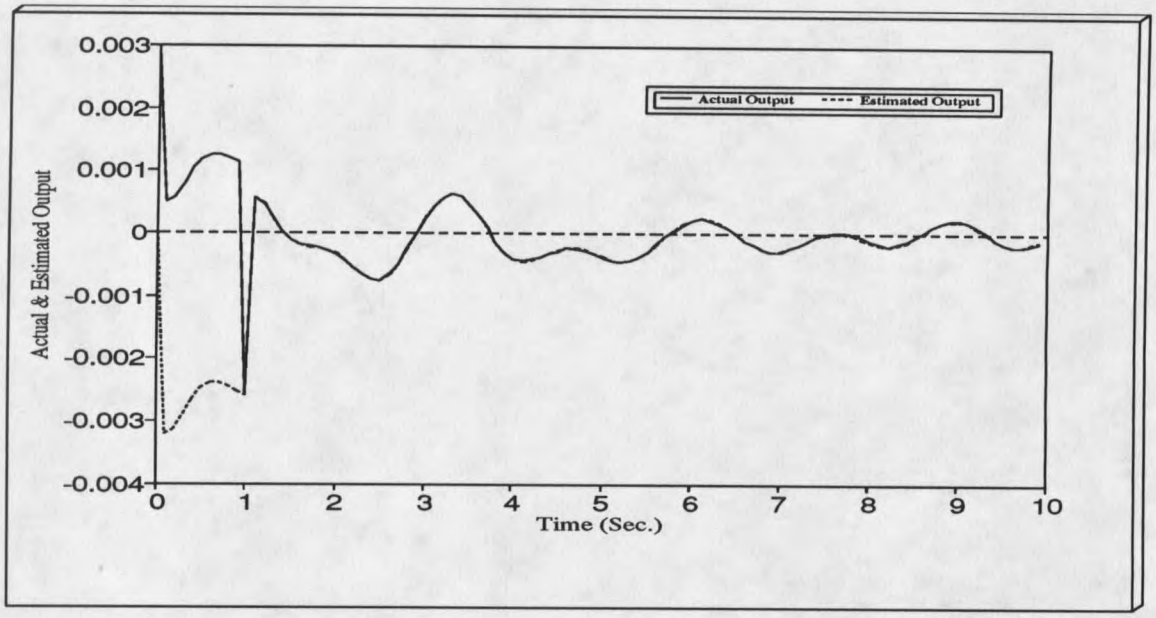

Figure 48. Transfer-function model output data versus actual data for frequency deviation signal.

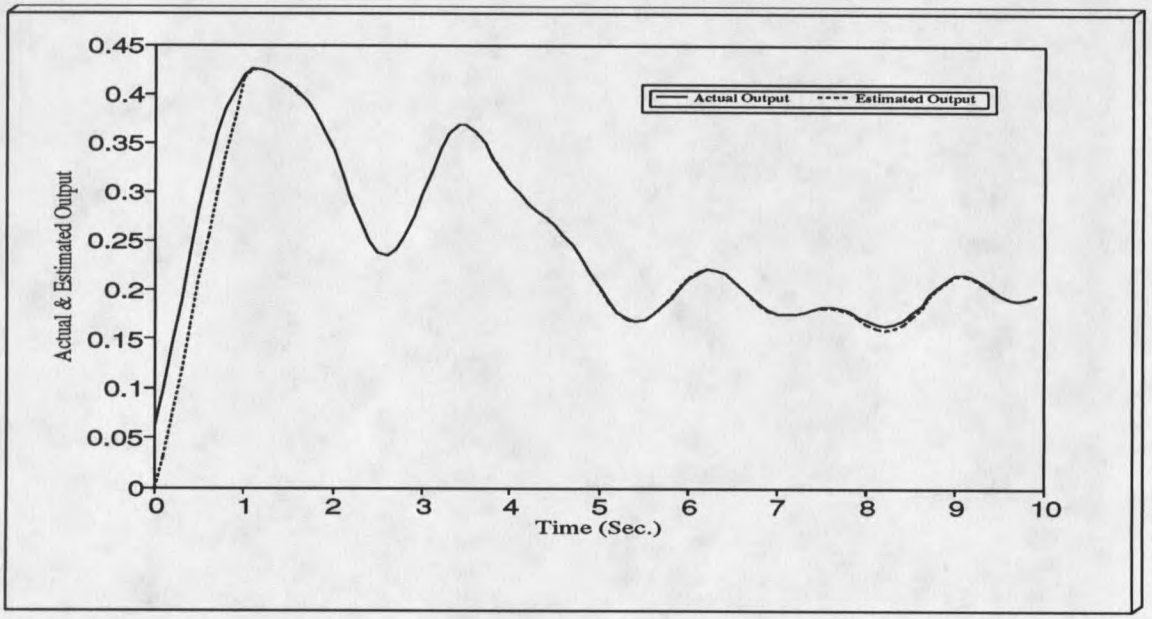

Figure 49. Transfer-function model output data versus actual data for voltage angle signal.

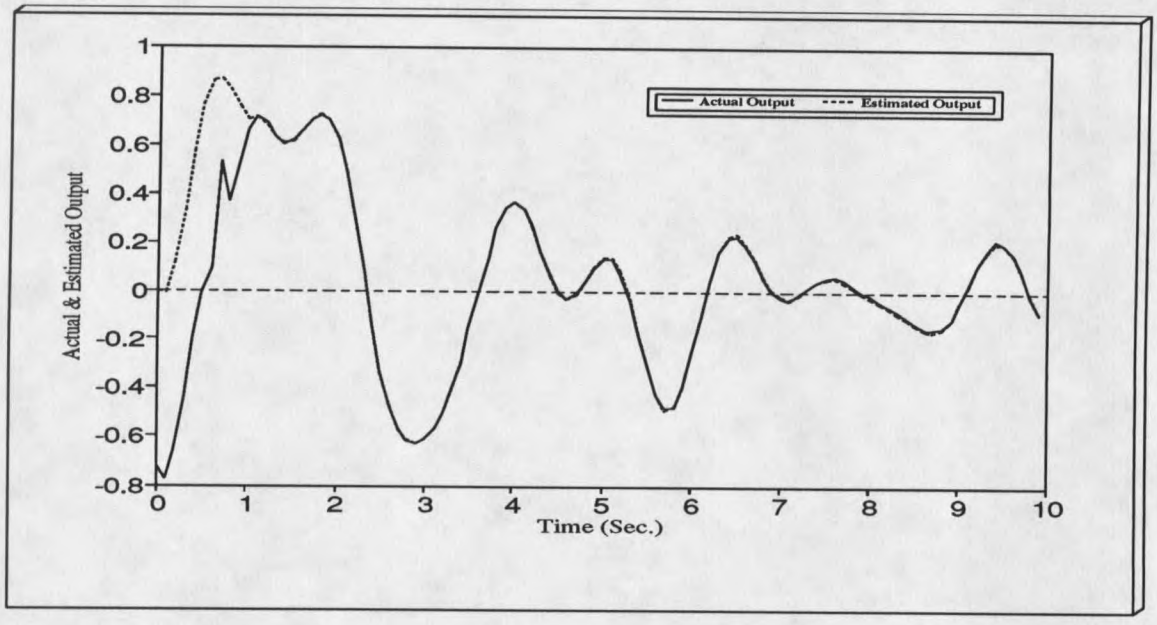

Figure 50. Transfer-function model output data versus actual data for rate of change of current signal.

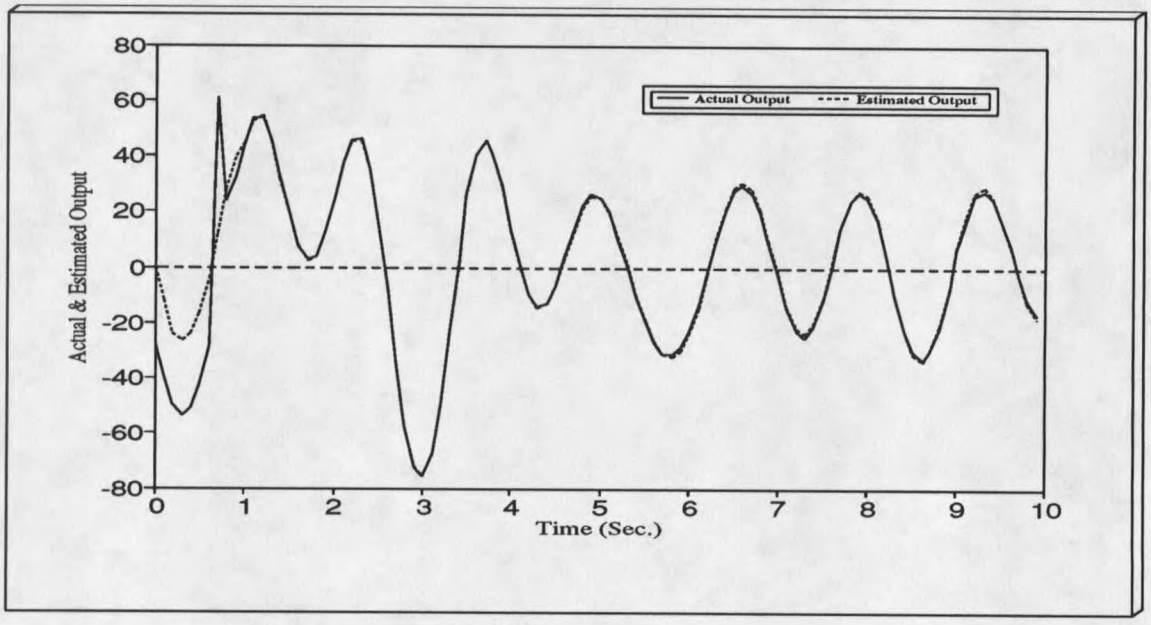

Figure 51. Transfer-function model output data versus actual data for rate of change of power signal.

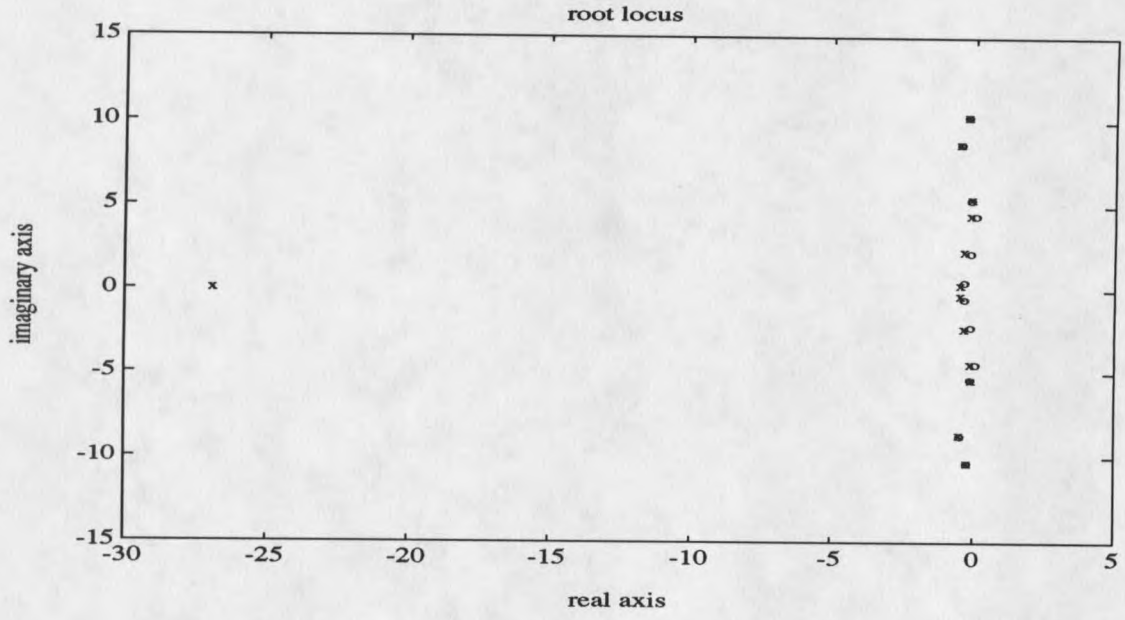

Overall root locus

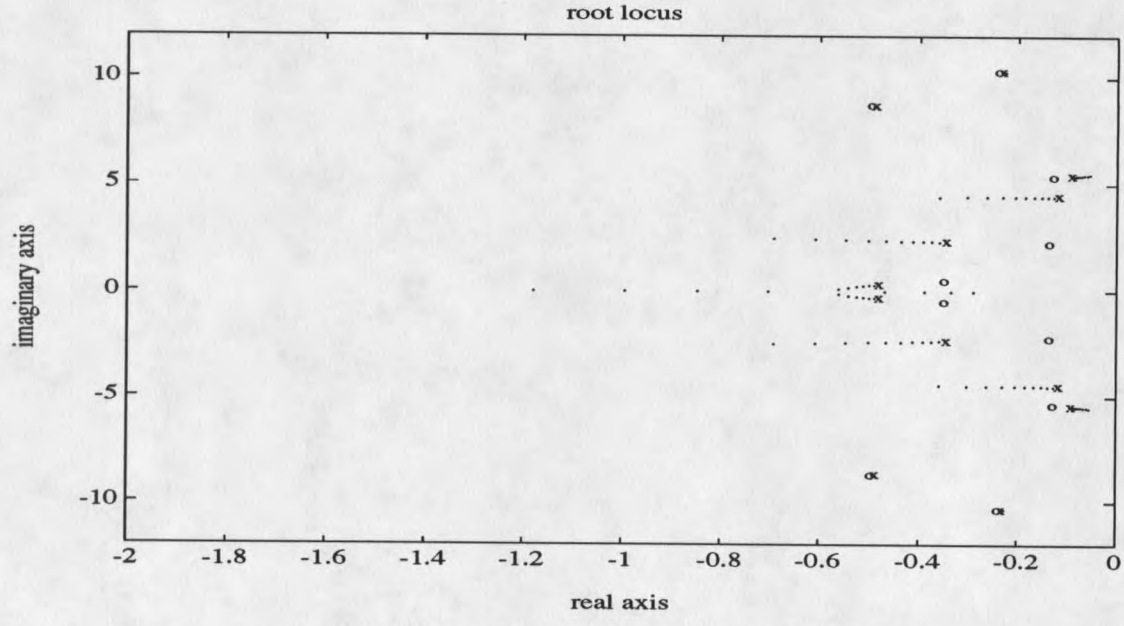

Portion of interest expanded

Figure 52. Root-locus plot for frequency deviation signal.

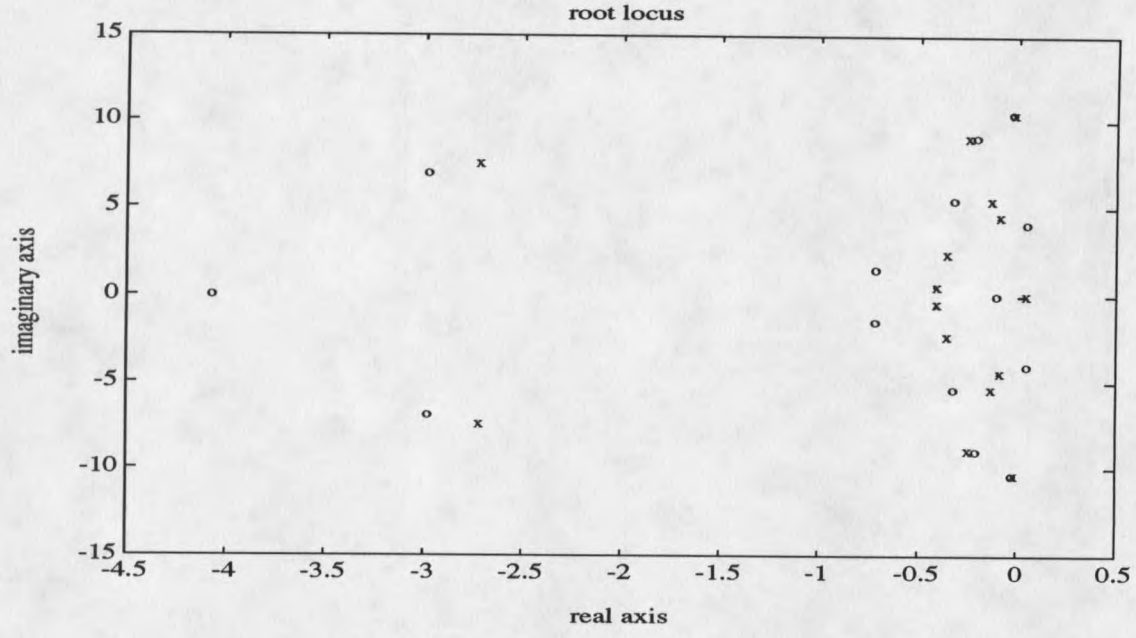

Overall root locus

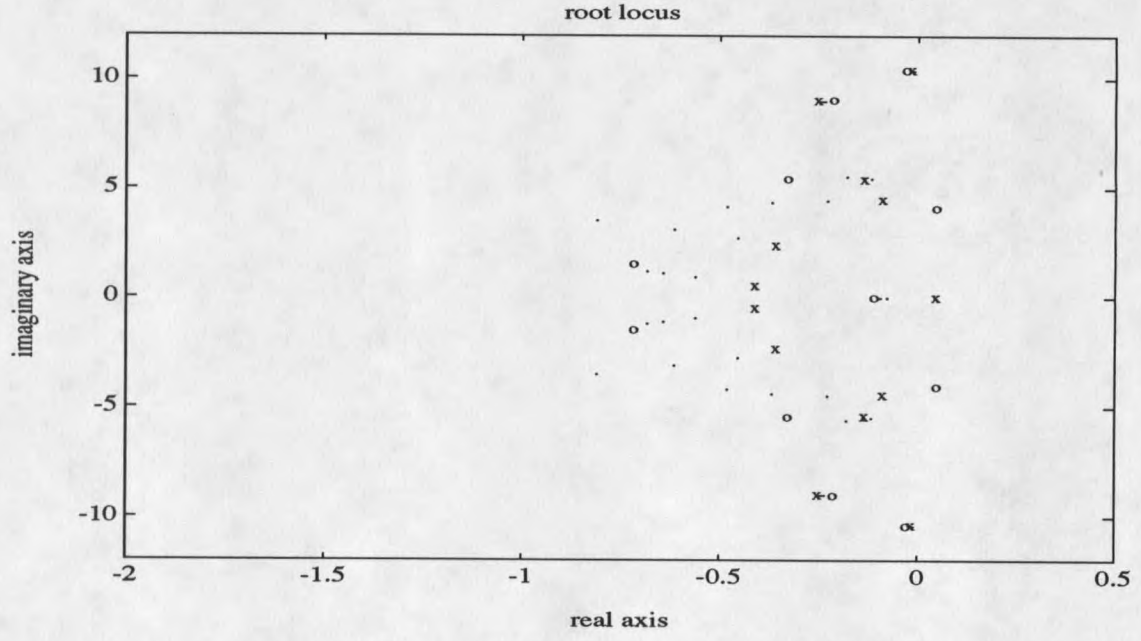

Portion of interest expanded

Figure 53. Root-locus plot for voltage angle signal.

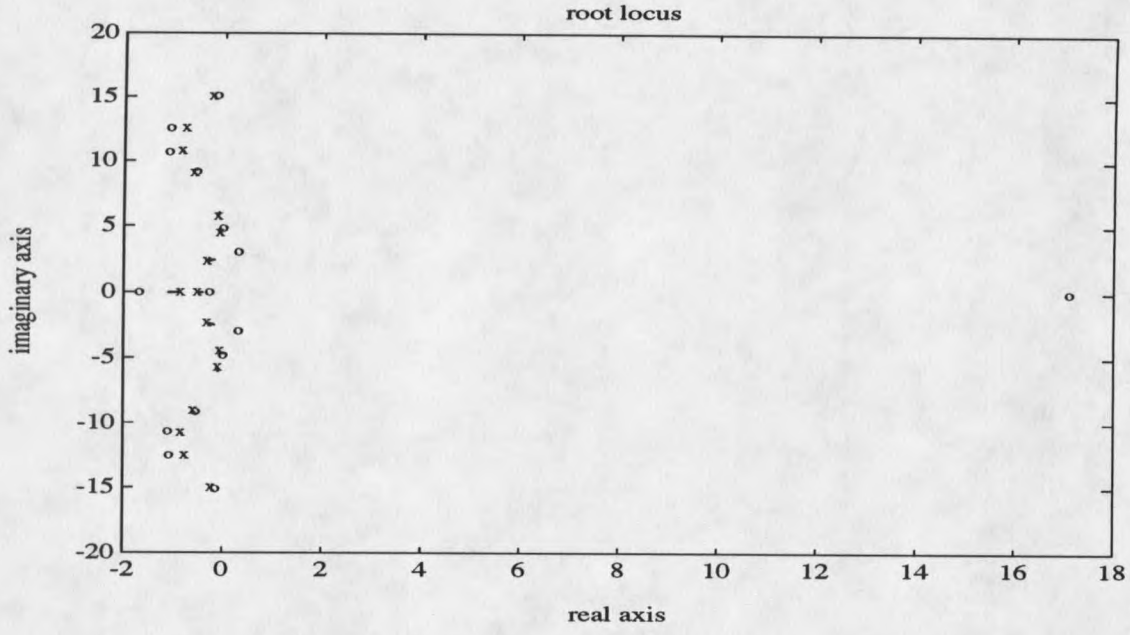

Overall root locus

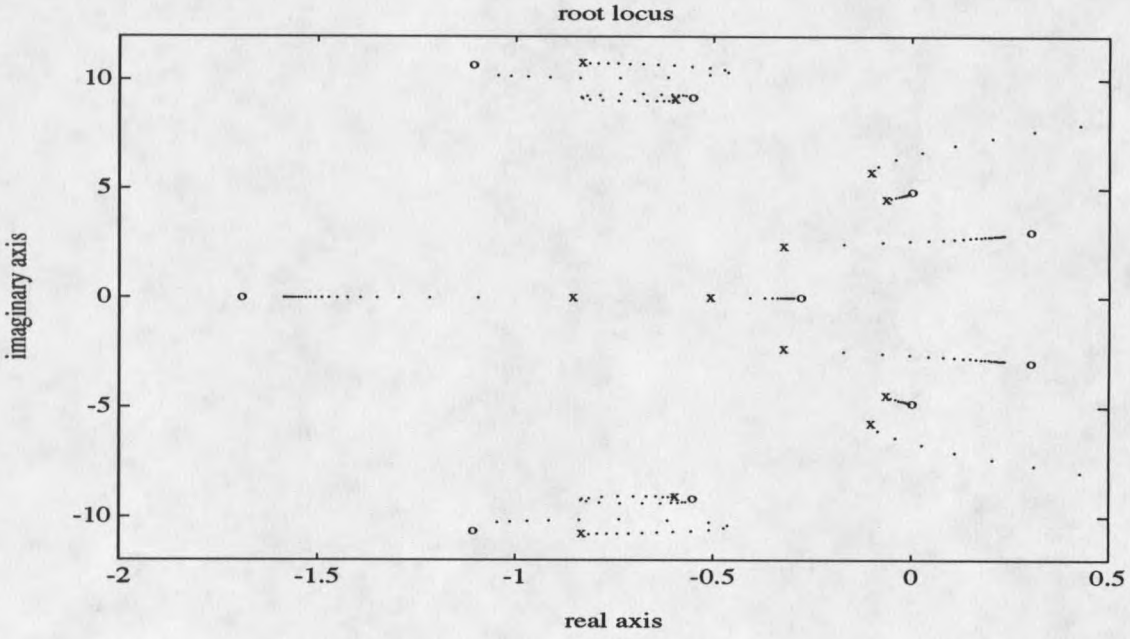

Portion of interest expanded

Figure 54. Root-locus plot for rate of change of current.

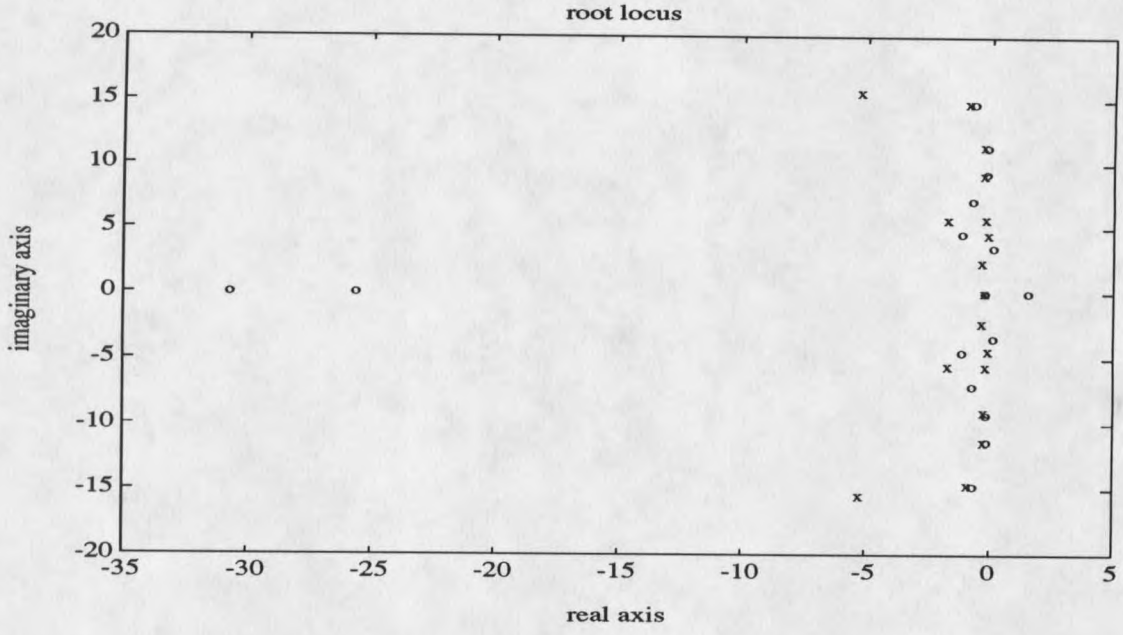

Overall root locus

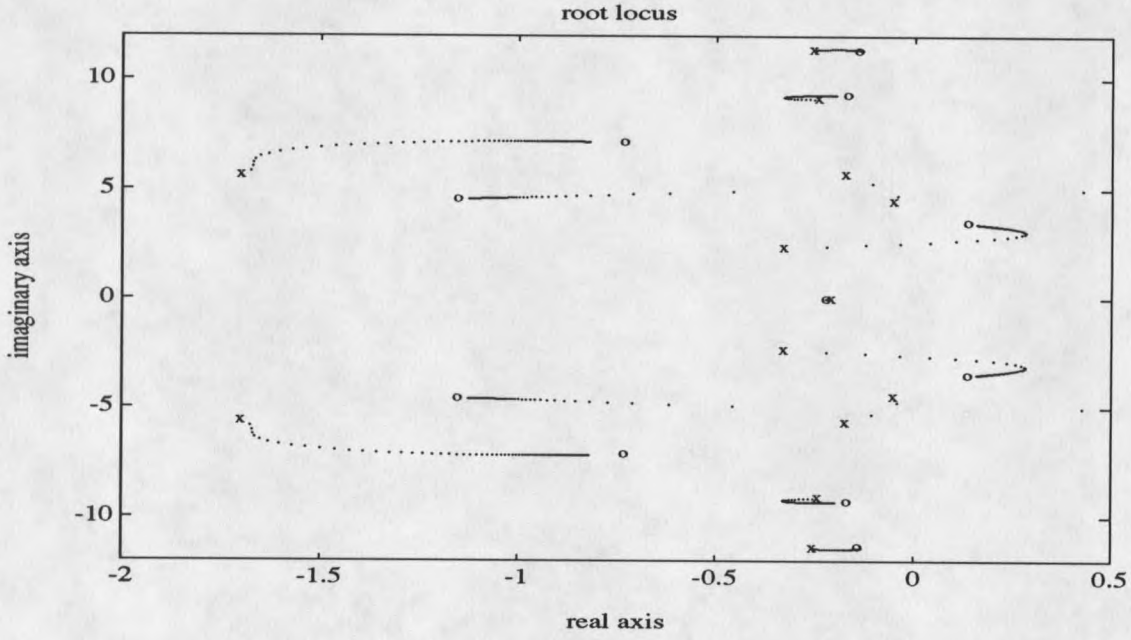

Portion of interest expanded

Figure 55. Root-locus plot for rate of change of real power.

CHAPTER 7

SYSTEM IDENTIFICATION USING MODIFIED PRONY ANALYSIS

Introduction

Prony signal analysis is an off-line identification technique to determine modal, damping, phase, and magnitude information of a signal. A standard Prony signal analysis method is described in [56]. This standard Prony signal analysis method does not use knowledge of the system input and therefore is not a system identification technique. If the input to a system is restricted to be of a certain class and knowledge of the input is used in a particular way [7] along with Prony analysis of the output signal, then a system model can be obtained. However, in [7] it is assumed that the model of the system does not contain a feedforward or throughput term; i.e., the identified model is a strictly proper transfer function where the order of the numerator is strictly less than that of the denominator. This chapter describes a generalization of the method in [7] to include a feedforward or throughput term.

Modified Prony Analysis

Figure 56 shows a block diagram of a general linear system with input u(t), output y(t), and unit impulse response g(t).

In the same figure w(t) represents any non-zero initial conditions present in the system. For the sake of simplicity in this analysis it is assumed that the system has zero initial conditions.

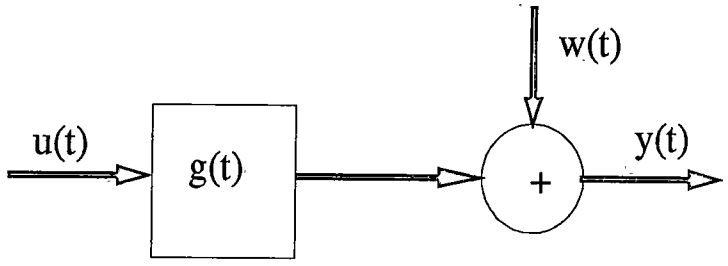

Figure 56. System model with initial conditions.

The objective is to use sampled values of u(t) and y(t) to obtain an estimate of G(s), the Laplace transform of g(t). G(s) is assumed to be of the form

$$G(s) = e^{-sD'}\left\{R_o + \sum_{i=1}^{n}\frac{R_i}{s-\lambda_i}\right\} \tag{7.1}$$

where $D' \in \Re$ is a known system time delay $R_o \in \Re$ is the feedforward or throughput term, $R_i \in C$ is the transfer function residue associated with the ith eigenvalue λ_i, and n is the order of the model. λ_i's are assumed to be distinct. As in [7], the input is restricted to be of the form

$$U(s) = \sum_{j=0}^{q} c_j \frac{e^{-sD_j} - e^{-sD_{j+1}}}{s - \lambda_{n+1}} \tag{7.2}$$

where $U(s)$ is the Laplace transform of $u(t)$, c_i's are arbitrary real constants, $D_j < D_{j+1}$ represent instants in time where u(t) is discontinuous, and $\lambda_{n+1} \neq \lambda_i$, $i = 1,2,\ldots,n$. Without loss of generality $D_o \equiv 0$. The transform $\hat{Y}(s)$ of the identified system model output is

$$\hat{Y}(s) = U(s)G(s) + W(s) \tag{7.3}$$

Substituting $W(s) = 0$ and expressions for $G(s)$ and $U(s)$ from (7.1) and (7.2), respectively, it follows that

$$\hat{Y}(s) = \sum_{j=0}^{q} c_j \frac{(e^{-sD_j} - e^{-sD_{j+1}})}{(s-\lambda_{n+1})} e^{-sD'} \left\{ R_o + \sum_{i=1}^{n} \frac{R_i}{(s-\lambda_i)} \right\} \tag{7.4}$$

Using partial fraction expansion,

$$\hat{Y}(s) = \sum_{j=0}^{q} c_j \left(e^{-sD_j} - e^{-sD_{j+1}}\right) e^{-sD'} \left\{ \frac{Q_{n+1}}{(s-\lambda_{n+1})} + \sum_{i=1}^{n} \frac{Q_i}{(s-\lambda_i)} \right\} \tag{7.5}$$

where

$$Q_i \equiv \frac{R_i}{\lambda_i - \lambda_{n+1}} \; ; \quad i = 1,2,\ldots,n \tag{7.6a}$$

and

$$Q_{n+1} \equiv -\sum_{i=1}^{n} Q_i + R_o \tag{7.6b}$$

Rearranging equation (7.5)

$$\hat{Y}(s) = \sum_{j=0}^{q} c_j \left(\sum_{i=1}^{n} Q_i \frac{(e^{-s(D_j+D')} - e^{-s(D_{j+1}+D')})}{(s-\lambda_i)} \right) + Q_{n+1} e^{-sD'} U(s) \tag{7.7}$$

Taking inverse Laplace transform of (7.7)

$$\hat{y}(t) = \sum_{j=0}^{q} c_j \Big(\sum_{i=1}^{n} Q_i \Big\{ e^{\lambda_i (t - D_j - D')} \mu(t - D_j - D') - e^{\lambda_i (t - D_{j+1} - D')} \mu(t - D_{j+1} - D') \Big\} + Q_{n+1} u(t - D') \Big) \tag{7.8}$$

where $\mu(.)$ denotes the unit step function and $u(.)$ is the input applied to the system. For $t \geq D_{q+1} + D'$ output $\hat{y}(t)$ in (7.8) can be written as

$$\hat{y}(t) = \sum_{i=1}^{n} e^{-\lambda_i D'} Q_i \sum_{j=0}^{q} c_j \Big(e^{-\lambda_i D_j} - e^{-\lambda_i D_{j+1}} \Big) e^{\lambda_i t} \tag{7.9}$$

because, for $t \geq D_{q+1} + D'$,

$$\begin{aligned} &\mu(t - D_j - D') = 1; \\ &\mu(t - D_{j+1} - D') = 1; \quad \text{and} \\ &u(t - D') = 0 \end{aligned} \tag{7.10}$$

Let $\tau = t - D_{q+1} - D'$ and define

$$\hat{v}(\tau) \overset{\Delta}{=} \hat{y}(\tau + D_{q+1} + D') \tag{7.11}$$

Substituting $t - D' = \tau + D_{q+1}$ in equation (7.9)

$$\hat{v}(\tau) = \sum_{i=1}^{n} Q_i \sum_{j=0}^{q} c_j \Big(e^{\lambda_i (D_{q+1} - D_j)} - e^{\lambda_i (D_{q+1} - D_{j+1})} \Big) e^{\lambda_i \tau} \tag{7.12}$$

which can also be written as

$$\hat{v}(\tau) = \sum_{i=1}^{n} B_i e^{\lambda_i \tau} \quad , \quad \tau \geq 0 \tag{7.13}$$

where

$$B_i = Q_i \sum_{j=0}^{q} c_j \Big(e^{\lambda_i (D_{q+1} - D_j)} - e^{\lambda_i (D_{q+1} - D_{j+1})} \Big) \quad ; \quad i = 1, 2, \ldots, n \tag{7.14}$$

Equation (7.14) is solved for Q_i:

$$Q_i = \frac{B_i}{c_o e^{\lambda_i D_{q+1}} - c_q + \sum_{j=1}^{q} (c_j - c_{j-1}) e^{\lambda_i (D_{q+1} - D_j)}} \quad ; \quad i = 1, 2, \ldots, n \tag{7.15}$$

and the transfer function residues are obtained by combining (7.6) and (7.13) to obtain

$$R_i = \frac{B_i(\lambda_i - \lambda_{n+1})}{c_o e^{\lambda_i D_{q+1}} - c_q + \sum_{j=1}^{q} (c_j - c_{j-1}) e^{\lambda_i (D_{q+1} - D_j)}} \quad ; \quad i = 1, 2, \ldots, n \tag{7.16}$$

The following relationships will be used later to determine R_o. For some specific time interval $D_\eta + D' \le t < D_{\eta+1} + D'$, output $\hat{y}(t)$ in (7.8) can be written as

$$\hat{y}(t) = \sum_{i=1}^{n} Q_i \left\{ \sum_{j=0}^{\eta-1} c_j \left(e^{\lambda_i (t - D_j - D')} - e^{\lambda_i (t - D_{j+1} - D')} \right) + c_\eta e^{\lambda_i (t - D_\eta - D')} \right\} + Q_{n+1} u(t - D') \tag{7.17}$$

which can be simplified to

$$\hat{y}(t) = \sum_{i=1}^{n} B_i' e^{\lambda_i t} + B_{n+1}' e^{\lambda_{n+1} t} \tag{7.18}$$

where

$$B_i' = Q_i \left\{ \sum_{j=0}^{\eta-1} c_j \left(e^{-\lambda_i (D_j + D')} - e^{-\lambda_i (D_{j+1} + D')} \right) + c_\eta e^{-\lambda_i (D_\eta - D')} \right\} \tag{7.19a}$$

and

$$B_{n+1}' = \frac{Q_{n+1} u(t - D')}{e^{\lambda_{n+1} t}} = K' Q_{n+1} \tag{7.19b}$$

As already mentioned Prony analysis is an off-line signal analysis technique that fits a weighted summation of damped modal components in the form

$$\hat{y}(t) = \sum_{i=1}^{n} B_i e^{\lambda_i t} \tag{7.20}$$

to a given signal $y(t)$, where $B_i \in C$ is the signal or output residue associated with the ith eigenvalue $\lambda_i \in C$, and the λ_i's are distinct. The discrete form of $\hat{y}(t)$ is

$$\hat{y}_k \equiv \hat{y}(kT_s) = \sum_{i=1}^{n} B_i z_i^k \quad : \quad k = 0,1,\ldots,N-1 \tag{7.21}$$

where $\hat{y}_k$ is the sampled value of $\hat{y}(t)$, sampled at a sample period (T_s) smaller than the Nyquist period, B_i is the output residue in (7.20), N is the total number of sampled output data, and

$$z_i = e^{\lambda_i T_s} \tag{7.22}$$

which is called a discrete-time eigenvalue. The objective of the Prony analysis is to find the B_i's, λ_i's, and n that result in $\hat{y}_k$ being the best fit to y_k in a least-squares error sense. Assuming $N > 2n$, equation (7.21) can be expanded and equated to y_k resulting in

$$\begin{pmatrix} z_1^o & z_2^o & \cdots & z_n^o \\ z_1^1 & z_2^1 & \cdots & z_n^1 \\ \cdot & \cdot & & \cdot \\ \cdot & \cdot & & \cdot \\ \cdot & \cdot & & \cdot \\ z_1^{N-1} & z_2^{N-1} & \cdots & z_n^{N-1} \end{pmatrix} \begin{pmatrix} B_1 \\ B_2 \\ \cdot \\ \cdot \\ \cdot \\ B_n \end{pmatrix} = \begin{pmatrix} y_o \\ y_1 \\ \cdot \\ \cdot \\ \cdot \\ y_{N-1} \end{pmatrix} \qquad (7.23a)$$

or in a compact form

$$ZB = Y \qquad (7.23b)$$

where $Z \in C^{Nxn}$, $B \in C^n$, and $Y \in \Re^N$. If z_i's are known then the above overdetermined set of equations can be solved using least-squares error technique to obtain the optimal B_i's. Since discrete-time eigenvalues are the roots of the characteristic equation, they can be obtained by solution of following set of over-determined equations [7]

$$\begin{pmatrix} y_o & y_1 & \cdots & y_{n-1} \\ y_1 & y_2 & \cdots & y_n \\ \cdot & \cdot & & \cdot \\ \cdot & \cdot & & \cdot \\ \cdot & \cdot & & \cdot \\ y_{N-n-1} & y_{N-n} & \cdots & y_{N-2} \end{pmatrix} \begin{pmatrix} a_n \\ a_{n-1} \\ \cdot \\ \cdot \\ \cdot \\ a_1 \end{pmatrix} = \begin{pmatrix} y_n \\ y_{n+1} \\ \cdot \\ \cdot \\ \cdot \\ y_{N-1} \end{pmatrix} \qquad (7.24)$$

where a_i's $\in \Re$, $i = 1,2,...,n$ are the coefficients of the characteristic polynomial

$$z_i^n - (a_1 z_i^{n-1} + a_2 z_i^{n-2} + \ldots + a_n) = 0 \;\; ; \;\; i = 1,2,...,n \qquad (7.25)$$

The standard Prony analysis for signal identification involves the following steps: first the optimal least-squares solution of the over-determined set of equations (7.24) is carried out to obtain a_i's; equation (7.25) is then factored to obtain the discrete-time eigenvalues, the z_i's; solution of (7.22) then gives the continuous time eigenvalues λ_i's; and finally the overdetermined set of equations (7.23) is solved to obtain optimal least-squares solution for B_i's.

However to obtain the system transfer function as given in (7.1) the standard Prony signal analysis is used along with the knowledge of the input and some modifications. First a standard Prony analysis is carried out using v_i's, corresponding to $\hat{v}(\tau)$ in (7.13) which is delayed version of the corresponding output $\hat{y}(t)$, to obtain the continuous time eigenvalues λ_i's and the corresponding B_i's. Knowing c_i's, D_i's, and λ_{n+1} from the known applied input, equations (7.15) and (7.16) can then be solved to obtain Q_i's and the transfer function residues R_i's, respectively. The only remaining unknown is R_o which requires knowledge of Q_{n+1} or B_{n+1}'.

The discrete form of the equation (7.18) is

$$\hat{y}_k = \sum_{i=1}^{n} B_i' z_i^k + B_{n+1}' z_{n+1}^k \qquad (7.26)$$

A Prony matrix for the interval $D' \le t < D_1 + D'$ is obtained by expanding equation (7.26) and equating it to $\hat{y}_k$

$$\begin{pmatrix} z_1^o & z_2^o & \cdots & z_n^o & z_{n+1}^o \\ z_1^1 & z_2^1 & \cdots & z_n^1 & z_{n+1}^1 \\ \cdot & \cdot & & \cdot & \cdot \\ \cdot & \cdot & & \cdot & \cdot \\ \cdot & \cdot & & \cdot & \cdot \\ z_1^{m_1-1} & z_2^{m_1-1} & \cdots & z_n^{m_1-1} & z_{n+1}^{m_1-1} \end{pmatrix} \begin{pmatrix} B_1' \\ B_2' \\ \cdot \\ \cdot \\ \cdot \\ B_n' \\ B_{n+1}' \end{pmatrix} = \begin{pmatrix} y_o \\ y_1 \\ \cdot \\ \cdot \\ \cdot \\ y_{m_1-2} \\ y_{m_1-1} \end{pmatrix} \qquad (7.27a)$$

where m_1 is the number of sampled output values during the interval $D' \le t < D_1 + D'$. Similarly the Prony matrix for the interval $D_1 + D' \le t < D_2 + D'$ having m_2 data point is

$$\begin{pmatrix} z_1^{m_1} & z_2^{m_1} & \cdots & z_n^{m_1} & z_{n+1}^{m_1} \\ z_1^{m_1+1} & z_2^{m_1+1} & \cdots & z_n^{m_1+1} & z_{n+1}^{m_1+1} \\ \cdot & \cdot & & \cdot & \cdot \\ \cdot & \cdot & & \cdot & \cdot \\ \cdot & \cdot & & \cdot & \cdot \\ z_1^{m_{12}-1} & z_2^{m_{12}-1} & \cdots & z_n^{m_{12}-1} & z_{n+1}^{m_{12}-1} \end{pmatrix} \begin{pmatrix} B_1'' \\ B_2'' \\ \cdot \\ \cdot \\ \cdot \\ B_n'' \\ B_{n+1}'' \end{pmatrix} = \begin{pmatrix} y_{m_1} \\ y_{m_1+1} \\ \cdot \\ \cdot \\ \cdot \\ y_{m_{12}-2} \\ y_{m_{12}-1} \end{pmatrix} \qquad (7.27b)$$

where $m_{12} = m_1 + m_2$. Similarly for the last input interval $D_q + D' \le t < D_{q+1} + D'$ having m_{q+1} data points the Prony matrix is

$$\begin{pmatrix} z_1^m & z_2^m & \cdots & z_n^m & z_{n+1}^m \\ z_1^{m+1} & z_2^{m+1} & \cdots & z_n^{m+1} & z_{n+1}^{m+1} \\ \cdot & \cdot & & \cdot & \cdot \\ \cdot & \cdot & & \cdot & \cdot \\ \cdot & \cdot & & \cdot & \cdot \\ z_1^{M-1} & z_2^{M-1} & \cdots & z_n^{M-1} & z_{n+1}^{M-1} \end{pmatrix} \begin{pmatrix} B_1''^{\cdots} \\ B_2''^{\cdots} \\ \cdot \\ \cdot \\ \cdot \\ B_n''^{\cdots} \\ B_{n+1}''^{\cdots} \end{pmatrix} = \begin{pmatrix} y_m \\ y_{m+1} \\ \cdot \\ \cdot \\ \cdot \\ y_{M-2} \\ y_{M-1} \end{pmatrix} \qquad (7.27c)$$

where $M = m_1 + m_2 + \ldots + m_{q+1}$. Using the same compact vector form as in (7.23b), (7.27) is expressed as

$$ZB' + Z_{n+1}B_{n+1}' = Y \tag{7.28}$$

Next, the expression for B_{n+1}' of (7.19b) is used in (7.28) to obtain

$$ZB' + Z_{n+1}K'Q_{n+1} = Y \tag{7.29}$$

which can be written as

$$Z_{n+1}'Q_{n+1} = Y' \tag{7.30}$$

where

$$\begin{aligned} Z_{n+1}' &= Z_{n+1}K' \\ Y' &= Y - ZB' \end{aligned} \tag{7.31}$$

Knowing Q_i's from the standard Prony analysis and the knowledge of the input, equation (7.19a) can be solved to obtain B_i'. The only unknown in equation (7.30) is Q_{n+1}. Writing equation (7.30) for each input interval and combining them, an over-determined set of equations can be obtained which can then be solved using the least-squares technique to obtain Q_{n+1}. By substituting values of Q_i and Q_{n+1} in (7.6b), the remaining transfer function residue R_o can be evaluated.

Application

From the results obtained in Chapter 6, where the Prony-based identification technique of [7] is used, it is evident that the estimated output during the application of the input does not match the actual output. This suggests that the system transfer function contains a throughput or feedforward term. Here the modified Prony-based identification technique of this Chapter is used to obtain a proper transfer function for the system. A FORTRAN computer package that implements the modified Prony based identification method has been developed. A listing of the package is given in Appendix A. Only two signals, change of frequency and voltage angle which showed better promise for system damping, are considered here.

A system transfer function for each of the modulation signals is obtained using the above package. The test system used is the same as that described in Chapter 6, as also is the block diagram and the input pulse. The transfer-function responses and the actual responses are shown in Figures 57 and 58. In both cases the linear low-order model output fits the actual system response quite well even during the application of the input signal. Responses of the linearized models obtained are then used in root-locus studies to see how the feedback of these signals affects the system eigenvalues.

Also a simple modulation controller is designed for each of the above modulation signals primarily to add damping to the interarea modes, but at the same time to dampen other local modes if possible. The controller is not allowed to decrease the damping of any electromechanical mode and consists of a simple band-pass compensator to extract the interarea and local electromechanical modes. The compensator for voltage angle signal is characterized by

$$\frac{K(s+0.063)(s+30)}{(s+0.63)(s+12.56)} \tag{7.32}$$

while compensator for frequency deviation is characterized by

$$\frac{Ks(s+500)}{(s+0.3)(s+20.0)} \tag{7.33}$$

and gain K is adjusted to obtain the desired damping. Root-locus plots of the system transfer function with the compensator are used to obtain the feedback gain. The transfer function obtained from the Prony-based analysis of each signal is used as the forward transfer function, and the compensator as the feedback. The compensator time constants are chosen to make the loci move to the left as they departed from their open-loop poles. Figures 59 and 60 show the root-locus plots of the closed-loop feedback systems.

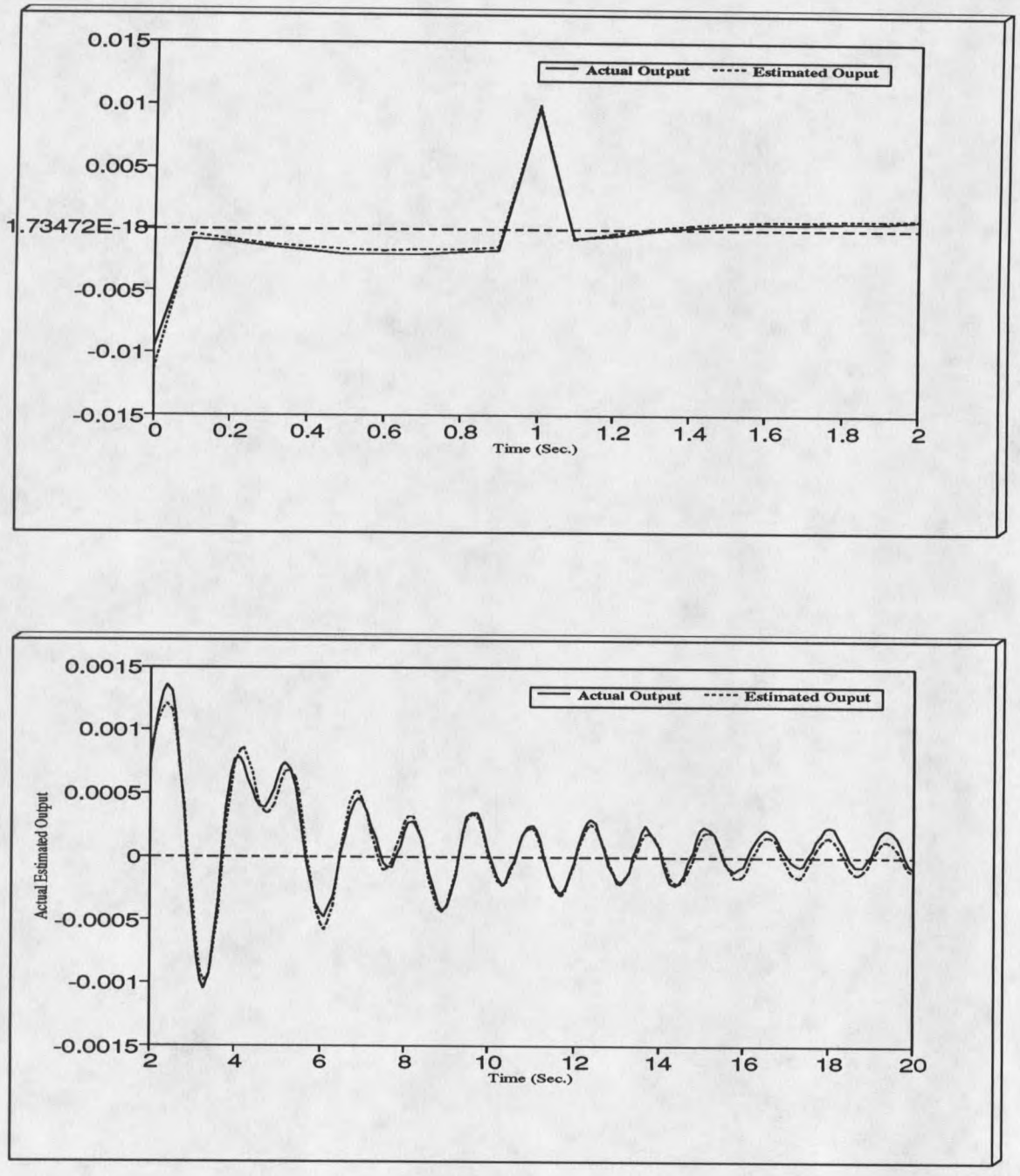

Figure 57. Transfer-function model output data versus actual data for frequency deviation signal.

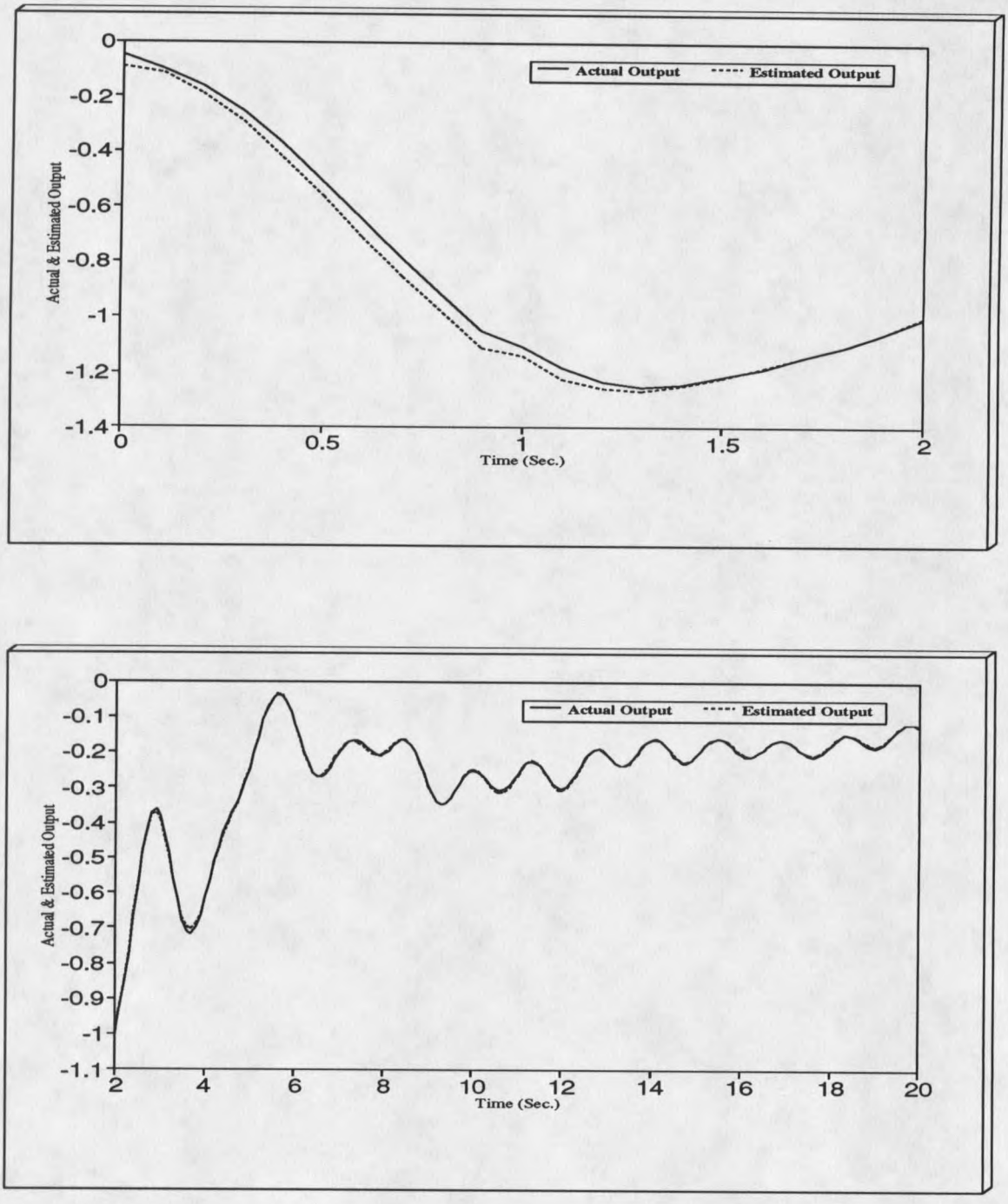

Figure 58. Transfer-function model output data versus actual data for voltage angle signal.

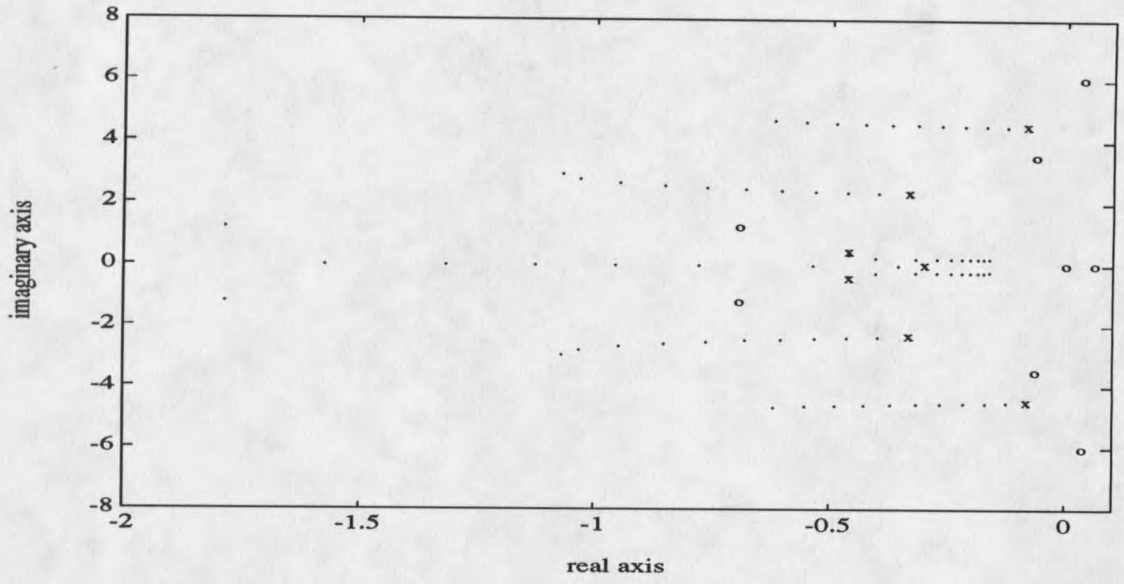

Figure 59. Root-locus plot with compensator for frequency deviation signal; gain K = 0 to 1000.

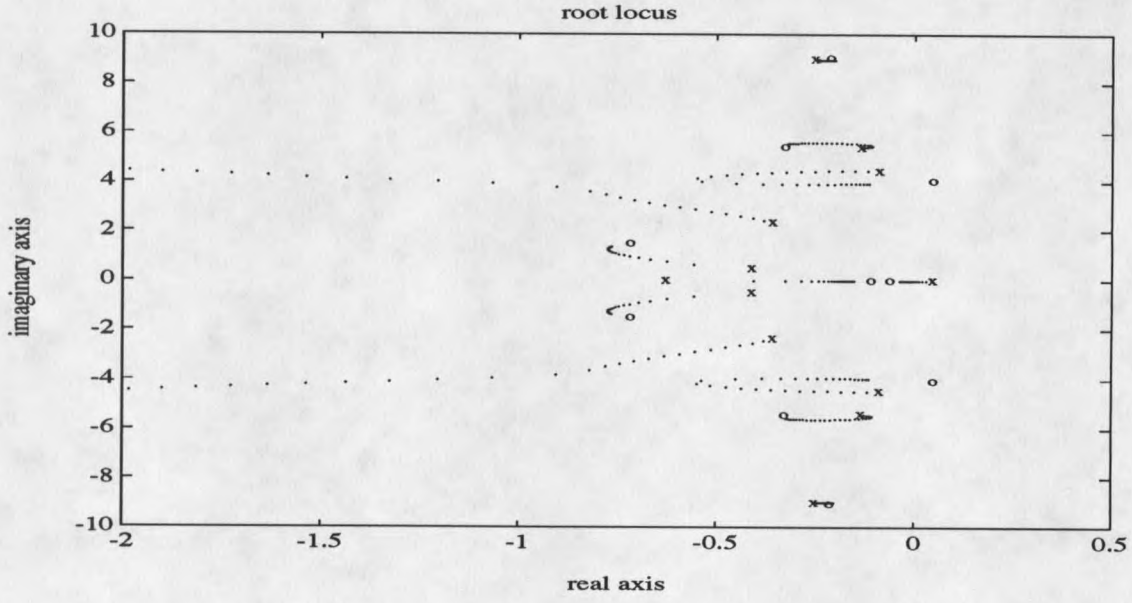

Figure 60. Root-locus plot with compensator for voltage angle signal; gain K = 0 to 30.

CHAPTER 8

TIME DOMAIN SIMULATION RESULTS FOR SMALL SIGNAL MODULATION SCHEMES

Introduction

This Chapter presents computer simulation results for small signal modulation of the ac/dc test system using frequency deviation and voltage angle as modulating signals. Time domain performance of the voltage angle and the frequency deviation feedback signal are presented without and with their respective compensator described in Chapter 7.

Simulation Results

The small signal modulation schemes described in Chapters 6 and 7 are applied to the 42-bus, 17-machine test system. No significant damping is observed except when voltage angle or frequency deviation at a bus near the rectifier is used as the modulating signal. A given modulating signal is used as a feedback signal and modulates the error signal of the current regulator at the rectifier end. The gain values used for both rectifier and inverter conventional PI current controller are $K_p = 0.05$ for the proportional controller and $K_I = 1.0$ for the integral controller. The generator swing curves to disturbance

#2 (line outage from bus P to bus SC2 in Figure 1 for 0.5 s) are as shown in Figures 61 through 65. Figure 61 shows the relative generator angle time variations without any modulation signal used. Comparison of Figure 61 with Figure 42 (Chapter 5) show that use of lower value of gains for the conventional PI current controller results in improved damping. Figures 62 and 63 show the generator angle responses without and with compensator, respectively, when voltage angle is used as modulating signal with feedback gain K = 20. Similarly, Figures 64 and 65 show the generator angle responses without and with compensator, respectively, when frequency deviation is used as modulating signal with feedback gain K = 100. From these figures, the positive effect of modulation when bus voltage angle or frequency deviation is used as the modulating signal is clearly evident in damping of generator angle oscillations. However, in comparing the modulation results when voltage angle is used as the modulating signal, somewhat better damping is observed when straight modulation is used (Figure 62) as compared to the damping obtained with the modulation and the compensator (Figure 63). It is also noticed that the feedback gain values used are much lower than the range obtained from the root-locus studies. This can be due to the lack of necessary voltage support at the inverter end as is required in large interconnected ac/dc systems.

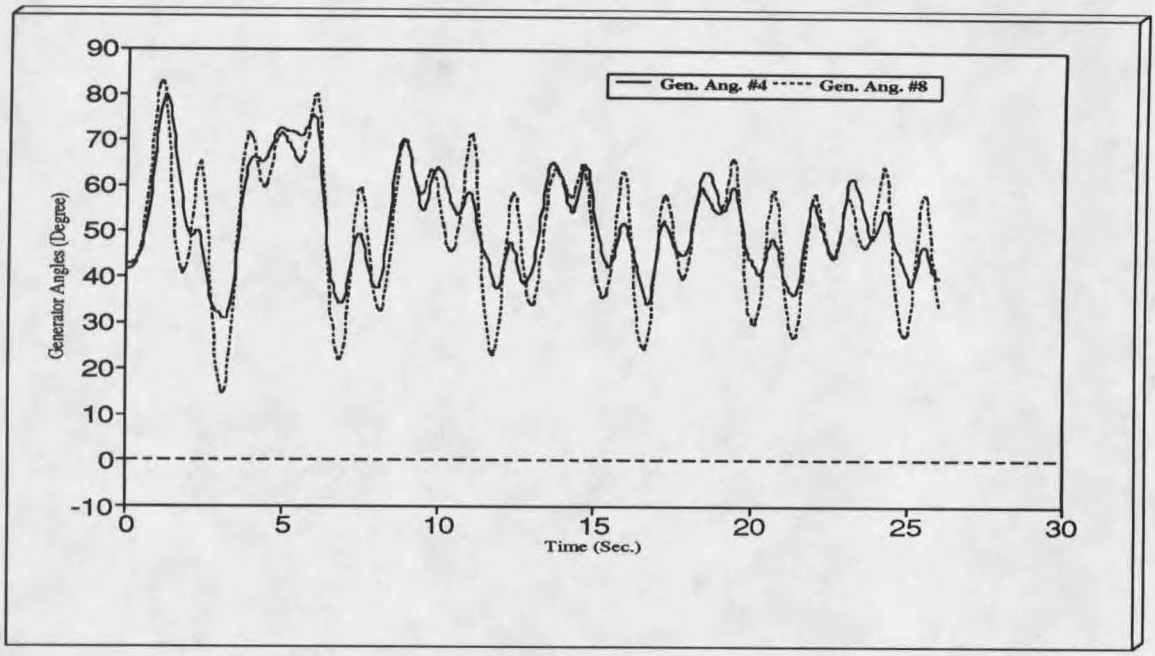

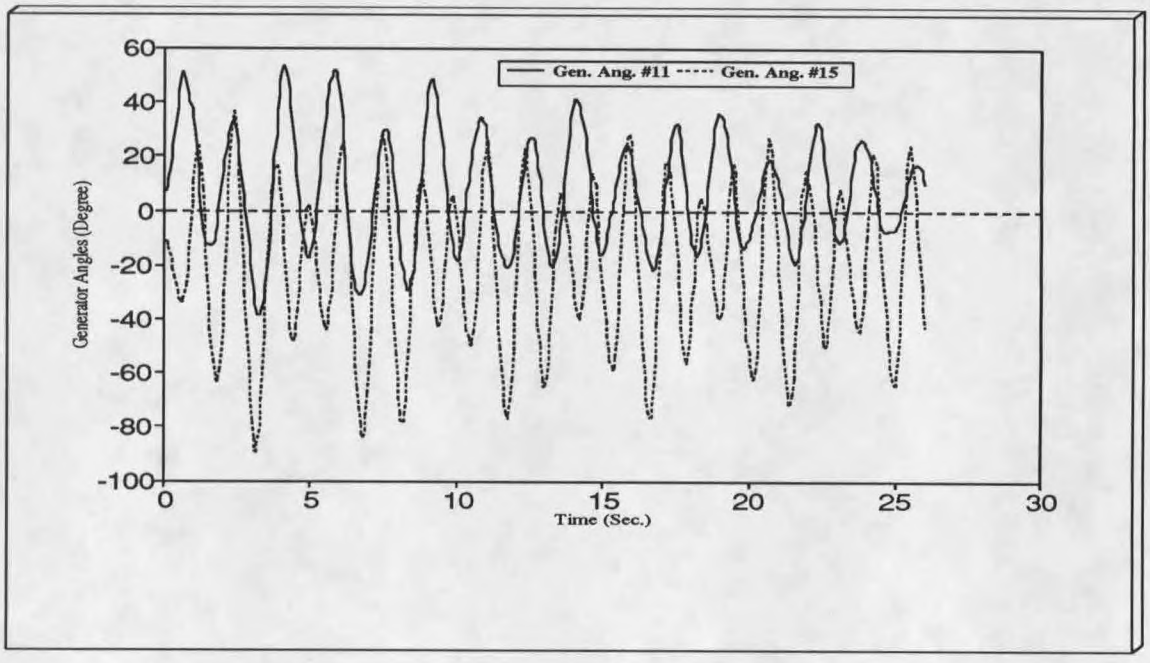

Figure 61. Relative generator angles for fault 2 without any modulation.

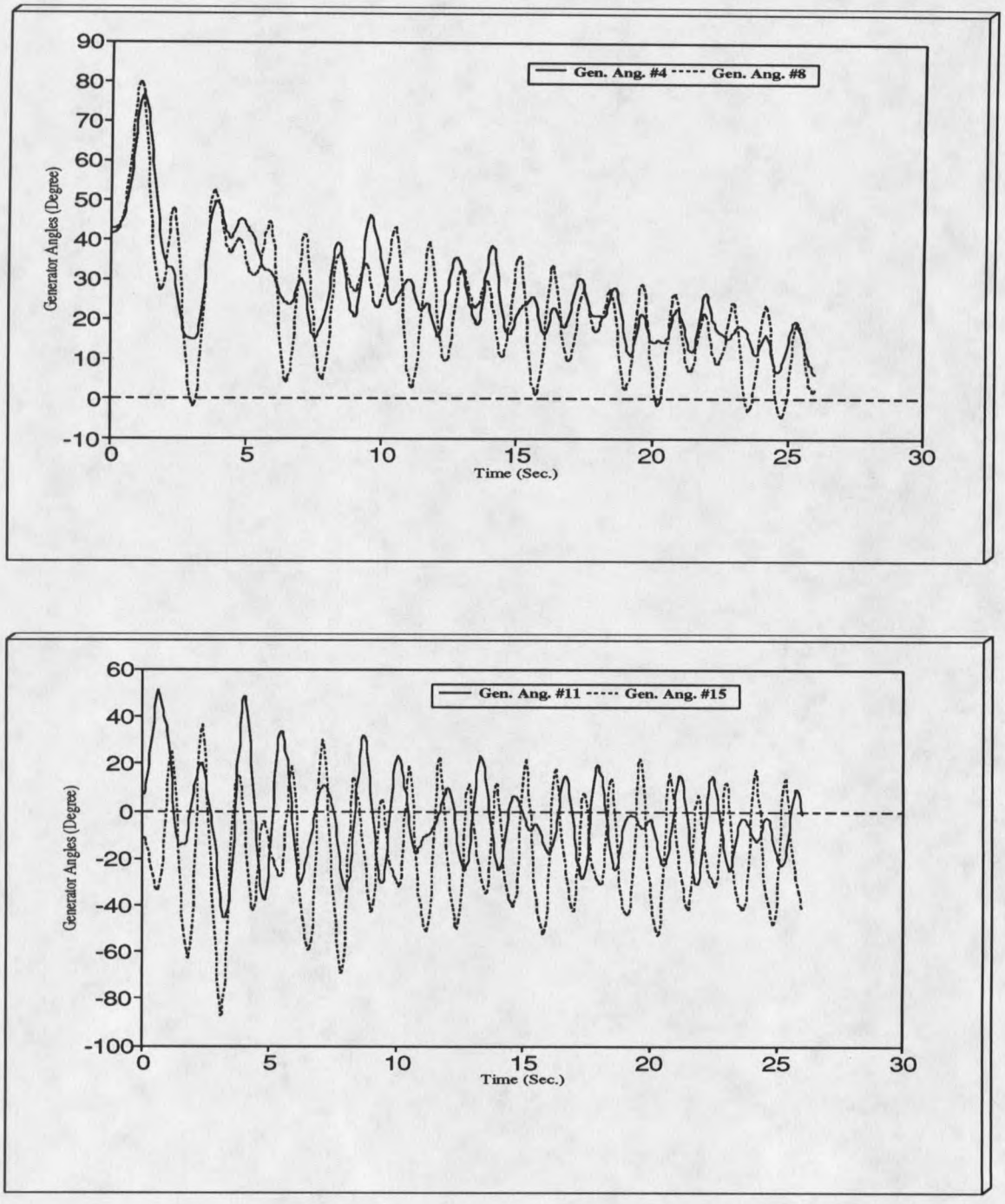

Figure 62. Relative generator angles for fault 2 for small signal modulation using voltage angle signal without compensator and feedback gain K = 20.

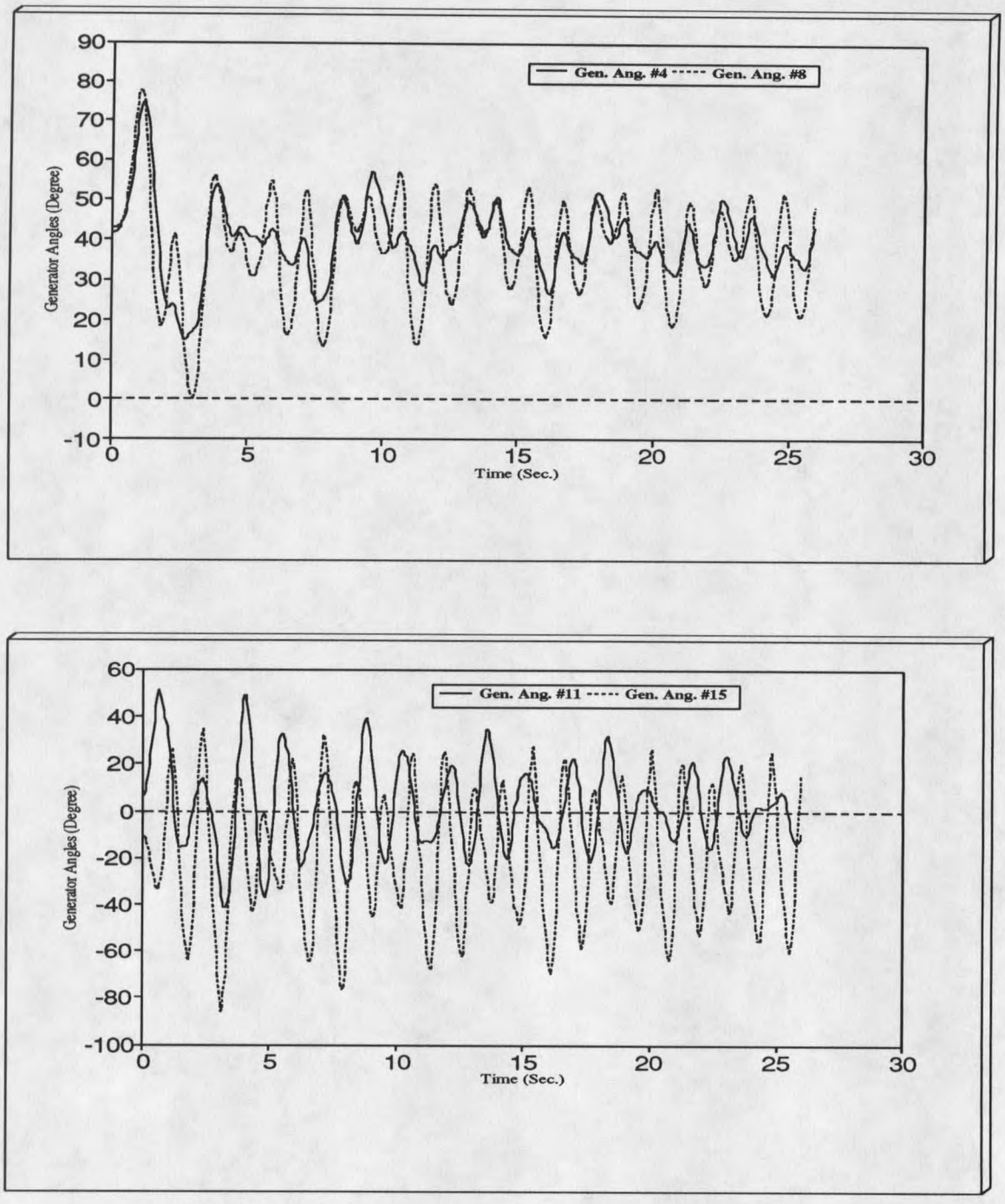

Figure 63. Relative generator angles for fault 2 for small signal modulation using voltage angle signal with compensator and feedback gain K = 20.

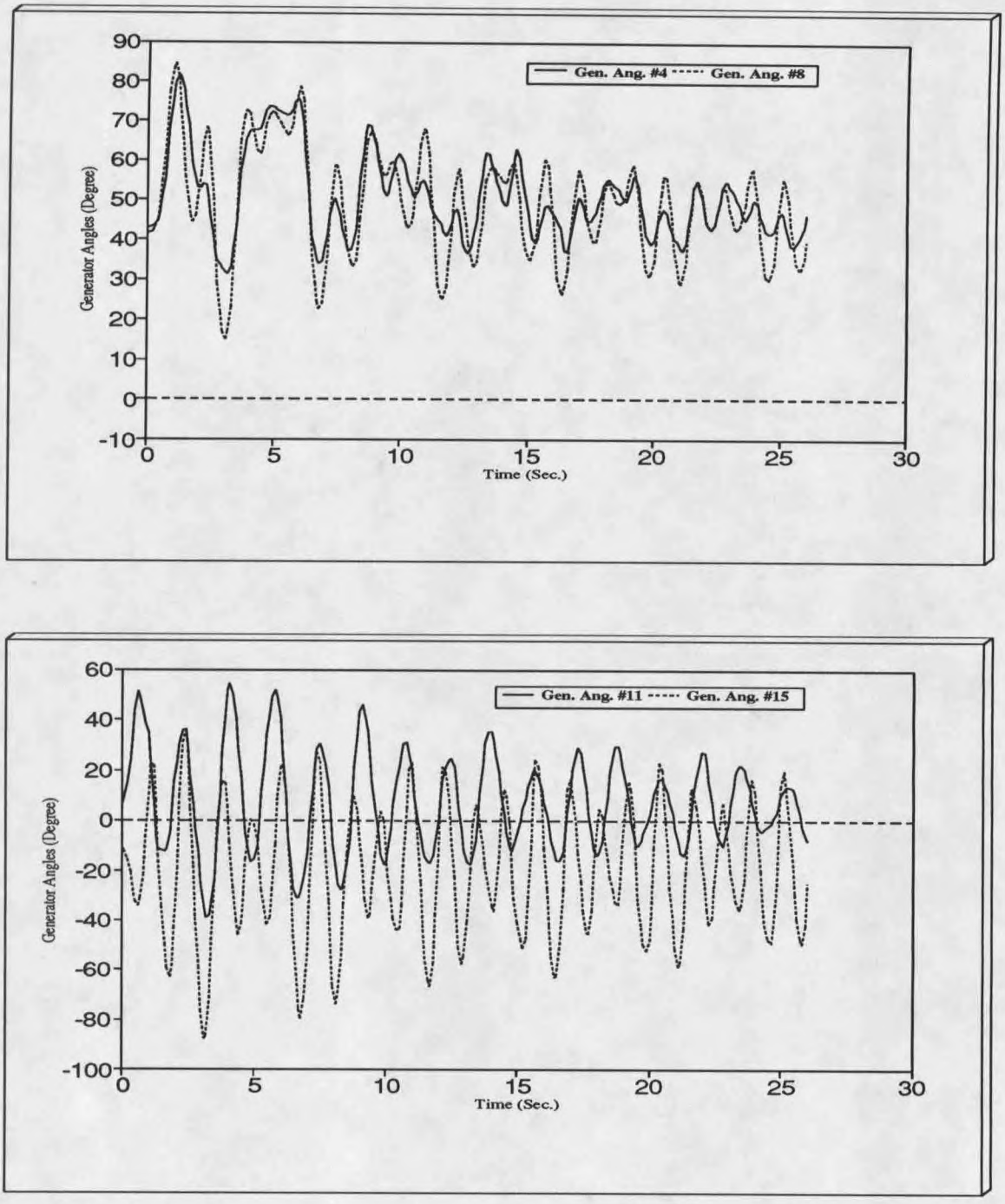

Figure 64. Relative generator angles for fault 2 for small signal modulation using frequency deviation without compensator and feedback gain K = 100.

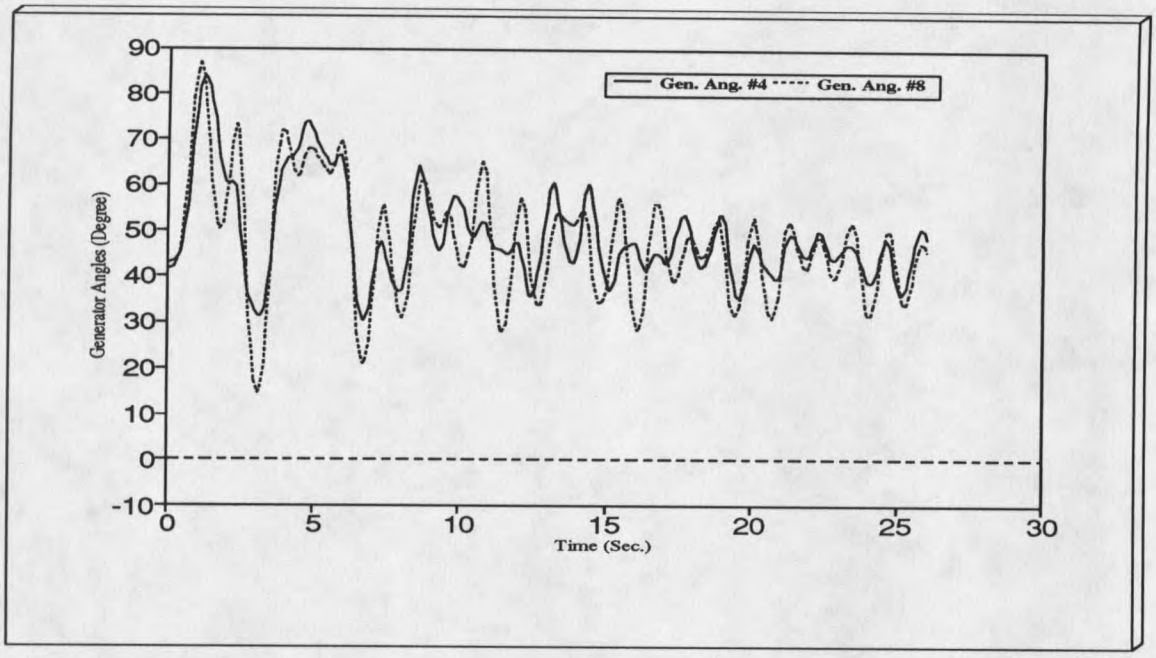

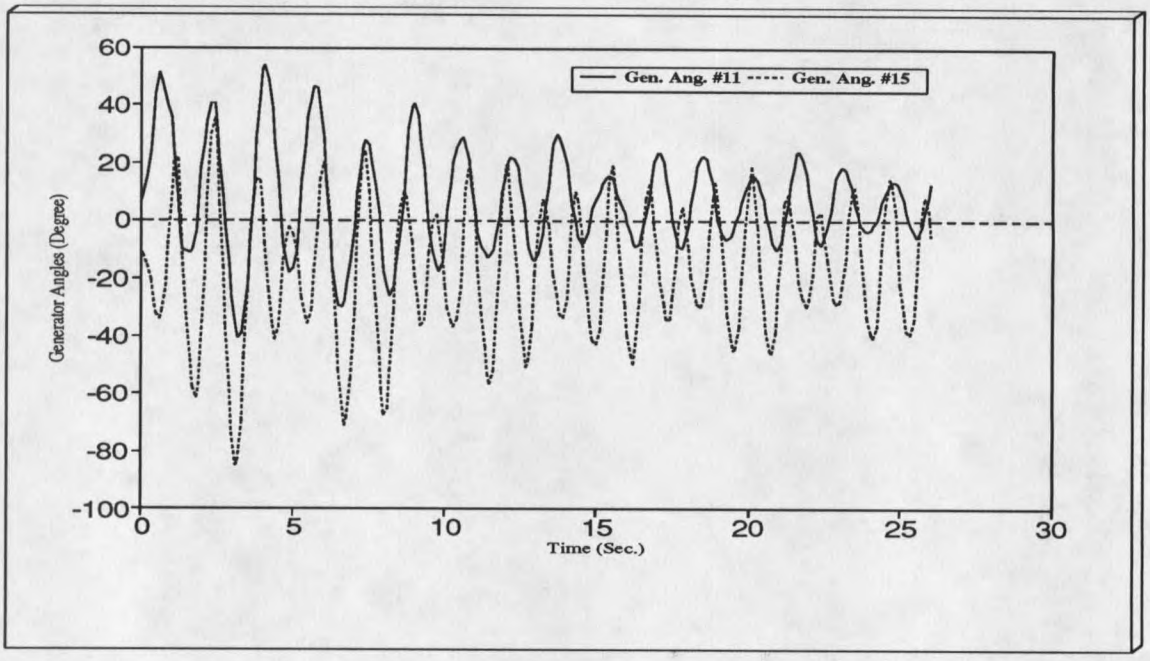

Figure 65. Relative generator angles for fault 2 for small signal modulation using frequency deviation with compensator and feedback gain K = 100.

CHAPTER 9

COMBINED SMALL SIGNAL MODULATION AND SVC CONTROL

Introduction

A Static Var Compensator (SVC) also known as a Static Var System (SVS) is a dynamic or continuously adjustable reactive power compensation device. Reactive compensation is generally required for voltage regulation, reactive power support, and enhancement of stability in a large power system. The steady-state control of reactive power using an SVC helps in maintaining the desired voltage profile in the power system network and minimizes excessive system losses. Additionally, the dynamic control of an SVC helps in reducing voltage variations caused by synchronizing power flow swings and dynamic variations in hvdc converter real and reactive power. Some of the other functions that can be performed by an SVC are: maintaining steady-state power transfer capability; preventing transient, electromechanical, and subsynchronous instability; and preventing voltage collapse.

From the results obtained using the modulation scheme (Chapter 8), it is evident that the modulation of power at the rectifier end without sufficient voltage support at the inverter end does not provide the desired damping as envisaged from the root-locus plot. The absence of suitable voltage support leads

to commutation failure, thereby restricting the gain of the modulating compensator to a low value. To overcome this difficulty, the application of multi-mode control is necessary. In this chapter a combination of small signal modulation control and SVC control is used to enhance the damping of the oscillatory modes. This is not a new technique, but it is presented here to show that the use of nonconventional converter controllers and modulation schemes without proper voltage support, as provided by the SVC, is not sufficient for damping.

Implementation

The combined small signal modulation scheme with SVC control is implemented on the 42-bus, 17-machine test system. Here in addition to providing a modulation compensator (described in Chapter 7 and implemented in Chapter 8) at the rectifier end, an SVC controller is provided at the inverter commutating bus (Bus SC1 in Figure 1 of Chapter 2). The voltage angle at the bus near the rectifier (Bus NW1 in Figure 1) is used as a feedback signal for modulation control while frequency deviation at the inverter commutating bus is used as the feedback signal for controlling the SVC. The generator swing responses to disturbance #2 (line outage from bus P to bus SC2 for 0.5 s) are as shown in Figure 66. As in the case of the modulation scheme simulations, the variation of generator

angles #4, #8, #11 and #15 relative to generator #1 are presented. With the use of SVC control at the inverter end it is possible to increase the modulation compensator gain at the rectifier from 20 to 100 without any commutation failure. The SVC controller has the feedback gain of 60. As compared to the results displayed in Chapter 8, the results here show considerable improvement in the damping.

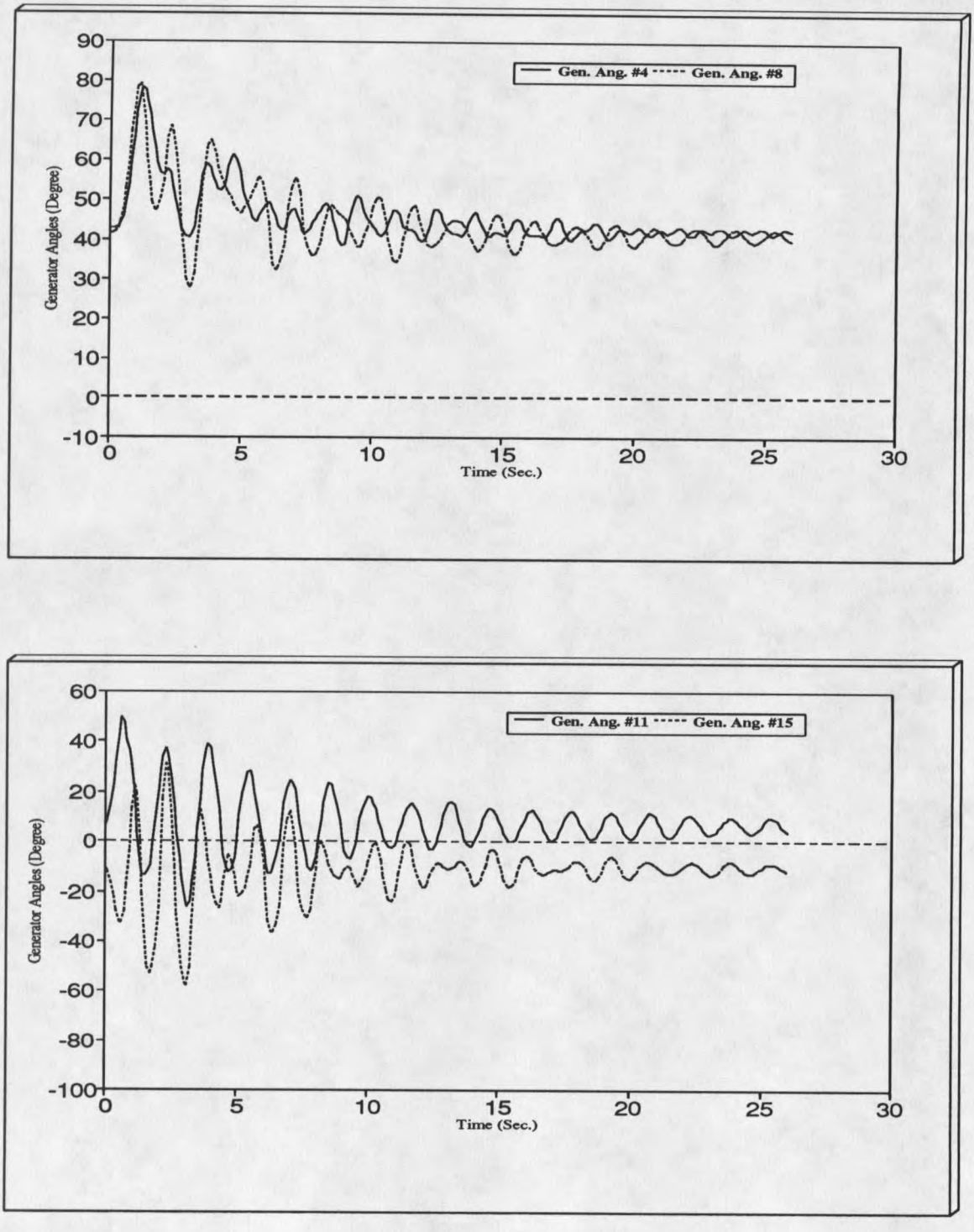

Figure 66. Relative generator angles for combined small signal modulation and SVC control.

CHAPTER 10

A SUPPLEMENTARY ADAPTIVE CONVERTER CONTROLLER FOR DAMPING OF POWER SYSTEM OSCILLATIONS

Introduction

The "steady-state" operating points of power systems may vary from hour to hour and season to season because of variation in the load demand and other foreseeable and unforeseeable circumstances. Because the dynamics of power systems depend on their operating point under steady-state conditions, it may be difficult or even impossible for a conventional controller of a dc transmission system designed for one operating point to damp out the unwanted oscillations at certain other operating points. This time varying nature of power systems, combined with their nonlinear characteristics, makes them suitable candidates for application of adaptive control strategies. In comparison to a conventional controller with fixed parameters, an adaptive regulator can modify its behavior according to the changes in the dynamics of the system it is controlling [23]. Hence, when applied to a power system, an adaptive controller can provide damping of low frequency oscillations at each operating point [57,58].

In this chapter a supplementary adaptive control scheme, similar to the one described in [58], is used along with a fixed hvdc regulator to enhance its robustness and effectiveness in damping power system oscillations.

Supplementary Adaptive Control Scheme

The supplementary adaptive control scheme uses an indirect self-tuning adaptive enhanced LQ controller as described in [59], in conjunction with a conventional fixed proportional-plus-integral (PI) controller to determine the appropriate time-varying effective converter firing angle required to dampen electromechanical oscillations. The conventional PI controller regulates the dc current in the link and as already seen (from the time-domain simulation results shown in Chapter 5) is not capable of providing significant damping of oscillations. However, it is effective in forcing the steady-state error to zero. The adaptive controller provides most of the damping under changing system conditions. Various signals available on the ac system, like bus voltage angle or frequency deviation can be used as control signals to regulate the converter firing angle. The most attractive feature of this scheme is that it can be used with an already existing conventional PI current regulator without modifying it.

The block diagrams given in Figures 67 and 68 show two different methods in which the supplementary adaptive controller described in [58] is applied to control the dc converter firing angle. In both cases the ac system output signal (Y which is frequency deviation) and the adaptive control input signal (U) are given to the adaptive controller which consists of an on-line identifier, an adaptive observer, and an adaptive enhanced LQG regulator [57]. The identifier identifies a discrete low-order model for the ac/dc system. The identifier used here is a recursive least-squares type with an exponential forgetting factor [23]. The identified model parameters are then given to the adaptive observer and the adaptive regulator. The observer estimates the inaccessible states of the system. Because the observer used is a reduced-order one, its states do not have one-to-one correspondence with the actual system states. It is a special case of a finite-settling-time observer [57,58]. The observer given in [7] which allows the placement of observer poles arbitrarily inside the unit circle also has been tried. The regulator calculates the gain of the optimal feedback control law from the iterative solution of the Riccati equations and is taken from [59]. Using the states estimated by the observer (X) and the gains calculated by the adaptive regulator (G), an adaptive feedback control signal (U) is obtained which is used as the modulating signal at the converter.

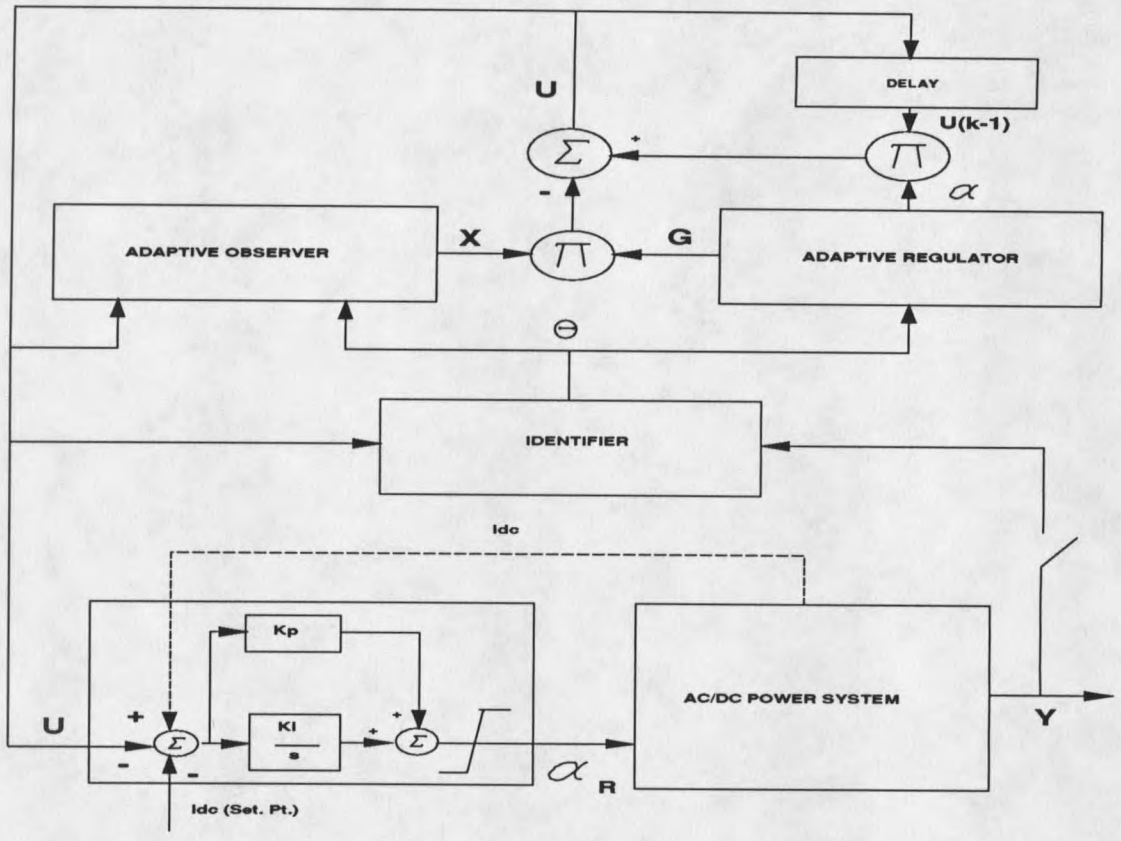

Figure 67. A supplementary adaptive control scheme 1 for modulation of dc line current.

In the first scheme (Figure 67) the adaptive signal is added at the point where the current error signal for the rectifier PI controller is obtained, and hence it modulates the dc line current. In the second scheme (Figure 68) the adaptive signal is directly added to the rectifier firing angle obtained from the PI controller, and hence it modulates the firing angle. In both cases the input to the power system is the effective firing angle that the rectifier controller

presents to the ac/dc power system. The system output is taken to be either unfiltered or a filtered version of the ac bus frequency deviation. The underlying damping philosophy here is that the process of minimizing the variation of any output will minimize transient power fluctuations in the system and thereby reduce the electromechanical oscillations in the system [58].

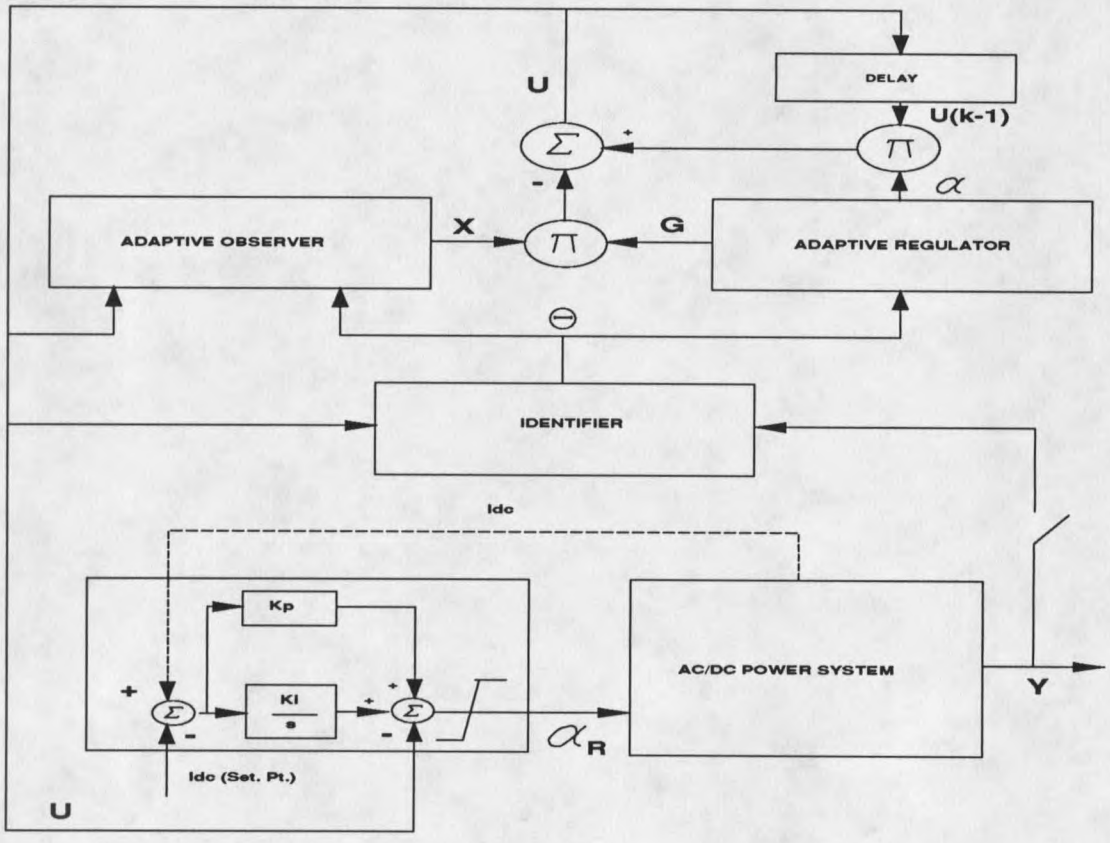

Figure 68. A supplementary adaptive control scheme 2 for modulation of rectifier firing angle.

CHAPTER 11

TIME DOMAIN SIMULATION RESULTS FOR THE SUPPLEMENTARY ADAPTIVE CONTROLLER

Introduction

This chapter presents the time domain simulation results for the supplementary adaptive control schemes introduced in Chapter 10.

Simulation Results

The supplementary adaptive control schemes described in Chapter 10 were applied to the 42-bus, 17-machine test system. Both schemes were implemented using unfiltered and filtered versions of the frequency deviation signal at an ac bus (NW1 in Figure 1 of Chapter 2) as input signal to the adaptive controller. The filter used is a band pass filter which blocks the dc component of the signal and also attenuates frequency components above the electromechanical swing modes. The corner frequencies of this filter are set at 0.05 and 3.0 Hz.

In order to facilitate the identification of the parameters of the reduced-order model of the system, a probing signal is used as an input to the system whose magnitude is kept as small as possible so as to just excite the natural modes of the system. Two different types of observers were implemented:

one is a finite-settling-time observer and other allows the placement of observer poles arbitrarily inside the unit circle. Two different identified model types were implemented: one having a strictly proper transfer function where the order of the numerator is one less than that of the denominator, and the other having a proper transfer function with the numerator order being the same as that of the denominator.

The adaptive controller operates as follows. Over the initial 2.1 s of operation, the probing signal is applied to the system and is changed at the sampling rate of 0.1 s. The identifier uses this system input in conjunction with the system output (here frequency deviation) and a recursive least-squares algorithm to update the parameters of the system model. At 2.1 s into the simulation, a disturbance is initiated on the power system. The identifier continues to operate, using the sampled input to the system (a combination of probing signal and calculated adaptive control action) along with the system output to update model parameters every 0.1 s. These parameters are supplied to the observer and to the ELQ regulator. The regulator gains are calculated by iterating the Riccati equations once during each sample period. The control signal is computed using the above Riccati gains and the values of the state vector estimated by the observer. This signal is updated every 0.1 s and is used as an adaptive modulating

signal to modulate the converter current or firing angle. The identifier, observer, and regulator are executed at a sampling period of 0.1 s; the ac/dc power system integration proceeds at a time step of 0.005 s.

The generator swing curves to disturbance #2 (line outage from bus P to bus SC2 in Figure 1 for 0.5 s) are as shown in Figures 69 through 76. Figures 69 and 70 show the relative generator angle time variation using unfiltered frequency deviation and filtered frequency deviation signals, respectively, for scheme 1. The finite-settling-time observer and the fourth order identified model with strictly proper transfer function are used. Figures 71 and 72 depict the same simulation condition except that the identified model is simply a proper transfer function of order three. Figures 73 and 74 are relative generator responses obtained when filtered and unfiltered frequency deviation signals, respectively, are used with scheme 2. Again a finite-settling-time observer and a third order identified model with proper transfer function are used. An observer with its poles placed at $0.5\ e^{\pm j30}$ was also tried, and Figures 75 and 76 show the results with this observer for schemes 1 and 2, respectively, using the unfiltered frequency deviation signal and the third order identified model having a proper transfer function. From these plots it is

evident that the supplementary adaptive controller provides slightly better damping than that obtained by small signal modulation schemes.

Comparisons of Figures 69 with 70 and 71 with 72 show that not much improvement in system damping is obtained when a filtered modulation signal is used versus an unfiltered signal. However, in actual practice a filter must be used for noise reduction. Also, these figures show that although use of proper transfer function in identified model slightly improves system damping, its effect is not significant in comparison with a strictly proper identifier. Comparisons of Figures 71 with 73 and 72 with 74 show that there is not much difference in system damping when scheme 1 or scheme 2 is used. Finally, use of an observer with non-zero pole placement (Figures 75 and 76) provides slightly better damping as compared to a finite settling time observer (Figures 69 through 74). This is because the observer poles are placed to obtain a filtering action on the controlled input and reduce the magnitude of initial swings thereby improving the system damping.

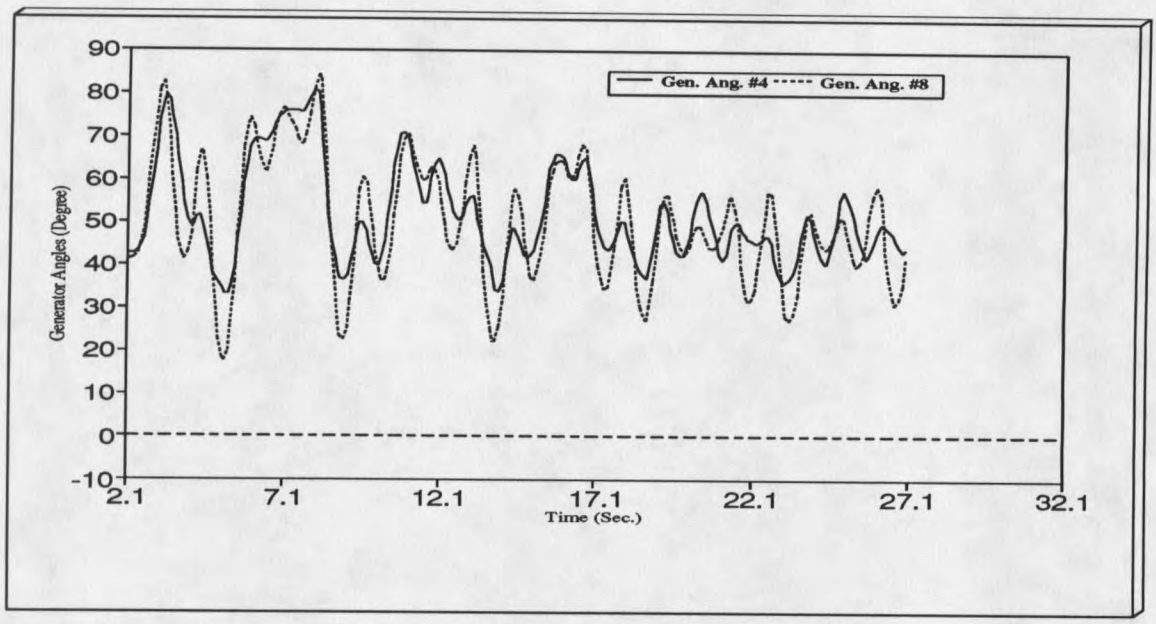

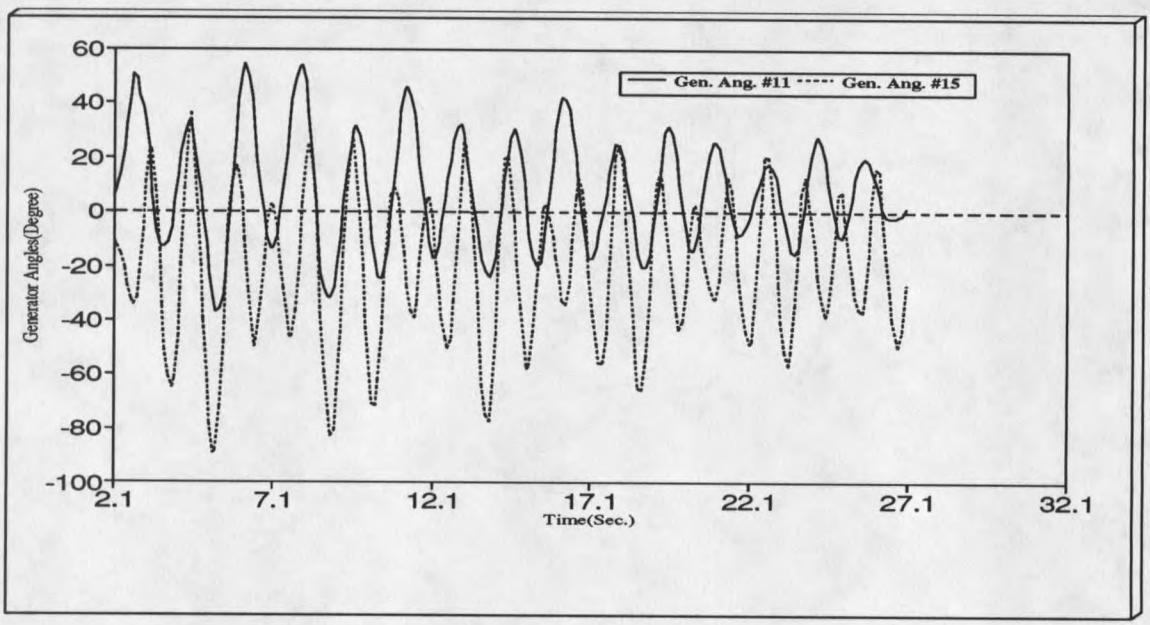

Figure 69. Relative generator angles for fault 2 (adaptive modulation scheme 1 using unfiltered frequency deviation signal, finite-settling time observer and identified model with strictly proper transfer function).

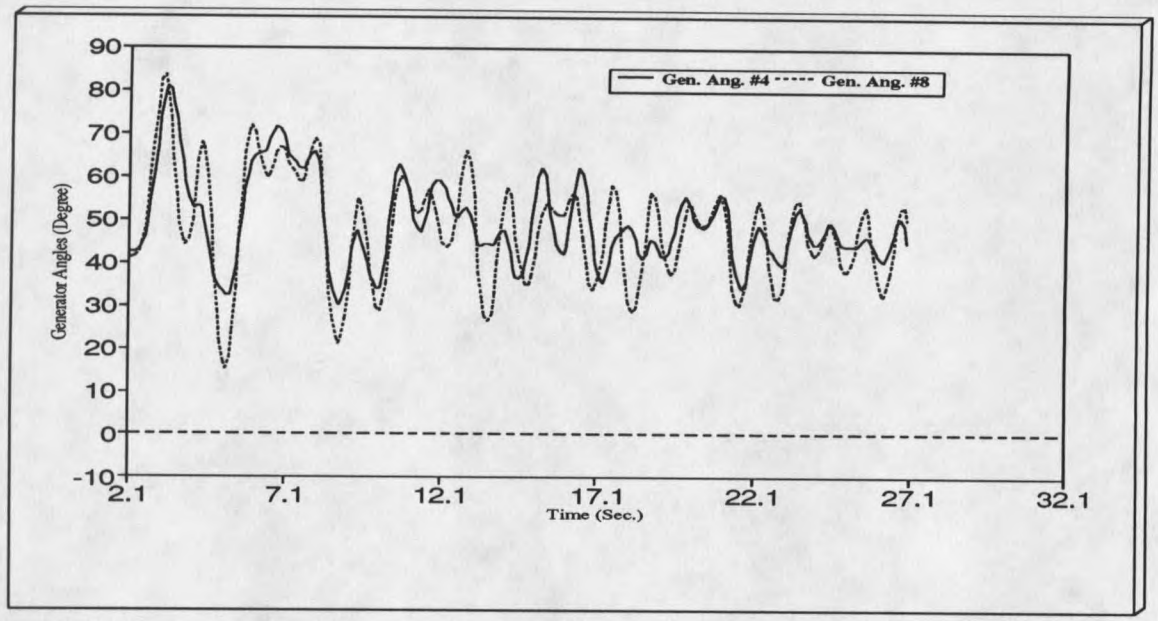

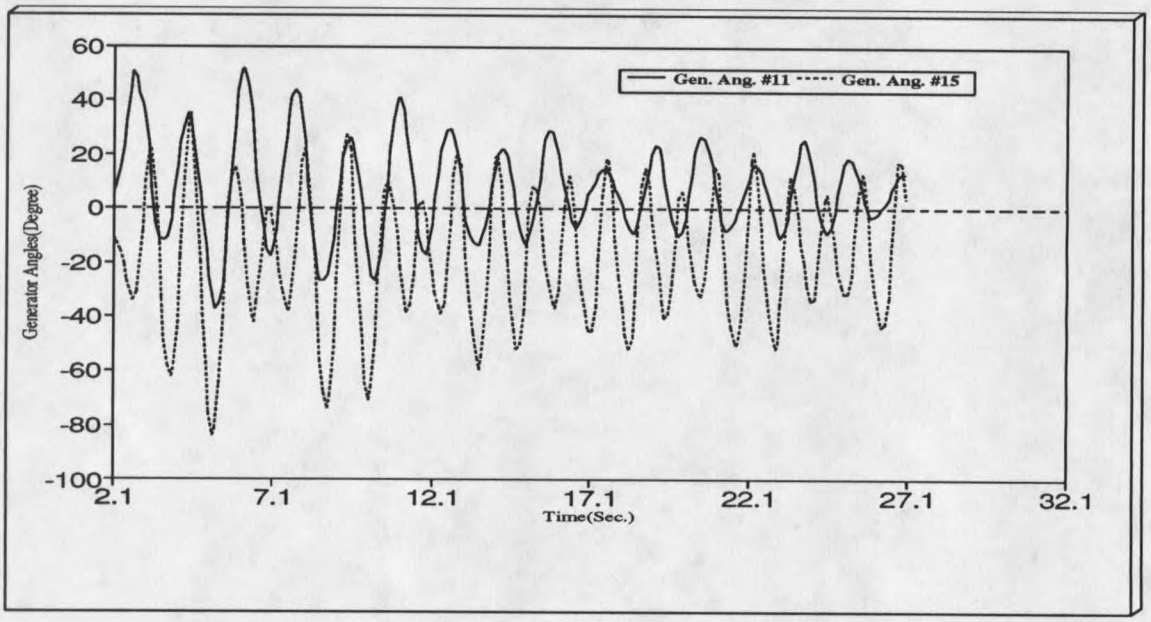

Figure 70. Relative generator angles for fault 2 (adaptive modulation scheme 1 using filtered frequency deviation signal, finite-settling time observer and identified model with strictly proper transfer function).

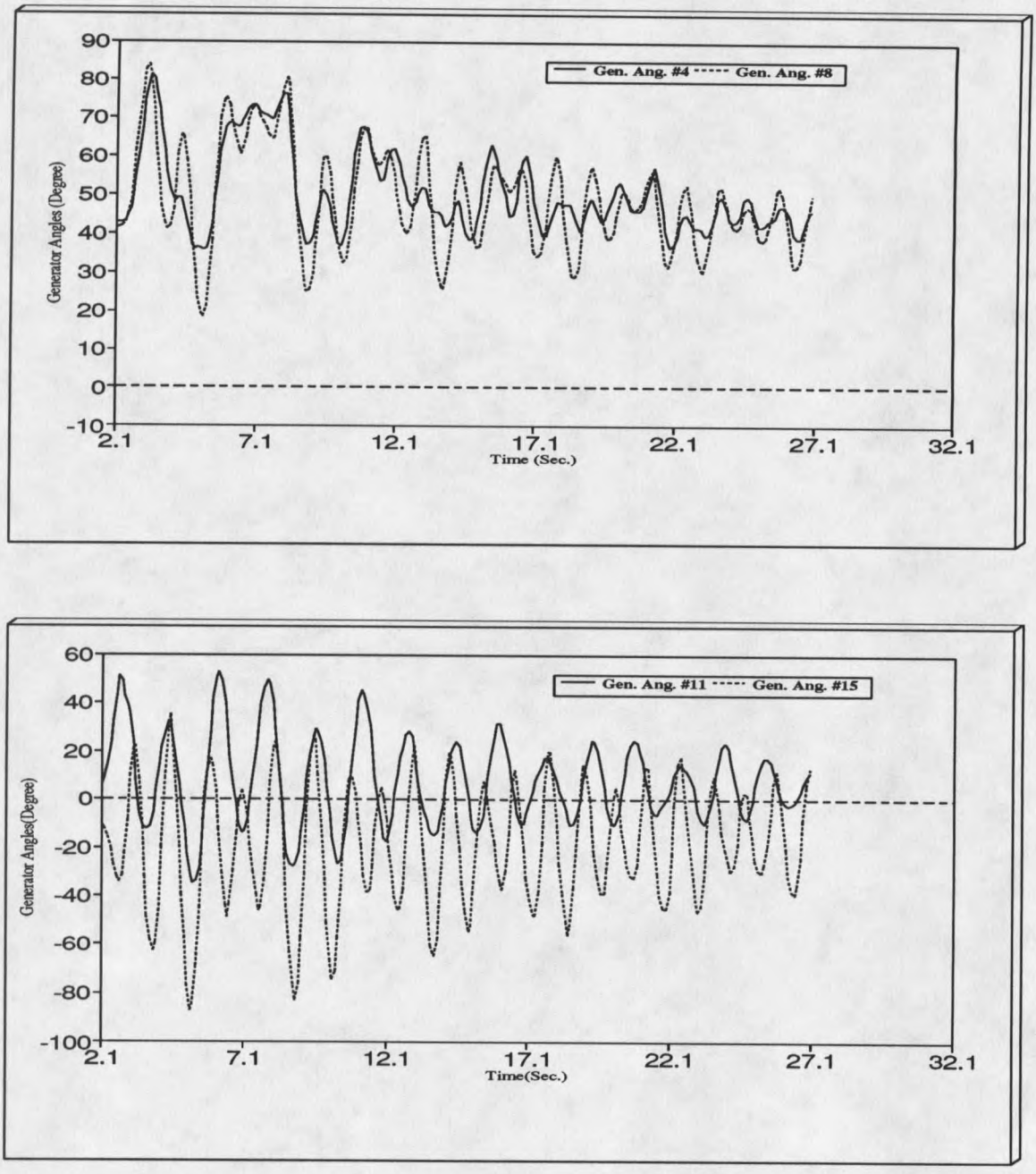

Figure 71. Relative generator angles for fault 2 (adaptive modulation scheme 1 using unfiltered frequency deviation signal, finite-settling time observer and identified model with proper transfer function).

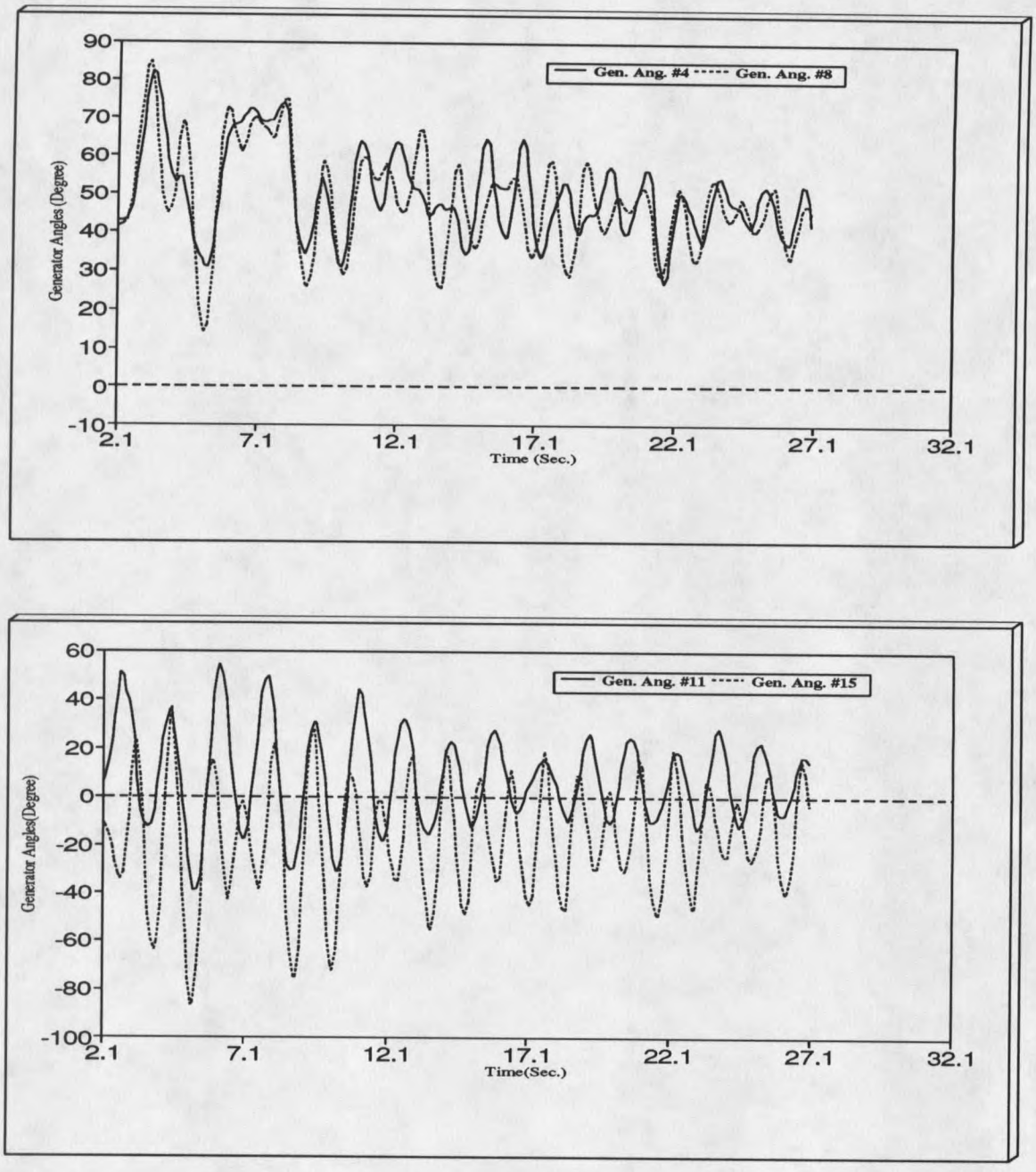

Figure 72. Relative generator angles for fault 2 (adaptive modulation scheme 1 using filtered frequency deviation signal, finite-settling time observer and identified model with proper transfer function).

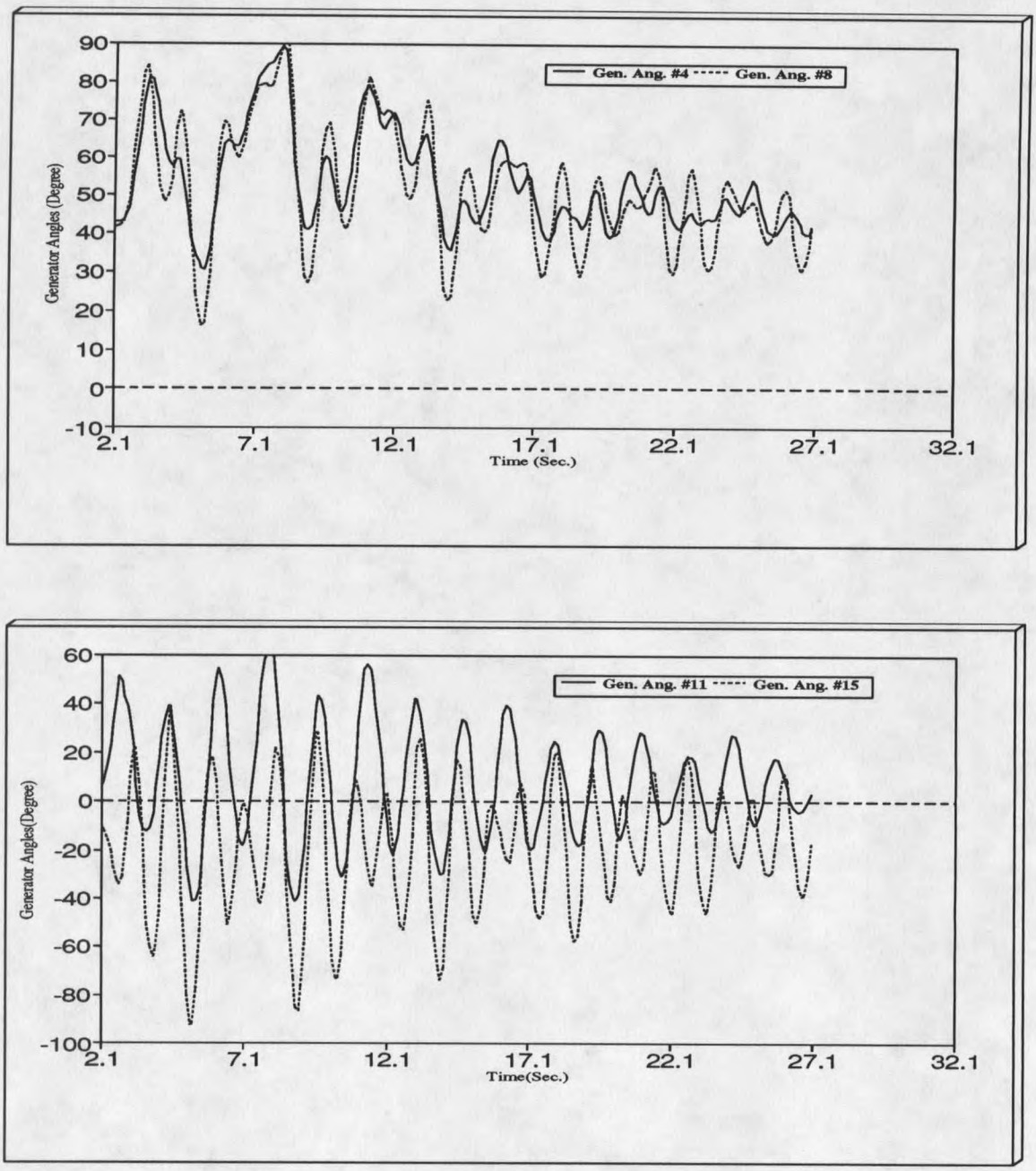

Figure 73. Relative generator angles for fault 2 (adaptive modulation scheme 2 using unfiltered frequency deviation signal, finite-settling time observer and identified model with proper transfer function).

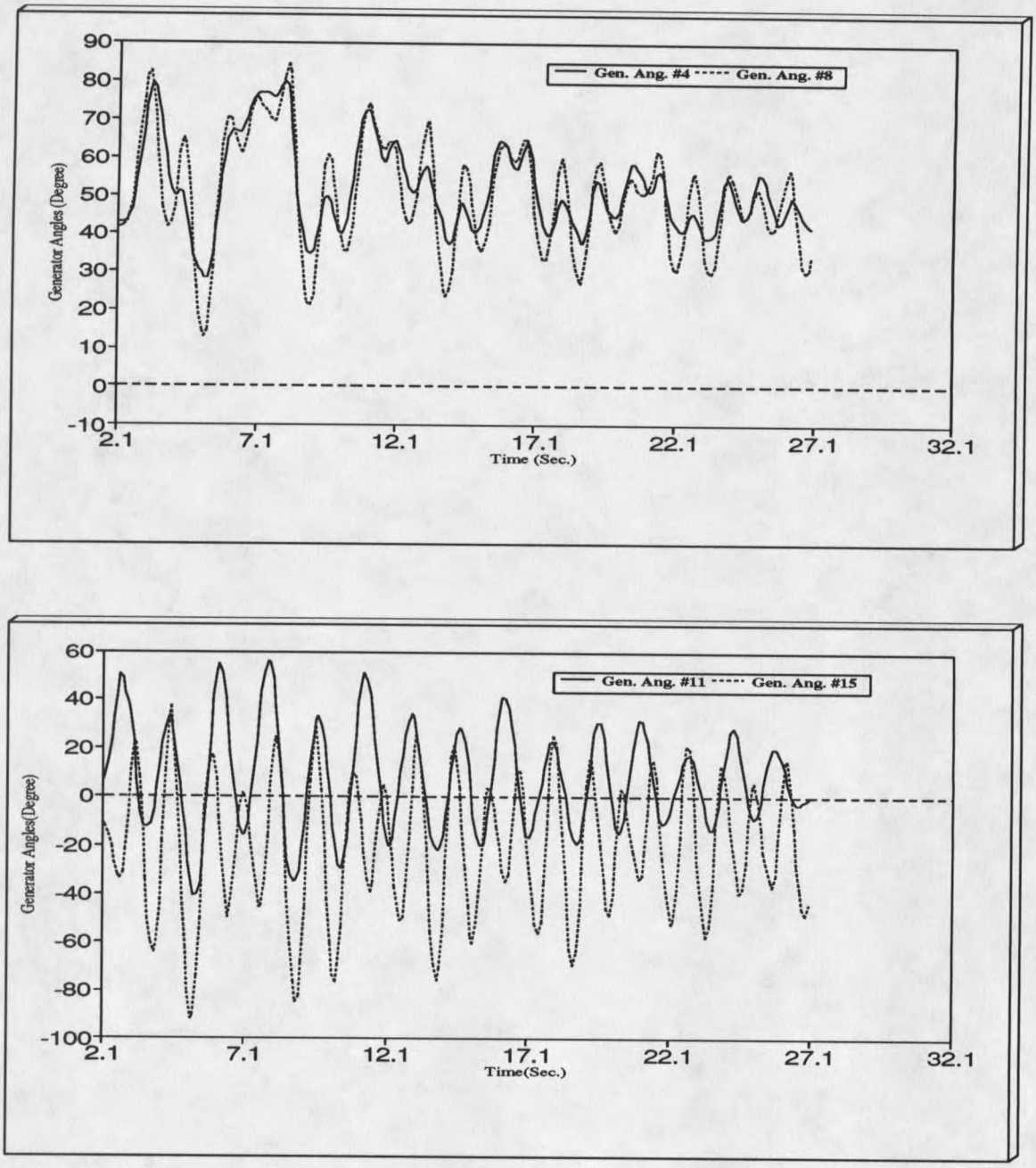

Figure 74. Relative generator angles for fault 2 (adaptive modulation scheme 2 using filtered frequency deviation signal, finite-settling time observer and identified model with proper transfer function).

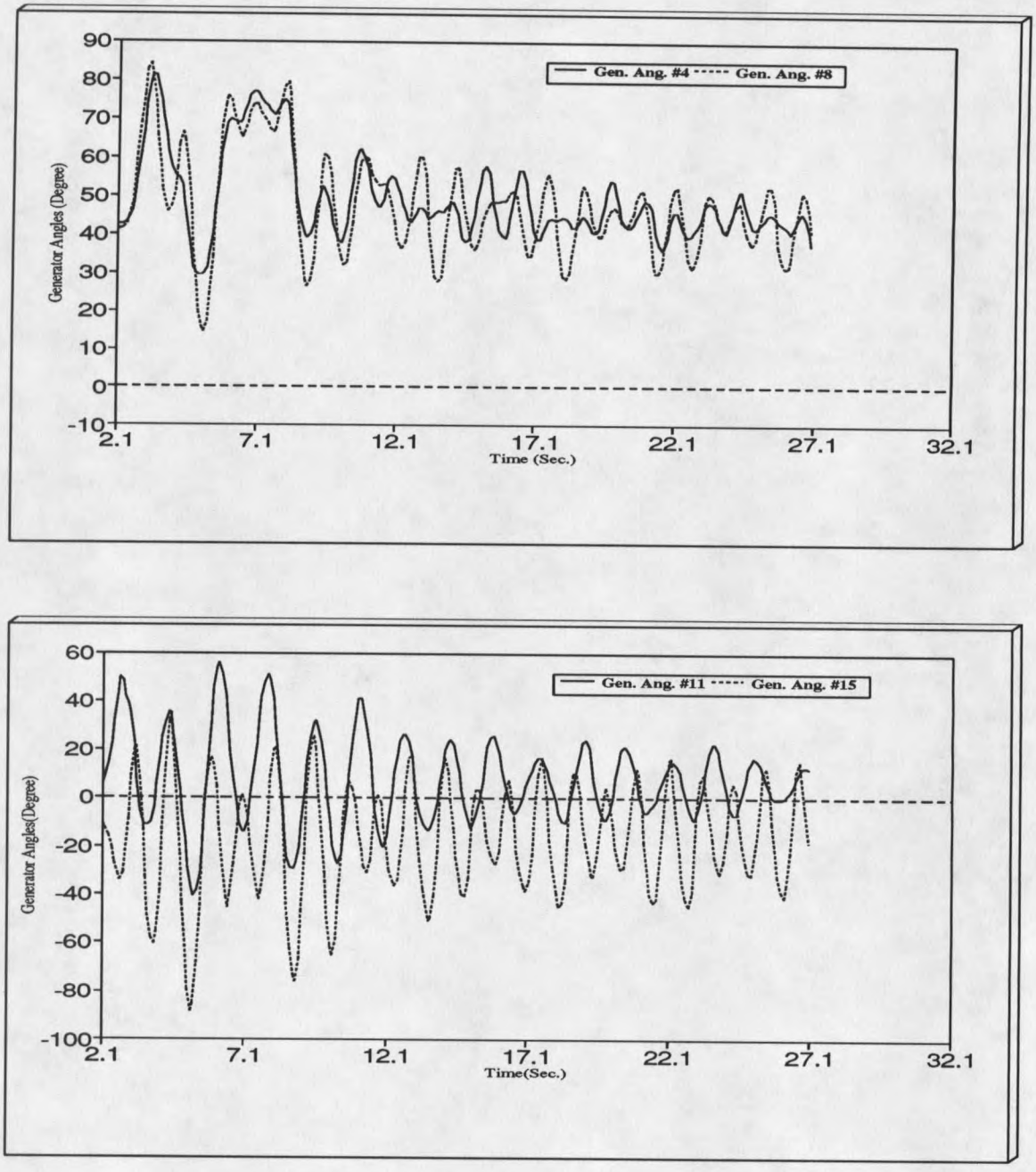

Figure 75. Relative generator angles for fault 2 (adaptive modulation scheme 1 using unfiltered frequency deviation signal, observer with non-zero pole placement, and identified model with proper transfer function).

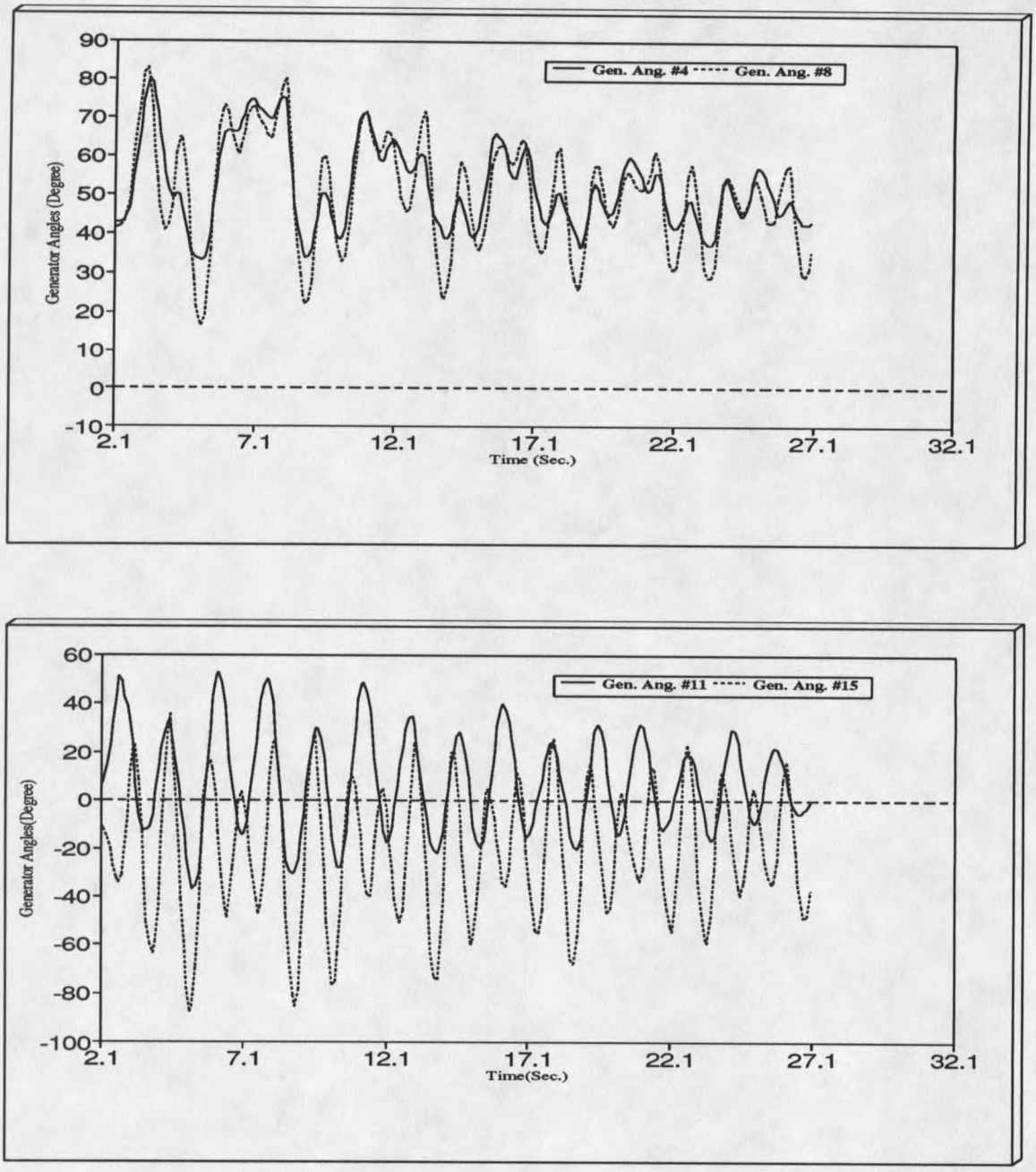

Figure 76. Relative generator angles for fault 2 (adaptive modulation scheme 2 using unfiltered frequency deviation signal, observer with non-zero pole placement, and identified model with proper transfer function).

CHAPTER 12

CONCLUSIONS AND FUTURE WORK

Various approaches to the problem of improving power system damping using hvdc converter control strategies have been presented. This chapter contains a number of conclusions concerning these approaches. It also gives some general directions for future work. The chapter is organized into four sections. The first section discusses the conventional and nonconventional converter control schemes. The performance of the small signal modulation scheme is discussed in the second section. The third section evaluates the generalized Prony system identification technique, and the fourth section evaluates the supplementary adaptive control scheme.

Nonconventional Hvdc System Control

One of the objectives of this thesis was to evaluate the performance of a set of nonconventional hvdc controllers relative to that of conventional controllers. Based on the Prony-based analysis and the root-locus study of the system presented in Chapter 4, and also the time-domain simulation results given in Chapter 5, it is evident that the damping effects of these nonconventional hvdc control schemes are not significant for a large interconnected system. However it has

been shown in the literature that some of these nonconventional control schemes do enhance the damping of the electromechanical oscillations in small systems.

The primary reason for this inconsistency is that the control action provided by the nonconventional controllers in large interconnected ac/dc systems may not be sufficient, as in the case of the 42-bus system studied, to provide satisfactory damping. This is particularly true if the ac/dc system has a high effective short-circuit ratio (ESCR) greater than about 2.5. The ESCR for an ac/dc system as defined in [11] is the ratio of the MVA short-circuit capacity of the ac system to the dc transmitted power. An ac/dc system is said to be strong in ac for an ESCR of 2.5. In such cases the ac system is too strong to be controlled by the dc line converter controllers using local signals only and without a supplementary signal. In the case of the 42-bus test system studied the ESCR is about 4. Also it should be mentioned that the time domain simulation results for the nonconventional controllers were obtained using typical values of gain for the proportional-plus-integral (PI) type compensator. The gain values used were quite high to force the steady-state error to zero. Other gain values might have produced better damping. This possibility should be explored further.

Small Signal Modulation Schemes

Another objective of this thesis was to determine the effectiveness of the small signal modulation schemes in damping low frequency oscillations. As shown in Chapters 6, 7, and 8, the modulation schemes can improve damping of system low frequency oscillations. The damping can be significantly improved with proper modulation signal compensator design and with proper voltage support at the inverter end. It has also been shown that reactive power modulation of the inverter ac bus using an SVC combined with real power modulation at the rectifier further improves system damping as is evident from the results presented in Chapter 9. However, the use of an SVC imposes additional financial cost. It is reported in [19,20] that reactive power modulation of the inverter coordinated with real power modulation at the rectifier can provide significant damping. This technique merits further research.

System Identification Using Modified Prony Analysis

A significant contribution of this thesis is the modified Prony Analysis technique presented in Chapter 7 for system identification. It is generalization of the method presented in [7] to include a feedforward or throughput term. From the results presented in Chapter 7 it is clear that the linear Prony fit matches very closely with the actual response even

during the application of the input pulse. Thus system identification using the modified Prony analysis has the advantage that it results in a reduced-order model of a large system and gives an estimate of the order of the system. However, the root-locus plots of the system transfer function with and without the compensator predict higher values of the feedback gain than the actual values which can be used in the time domain simulation results. Also from the response of the linear and the actual system with the same value of feedback gain, it is found that the damping is considerably more in the case of linear system. Lastly, Prony analysis of the actual system with a particular value of gain give a new set of eigenvalues which are very different from that predicted by the root-locus plot. Thus it is suggested that other off-line identification techniques like weighted least-squares should be considered. Preliminary work using weighted least-square has already been done but a detailed study is required.

Supplementary Adaptive Controller

Another contribution of this thesis is to present a suitable adaptive control strategy for damping of low frequency oscillations. In Chapter 10 a self-tuning supplementary adaptive converter controller is presented. It has the inherent capability of being more robust than the fixed converter

controllers as it adjusts its control based upon on-line identification of a reduced-order transfer function of the system. The biggest advantage of this type of controller is that the control action is automatically tuned as the system operating conditions change. Another attractive feature of this control is that it is used with an already existing conventional PI current regulator without modifying it. From the time domain simulation results obtained in Chapter 11 it is evident that supplementary adaptive modulation of the dc line current and the rectifier firing angle can improve system damping as compared to fixed modulation schemes. To improve system damping significantly, however, additional reactive support at the inverter is necessary.

There are still some aspects of the adaptive controller that warrant further investigation. One is the testing of the adaptive control scheme at some other operating point, very different from the test case operating point used in this thesis. Another is to use some other type of identification routine, other than the recursive least-squares routine used in this thesis. Also the use of a multivariable approach where there is more than one system output and one system input warrants further research.

REFERENCES CITED

1 C. Adamson and N. G. Hingorani, High Voltage Direct Current Power Transmission, Garroway, London, 1960.

2 E. W. Kimbark, Direct Current Transmission Vol. I, Wiley Interscience, New York, 1971.

3 E. Uhlmann, Power Transmission by Direct Current, Springer-verlag, New York, 1975.

4 J. Arillaga, High Voltage Direct Current Transmission, Peter Pergrinus Ltd., London, 1983.

5 J. Arillaga, C. P. Arnold, B. J. Harkar, Computer Modelling of Electrical Power Systems, John Wiley and Sons, New York, 1983.

6 J. R. Smith, "Robust Var Unit Control Strategies for Damping of Power System Oscillations," Ph. D. Thesis, Electrical Engineering Department, Montana State University, Bozeman, Montana, July, 1988.

7 D. J. Trudnowski, "Decentralized Control Strategies for Damping Power-system Electromechanical Oscillations," Ph. D. Thesis, Electrical Engineering Department, Montana State University, Bozeman, Montana, March 1991.

8 M. Z. Tarnawecky, "Hvdc Transmission Control Schemes," Proceedings, Manitoba Power Conference EHV-DC, June 7-10, 1971, Winnipeg, Canada.

9 C. E. Grund, T. H. Lee, S. R. Lightfoot, R. J. Piwko, R. V. Pohl, K. Mortensen, R. J. Newell, J. Reeve, and D. A. Woodford, "Functional Model of Two-terminal HVDC Systems for Transient and Steady-State Stability," IEEE Trans. Power Apparatus and Systems, vol. PAS-103, no. 6, June 1984, pp. 1249-1255.

10 IEEE Committee Report, "HVDC Modelling requirements for load-flow and stability simulation"' Report prepared for the IEEE working group on dynamic performance and modelling of dc system, January 1989, System Planning Division, Ontario Hydro, Totonto Canada.

11 M. Szechtman, W. W. Ping, E. Salgado, and J. P. Bowles, "Unconventional HVDC Control Technique for Stabilization of Weak Power System," IEEE Trans. On Power Apparatus and Systems, vol. PAS-103, no. 8, Aug. 1984, pp. 2244-2248.

12 A. E. Hammad, E. A. Woodford, and R. M. Mathur, "AC Voltage Control at an HVDC Terminal," Proceedings of the Canadian Communications and Power Conference, Montreal, Canada, 1978, pp. 341-349.

13 A. E. Hammad, K. Sadek, J. Koelsch, and G. Gueth, "Advanced Scheme for AC Voltage Control at HVDC Converter Terminals," IEEE Trans. on Power Apparatus and Systems, vol. PAS-104, no. 3, March 1985, pp. 697-703.

14 J. P. Bowles, "Alternative Techniques and Optimization of Voltage and Reactive Power Control at HVDC Converter Stations," Proceedings of IEEE Conference on Overvoltages and Compensation on Integrated AC/DC System, Winnipeg, Canada, July 1980.

15 Y. Yoshida, "Development of a Calculation Method of AC Voltage Stability in HVDC Transmission Systems," Electrical Engineering in Japan, vol. 94, no. 2, 1974, pp. 77-85.

16 F. Nishimura, A. Watanabe, N. Fujii, and F. Ogata, "Constant Power Factor Control System for HVDC Transmission," IEEE Trans. on Power Apparatus and Systems, vol. PAS-95, no. 6, Nov./Dec. 1976, pp. 1845-1853.

17 P. K. Kalra and R. M. Mathur, "Power Factor Control for HVDC Transmission System Feeding to Weak AC System," paper presented at IEEE Conference (MONTECH), Montreal, Sept. 29 - Oct. 1, 1986.

18 M. Yuki, T. Nambu, N. Nagai, K. Katsuki, and J. Tsukamoto, "Development of Digitalised Control Equipment for HVDC Transmission," IEEE Trans. on Power Apparatus and Systems, vol. PAS-103, no. 1, Jan. 1984, pp. 190-196.

19 C. E. Grund, R. V. Pohl, and J. Reeve, "Control Design of Active and Reactive Power HVDC Modulation Systems with Kalman Filtering," IEEE Trans. on Power Apparatus and Systems, vol. PAS-101, no. 10, Oct. 1982, pp. 4100-4111.

20 N. G. Hingorani, L. Cresap, R. Pohl, "Active and Reactive Power Modulation of HVDC System," Proceeding of IEEE Conference on Overvoltages and Compensation in Integrated AC-DC Systems, Winnipeg, July 1980, pp. 51-57.

21 C. E. Grund, M. P. Bahrman, N. Balu, L. Bergstrom, W. F. Long, R. J. Newell, D. Osborne, and R. V. Pohl, "Dynamic Performance Characteristics of North American HVDC Systems for Transient and Dynamic Stability Evaluations," IEEE Trans. Power Apparatus and Systems, vol. PAS-100, no. 7, July 1981, pp. 3356-3364.

22 R. Jotten, J. P. Bowles, G. Liss, C. J. B. Martin, and E. Rumpf, "Control in HVDC Systems, The State of the Art, Part I: Two-terminal Systems; Part II: Multiterminal System," Proceedings of the Cigre International conference on Large High Voltage Electric Systems, Paris, France, Aug. 30-Sept. 7, 1978.

23 K. J. Astrom and B. Wittenmark, Adaptive Control, Addison-Wesley, Reading, Massachusetts, 1989.

24 B. K. Johnson, "HVDC Models used in Stability Studies," Paper no. 88 SM 577-9, IEEE PES Summer Meeting, Portland, Oregon, July 24-29, 1988.

25 G. D. Breuer, J. F. Luini, and C. C. Young, "Studies of Large AC/DC Systems on the Digital Computer," IEEE Trans. on Power Apparatus and Systems, vol. PAS-85, no. 11, Nov. 1966, pp. 1107-1115.

26 T. Adielson, "Modelling of the Hvdc System for Digital Simulation of AC/DC Transmission interactions," paper 100-02, Cigre Symposium on AC/DC Interactions and Comparisons, Boston, Sept. 28-30, 1987.

27 P. Danfers, U. Lamm, and E. Uhlmann, "Some Aspects of Tapping hvdc Transmission Systems," Direct Current, vol. 10, no. 2, May 1963, pp. 124-129.

29 Panel Session, "Prospect of Multi-terminal Hvdc Transmission, IEEE PES Summer Meeting, Mexico City, July 1977.

30 W. F. Long, J. Reeve, J. R. McNichol, M. S. Holland, J. P. Taisne, J. LeMay, and D. J. Lorden, "Application aspects of Multi-terminal Dc Power Transmission," IEEE Trans. on Power Delivery, vol. PWRD-5, no. 4, Nov. 1990, pp. 2084-2098.

31 J. Reeve, "Multiterminal Hvdc Power Systems," IEEE Trans. Power Apparatus and Systems, vol. PAS-99, no. 3, March/April 1980, pp. 729-737.

32 N. Sato, N. V. Dravid, S. M. Chan, A. L. Burns, and J. J. Vithayathil, "Multiterminal Hvdc System representation in a Transient Stability Program," IEEE Trans. Power Apparatus and Systems, vol. PAS-99, no. 5, Sept./Oct. 1980, pp. 1927-1936.

33 Takeichi Sakurai, Kiyoshi Goto, Shoichi Irokawa, Koji Imai, and Takami Sakai, "A New Control Method for Multiterminal Hvdc Transmission without Fast Communication Systems," IEEE Trans. Power Apparatus and Systems, vol. PAS-102, no. 5, May 1983, pp. 1140-1150.

34 W. F. Long, J. Reeve, J. R. McNichol, R. E. Harrison, and J. P. Bowles, "Considerations for Implementing Multiterminal DC System," IEEE Trans. Power Apparatus and Systems, vol. PAS-104, no. 9, Sept. 1985, pp. 2521-2530.

35 S. Lefebvre, W. K. Wong, J. Reeve, M. Baker, and D. Chapman, "Considerations for Modelling MTDC Systems in Transient Stability Programs," IEEE Trans. on Power Delivery, vol. PWRD-6, no. 1, Jan. 1991, pp. 397-404.

36 H. Forsell, "The Gotland D. C. Link: The Grid Control and Regulation Equipment," - Part I, Direct Current, vol. 2, no. 7, 1955, pp 109-114; Part II, Direct Current, vol. 2, no. 7, 1955, pp. 166-170.

37 I. Liden, S. Sviden, and E. Uhlmann, "The Gotland D. C. Link: The Layout of the Plant," - Part I, Direct Current, vol. 2, no. 1, 1954, pp 2-7; Part II, Direct Current, vol. 2, no. 2, 1954, pp. 34-39.

38 C. Adamson and N. G. Hingorani, "Control of Hvdc Converters," Direct Current, vol. 7, no. 6, 1962, pp. 148-155.

39 J. D. Ainsworth, "Harmonic Instability between Controlled Static Converters and A.C. Networks," Proceedings IEE, vol. 114, no. 7, July 1967.

40 P. G. Engstrom, "Operation and Control of Hvdc Transmission," IEEE Trans. Power Apparatus and Systems, vol. PAS-83, no. 3, Jan. 1964, pp. 71-77.

41 J. D. Ainsworth, "The Phase-locked Oscillator - A new Control System for Controlled Static Converters," IEEE Trans. Power Apparatus and Systems, vol. PAS-87, no. 3, 1984, pp. 859-865.

42 A. Ekstrom and G. Liss, "A refined Hvdc Control Stystem," IEEE Trans. Power Apparatus and Systems, vol. PAS-89, no. 5/6, May/June 1970, pp.723-732.

43 E. Rumpf and S. Ranade, "Comparison of Suitable Control Systems for HVDC Stations Connected to Weak AC Systems, Part I: New Control Systems; Part II: Operational Behavior of the HVDC Transmission," IEEE Trans. on Power Apparatus and System, Vol. PAS-91, 1972, pp. 549-564.

44 J. J. Dougherty, T. Hillesland, Jr., "Power System Stability Considerations with Dynamically responsive DC Transmission Lines," IEEE Trans. Power Apparatus and Systems, vol. PAS-89, no. 1, Jan. 1970, pp. 34-41.

45 R. L. Cresap and W. A. Mittlestadt, "Small-Signal Modulation of the Pacific HVDC Intertie," IEEE Trans. Power Apparatus and Systems, vol. PAS-95, no. 2, March/April 1976, pp. 536-541.

46 R. L. Cresap, W. A. Mittlestadt, D. N. Scott, and C. W. Taylor, "Operating Experience with Modulation of the Pacific HVDC Intertie," IEEE Trans. Power Apparatus and Systems, vol. PAS-97, no. 4, July/Aug 1978, pp. 1053-1059.

47 R. L. Lee, D. Zollman, J. F. Tang, J. C. Hsu, J. R. Hunt, R. S. Burton, and D. E. Fletcher, "Enhancement of ac/dc System Perfromance by Modulation of a proposed Multiterminal DC System in the Southwestern U.S.," IEEE Trans. on Power Delivery, vol. PWRD-3, no. 1, Jan. 1988, pp. 307-316.

48 S. Lefebvre, M. Saad, and R. Hurtead, "Adaptive Control for HVDC Power Transmission System," IEEE Trans. on Power Appratus and System, vol. PAS-104, no. 9, Sept. 1985, pp. 2329-2335.

49 N. Rostamkolai, A. G. Phadke, W. F. Long, and J. S. Thorp, "An Adaptive Optimal Control Strategies for Dynamic Stability Enhancement of AC/DC Power System," IEEE Trans. on Power System, vol. 3, no. 3, Aug. 1988, pp. 1139-1145.

50 J. R. Smith, D. J. Trudnowski, P. A. Emmanuel, T. A. Short, D. A. Pierre, M. H. Nehrir, and G. L. Keenan, "A Low-order Transient Stability Model with Dynamic Characteristics of the Western North American Power Systems," MEPRA Report no. 291075-6, Electrical Engineering Department, Montana State University, Bozeman, Montana, Jan. 1990.

51 Users Manual, "Extended Transient Midterm Stability Package," Electrical Power Research Institute, Manual no. EPRI EL-2003-CCM, Jan. 1987.

52 IEEE Committee Report, "Excitation System Models for Power System Stability Studies," IEEE Trans. Power Apparatus and Systems, vol. PAS-100, no. 2, Feb. 1981, pp. 494-509.

53 R. L. Lee, J. H. Gee, and M. J. Beshir, "Planning considerations for the Intermountain HVDC Transmission System," IEEE Trans. on Power Delivery, vol. PWRD-1, no. 1, Jan. 1986, pp. 225-231.

54 C. T. Wu, "Operating and Maintenance Experience - Adelanto Converter Station of the Intermountain Power Project," IEEE Trans. on Power Delivery, vol. PWRD-1, no. 1, Jan. 1986, pp. 225-231.

55 C. T. Wu, P. R. Shockley, and L. Engstrom, "The Intermountain Power Project 1600 MW Hvdc Transmission System," IEEE Trans. on Power Delivery, vol. PWRD-3, no. 3, July 1988, pp. 1249-1256.

56 F. B. Hildebrand, Introduction to Numerical Analysis, McGraw Hill, New York, 1956.

57 J. R. Smith, D. A. Pierre, D. A. Rudberg, I. Sadighi, A. P. Johnson, and J. Hauer, "An Enhanced LQ Adaptive Var Unit Controller for Power System Damping," IEEE Trans. on Power System, vol. 4, no. 2, May 1989, pp. 443-451.

58 J. R. Smith, D. A. Pierre, I. Sadighi, and M. H. Nehrir, "A Supplementary Adaptive Var Unit Controller for Power System Damping," IEEE Trans. on Power System, vol. 4, no. 3, Aug. 1989, pp. 1017-1023.

59 D. A. Pierre, "Enhanced LQ Controllers and Adaptive Control," Proceedings of IEEE Conference on Decision and Control, Dec. 1988, pp. 782-785.

60 J. F. Hauer, C. J. Demeure, and L. L. Scharf, "Initial Results in Prony Analysis of Power System Response Signals," Paper no. 89SM702-2-PWRS, IEEE Summer Power Meeting, Long Beach, California, July 9-14, 1989.

APPENDIX

MODIFIED PRONY IDENTIFICATION SOFTWARE PACKAGE

```
C*************************************************************************
C**
C**   Progrm:  PRONYNEWID
C**
C**   by:  Dan Trudnowski, Montana State Univ., Sept. 1989, Oct. 1990.
C**        modified by Prince Emmanuel, Oct. 1990
C**
C**   This program uses the PRONY identification method to obtain a
C**   model for a system.  The method of analysis is described in Chap. 7
C**   of "Damping of Low Frequency Oscillations in an AC/DC Power Systems
C**   Using Converter Control," Ph.D. Thesis, EE Dept., Montana
C**   State Univ., 1991, by Prince Emmanuel and Chapter 3 of "Decentralized
C**   Control Strategies for Damping of Power-system Electromechanical
C**   Oscillations," Ph.D. Thesis, EE Dept., Montan State Univ., 1990
C**   by D. Trudnowski.
C**
C**   Two system cases are considered:
C**   1) the nonzero initial condition case; and
C**   2) the zero initial condition case.  With the case 1, a model is
C**   obtained for both the system and the initial conditions.  In the
C**   second case, a model is found for the system.
C**   The model is
C**
C**
C**                              W(s)
C**                               |
C**                  ----------  \|/
C**     U(s)  ----->I  G(s)  1-- + --->sampled at T----->
C**                  ----------     Y(s)                 Y(z)
C**
C**   A system model (G(s)) and initial-condition model are identified
C**   by this program where
C**
C**                   | n    RES(i)             |          n   RESINIL(i)
C**   G(s) = exp(-sD)|sum ------------ +RES(0)| W(s) = sum -----------
C**                   |i=1 s - EIGEN(i)         |         i=1 s - EIGEN(i)
C**
C**   where the eigenvalues (EIGEN's) are assumed distinct.  D is a pure
C**   system delay known by the user.
C**   U(s) is a known input of the form
C**
C**            NUMINPUTS-1        exp(-s*T*MDELAY(j)) - exp(-s*T*MDELAY(j+1))
C**      U(s) =   sum     AMP(j) ---------------------------------------------
C**               j=0                                 s
C**
C**   This program analyzes the sequence y(0) thru y(N-1) to find a yhat(k)
C**   that fits y(k) is a least-squares sense.  For the case where the initial
C**   conditions of G(s) are nonzero, two Prony analysis must be done.
C**   One Prony analysis is conducted from k=MDELAY(MSECDELAY) to
C**   k=MDELAY(MSECDELAY+1); the second analysis is conducted after
C**   k=MDELAY(NUMINPUTS).  Note that MSECDELAY must be less than
C**   NUMINPUTS.
C**
C**   This program gives least-squared model fits for n = 1,2,...,nmax,r
C**   where nmax is calculated by the program.
C**   How well the nth model fits the data is measured with
C**   Err:
C**
C**       Err = 20*log{2norm(yhat-y)/2norm(y)}
C**
```

Figure 77. Modified Prony identification programs.

```
C**   The smaller Err, the better the fit.  Output from this program is the
C**   nmax models, and their associated errors.  The program ORDER may be run
C**   to see how well each model fits the data.
C**
C**       Must be LINKED with:  QPOLYRT, DPINV (DLINPAK).
C**
C*************************************************************************
C**
C**   Inputs to PRONYID:
C**
C**      Y         = vector of output sequence, Y(1), Y(2), ..., Y(NSAM);
C**      TSAM      = sampling rate;
C**      NUMINPUTS = total number of delayed inputs (see above eqn.);
C**      SYSDELAY  = System delay in samples (D=SYSDELAY*TSAM above);
C**      AMP       = vector of input amplitude inputs, AMP(0), AMP(1), ...,
C**                  AMP(NUMINPUTS-1);
C**      MDELAY    = vector of integer delays, MDELAY(0), MDELAY(1),...,
C**                  MDELAY(NUMINPUTS);
C**      MSECDELAY = start of second prony analysis (see description above).
C**
C**   Y is input from a TEKPLOT file, other inputs are input iteractively.
C**
C**
C**   Outputs are contained in ORDER.IN, and ERROR.TEK.  ORDER.IN is read
C**   by the program ORDER.
C**     ORDER.IN:
C**
C**      Title
C**
C**      TSAM, NUMINPUTS, N (final order), MSECDELAY, SYSDELAY
C**
C**      MDELAY(1), ..., MDELAY(NUMINPUTS)
C**
C**      AMP(0), ..., AMP(NUMINPUTS-1)
C**
C**      Name of TEKPLOT file containing Y
C**
C**      INPUTTEK (The dependent variable column containing Y in the
C**                TEKPLOT file)
C**
C**      REAL AND DISCRETE -TIME EIGENVALUES
C**
C**      TRANSFER-FUNCTION RESIDUES
C**
C**      INITIAL-CONDITION RESIDUES
C**
C**    ERROR.TEK;
C**   Contains the Err(i), i=1,2,...,nmax; it is set up as a TEKPLOT file.
C**
C**
C*************************************************************************
C
C  MAX IS THE MAXIMUM LENTH OF Y, NMAX IS THE MAXIMUM SYSTEM ORDER,j
C  AND INMAX IS THE MAXIMUM NUMBER OF PULSES IN THE INPUT.
C
      PARAMETER(MAX=500, MAX2=2*MAX, NMAX=IINT(MAX/3.0)+1, INMAX=10)
C
C
      IMPLICIT REAL*8 (A-H,O-Z)
      INTEGER SYSDELAY
```

Figure 77. Continued.

```
      REAL*8 MATRIX
      COMPLEX*16 BRES, RES, ZEIGEN, EIGEN, RESINIL, DET
      CHARACTER NAME*20, TITLE*60, INICOND*1, NYQANS*1
      DIMENSION Y(MAX2), YHAT(MAX2), ISAVE(NMAX), ERR(NMAX),
     &          MATRIX(MAX2,NMAX*2)
      DIMENSION AMP(0:INMAX), MDELAY(0:INMAX+1)
      DIMENSION BRES(NMAX,2), RES(NMAX), ZEIGEN(NMAX), EIGEN(NMAX),
     &          RESINIL(NMAX)
      DIMENSION TEMP1(NMAX), TEMP2(NMAX), TEMP3(2*NMAX)
      DATA PIE/3.141592654/MDELAY(0)/0/IEIGEN/2/
      DATA (Y(I),I=1,MAX2)/MAX2*0.0D0/
C*************************************************************************
C**   Other Variables required for calculation of RES(0)
c
      complex*16 zmatrix(nmax,nmax), bnew(nmax,inmax), ynew(nmax)
      complex*16 znew(nmax), zsum, ysum, qnpls1, res0
      character thruput*1
c
C**
C*************************************************************************

C  OPEN OUTPUT DATA FILES:
      OPEN(15,FILE='ORDER.IN',STATUS='NEW')
      OPEN(17,FILE='ERROR.TEK',STATUS='NEW')
c     open(19,file='Test.out',status='new')
C
C------------------------------- INPUT DATA -----------------------------
      WRITE(*,5)
      READ(*,20) TITLE
      WRITE(*,10)
      READ(*,1000) NAME
      WRITE(*,15)
      READ(*,*) INPUTTEK
      WRITE(*,30)
      READ(*,*) TSAM
      WRITE(*,33)
      READ(*,*) NUMINPUTS
      WRITE(*,40) NUMINPUTS
      READ(*,*) (AMP(I), I=0,NUMINPUTS-1)
      WRITE(*,45) NUMINPUTS
      READ(*,*) (MDELAY(I),I=1,NUMINPUTS)
      WRITE(*,46)
      READ(*,*) SYSDELAY
      WRITE(*,47)
      READ(*,17) INICOND
      IF ((INICOND .EQ. 'N').OR.(INICOND .EQ. 'n')) THEN
         WRITE(*,50)
         READ(*,*) MSECDELAY
         IF (MSECDELAY .GE. NUMINPUTS) THEN
            WRITE(*,*)
            WRITE(*,*)'****************************************'
            WRITE(*,*)'    ERROR:  This value must be less '
            WRITE(*,*)'            than the number of input'
            WRITE(*,*)'            pulses.'
            WRITE(*,*)'****************************************'
            STOP
         ENDIF
         WRITE(*,55)
         READ(*,*) IEIGEN
```

Figure 77. Continued.

```
      ENDIF
      WRITE(*,60) 1.0D0/(4.0D0*TSAM)
      READ(*,17) NYQANS
C*************************************************************************
C**   Modified Part
C
      write(*,65)
      read(*,17)thruput
 65   FORMAT(/,'  Is throughput exist ? (Y/N) --> ',$)
C
C**   end of modified part
C*************************************************************************

  5   FORMAT(/,'  Title of run --> ',$)
 10   FORMAT(/,'  Name of TEKPLOT file containing output y(n) --> ',$)
 15   FORMAT(/,'  TEKPLOT variable to be analyzed  --> ',$)
 17   FORMAT(A1)
 20   FORMAT(A60)
 30   FORMAT(/,'  Sampling period --> ',$)
 33   FORMAT(/,'  Number of pulses in the input --> ',$)
 40   FORMAT(/,'      Amplitude of ',I2,' pulses --> ',$)
 45   FORMAT(/,'     ',I2,' delay integers of pulses --> ',$)
 46   FORMAT(/,'  System delay in samples --> ',$)
 47   FORMAT(/,'  Zero initial conditions? (Y/N) --> ',$)
 50   FORMAT(/,'      First Prony analysis done after pulse --> ',$)
 55   FORMAT(/,'      Which Prony analysis will be used to ',/,
     &  '      calculate the signal eigenvalues -- 1 or 2 (be ',/,
     &  '      careful to choose the one that contains',/,
     &  '      ALL possible eigenvalues including DC.) --> ',$)
 60   FORMAT(/,'  Delete modes above',F5.2,' hz? (Y/N) --> ',$)
C
C  READ IN SYSTEM OUPUT (Y) FROM TEKPLOT FILE:
      OPEN(11,FILE=NAME,STATUS='OLD')
      READ(11,*)
      READ(11,*)
      READ(11,*) MM
      I = 1
 100  READ(11,*,END=200) T,(TEMP1(J),J=1,MM)
      Y(I) = TEMP1(INPUTTEK)
      I = I + 1
      GOTO 100
 200  NSAM = I - 1
C---------------------------- END OF INPUT --------------------------------
C
C
C
C------- CHECK TO MAKE SURE VARIABLES ARE DIMENSIONED LARGE ENOUGH ------
      IF (NSAM .GT. MAX) THEN
         WRITE(*,*)
         WRITE(*,*)'  Increase parameter MAX in PRONYID.FOR'
         WRITE(*,*)
         STOP
      ENDIF
C--------------------------- END OF CHECK ---------------------------------
C
C
C
C---------- DETERMINE THE NUMBER OF COLUMNS NEEDED FOR ROBUST SVD -------
      IF ((INICOND .EQ. 'N').OR.(INICOND .EQ. 'n')) THEN
         IF ((NSAM-MDELAY(NUMINPUTS)-SYSDELAY) .LT.
     &       (MDELAY(MSECDELAY+1)-MDELAY(MSECDELAY))) THEN
```

Figure 77. Continued.

```
            NDATAPTS = NSAM - MDELAY(NUMINPUTS) - SYSDELAY
         ELSE
            NDATAPTS = MDELAY(MSECDELAY+1)-MDELAY(MSECDELAY)
         ENDIF
      ELSE
         NDATAPTS = NSAM - MDELAY(NUMINPUTS) - SYSDELAY
      ENDIF
      NCOL = IINT(NDATAPTS/3.0) - 1
C------------------ END OF DETERMINATION OF NUMBER OF COLUMNS-------------
C
C
C
C------------------ DETERMINE DISCRETE-TIME EIGENVALUES ------------------
C
C  FORM YMATRIX:
      IF (IEIGEN .EQ. 1) THEN
         M = MDELAY(MSECDELAY) + SYSDELAY
      ELSE
         M = MDELAY(NUMINPUTS) + SYSDELAY
      ENDIF
      DO I = 1,NDATAPTS-NCOL
         DO J = 1,NCOL
            MATRIX(I,J) = Y(NCOL+I-J+M)
         ENDDO
      ENDDO
C
C  SOLVE OVERDETERMINED SYSTEM FOR CHARACTERISTIC EQUATION
C  COEFFICIENTS (TEMP1(1) THRU TEMP1(NCOL)):
      MM = NDATAPTS-NCOL
      CALL PINV(MATRIX,MM,NCOL,MAX2,TEMP1,Y(NCOL+M+1))
C
C  FIND DISCRETE-TIME EIGENVALUES FROM TEMP1:
      DO I=1,NCOL
         TEMP3(I) = -TEMP1(NCOL-I+1)
      ENDDO
      CALL QPOLYRT(TEMP3,NCOL,TEMP1,TEMP2,IROOT)
      IF (IROOT .NE. 0) THEN
         WRITE(*,*)
         WRITE(*,*)'  WARNING! THE EIGENVALUES MAY BE WRONG'
         WRITE(*,*)'           DUE TO ILLCONDITIONING!'
      ENDIF
C---------------- END OF DISCRETE-TIME EIGENVALUE FINDING ----------------
C
C
C
C------------ FIND OUTPUT RESIDUES AND CONTINUOUS-TIME EIGENVALUES -------
C
C  FIRST SET UP Z MATRIX WITH REAL AND IMAGINARY PARTS SEPARATED:
      JCOLUMN = 2
      M = MDELAY(NUMINPUTS) + SYSDELAY
 210  DO J=1,NCOL
         ZMAG = (TEMP1(J)**2 + TEMP2(J)**2)**0.5D0
         PHI = DATAN(TEMP2(J)/TEMP1(J))
         IF ((TEMP1(J) .LT. 0.0D0).AND.(TEMP2(J) .NE. 0.0D0)) THEN
            IF (TEMP2(J) .LT. 0.0D0) THEN
               PHI = PHI - PIE
            ELSE
               PHI = PHI + PIE
            ENDIF
         ENDIF
         IF ((TEMP1(J) .LT. 0.0D0).AND.(TEMP2(J) .EQ. 0.0D0)) PHI=PIE
```

Figure 77. Continued.

```
          DO I=1,NDATAPTS
            MATRIX(I,J) =  ZMAG**(I-1)*DCOS(PHI*(DBLE(I-1)))
            MATRIX(I,J+NCOL) = -ZMAG**(I-1)*DSIN(PHI*(DBLE(I-1)))
            MATRIX(I+NDATAPTS,J) = -MATRIX(I,J+NCOL)
            MATRIX(I+NDATAPTS,J+NCOL) = MATRIX(I,J)
          ENDDO
          IF (JCOLUMN .EQ. 2) THEN
             ZEIGEN(J) = DCMPLX(TEMP1(J),TEMP2(J))
             X1 = DLOG(ZMAG)/TSAM
             X2 = PHI/TSAM
             EIGEN(J) = DCMPLX(X1,X2)
          ENDIF
       ENDDO
C
C-------------- GET RID OF EIGENVALUE ON THE NEG. REAL AXIS -------------
       KCOL = NCOL
       I = 1
       DO WHILE (I .LE. KCOL)
          IF ((DREAL(ZEIGEN(I)) .LT. 0.D0).AND.
     &     (DIMAG(ZEIGEN(I)) .EQ. 0.0D0)) THEN
            KCOL = KCOL - 1
            IF (I .EQ. (KCOL+1)) GOTO 220
            DO J=I,KCOL
               EIGEN(J) = EIGEN(J+1)
               ZEIGEN(J) = ZEIGEN(J+1)
               BRES(J,1) = BRES(J+1,1)
               BRES(J,2) = BRES(J+1,2)
            ENDDO
          ELSE
            I = I + 1
          ENDIF
        ENDDO
 220    NCOL = KCOL
C-------------- END OF DELETING EIGENVALUES ON NEG. REAL AXIS ------------
C
C ------------ remove eigen values having very high damping  ------------
C
       KCOL = NCOL
       I = 1
       DO WHILE (I .LE. KCOL)
          IF (ABS(DREAL(ZEIGEN(I))) .LT. 0.606) THEN
             KCOL = KCOL - 1
             IF (I .EQ. (KCOL+1)) GOTO 222
             DO J=I,KCOL
                EIGEN(J) = EIGEN(J+1)
                ZEIGEN(J) = ZEIGEN(J+1)
                BRES(J,1) = BRES(J+1,1)
                BRES(J,2) = BRES(J+1,2)
             ENDDO
          ELSE
             I = I + 1
          ENDIF
        ENDDO
 222    NCOL = KCOL
C
C --------  end of removal of eigne values having very high damping ------
C
C  NOW SOLVE THE OVER-DETERMINED SYSTEMS FOR OUTPUT RESIDUE:
       DO I=1,NDATAPTS
          YHAT(I) = Y(M+I)
```

Figure 77. Continued.

```
            YHAT(NDATAPTS+I) = 0.0D0
         ENDDO
         CALL PINV(MATRIX,2*NDATAPTS,2*NCOL,MAX2,TEMP3(1),YHAT)
         DO I=1,NCOL
            BRES(I,JCOLUMN) = DCMPLX(TEMP3(I),TEMP3(I+NCOL))
         ENDDO
         IF ((INICOND .EQ. 'N').OR.(INICOND .EQ. 'n')) THEN
            M = MDELAY(MSECDELAY) + SYSDELAY
            JCOLUMN = JCOLUMN - 1
            IF (JCOLUMN .EQ. 1) GOTO 210
         ENDIF
C------------------ END OF OUTPUT RES. AND EIGEN. ------------------------
C
C
C
C---------- GET RID OF ALL MODES ABOVE NYQUIST/2 IF USER DESIRES --------
         IF ((NYQANS .EQ. 'Y').OR.(NYQANS .EQ. 'y')) THEN
            I = 1
            DO WHILE (I .LE. KCOL)
               IF (DREAL(ZEIGEN(I)) .LT. 0.D0) THEN
                  KCOL = KCOL - 1
                  IF (I .EQ. (KCOL+1)) GOTO 230
                  DO J=I,KCOL
                     EIGEN(J) = EIGEN(J+1)
                     ZEIGEN(J) = ZEIGEN(J+1)
                     BRES(J,1) = BRES(J+1,1)
                     BRES(J,2) = BRES(J+1,2)
                  ENDDO
               ELSE
                  I = I + 1
               ENDIF
            ENDDO
         ENDIF
 230     NCOL = KCOL
C------------- END OF DELETING MODES ABOVE THE NYQUIST/2 RATE -----------
C
C
C
C--------- CALCULATE TRANSFER-FUNCTION INITIAL-CONDITION RESIDUES -------
         AMP(NUMINPUTS) = 0.0D0
C
C  IF THE USER SPECIFIES THE INITIAL-CONDITION RESIDUES ARE ZERO:
         IF ((INICOND .EQ. 'Y').OR.(INICOND .EQ. 'y')) THEN
            DO I=1,NCOL
               RESINIL(I) = DCMPLX(0.0D0,0.0D0)
               DET = AMP(0)*ZEIGEN(I)**MDELAY(NUMINPUTS)
     &               - AMP(NUMINPUTS-1)
               DO J=1,NUMINPUTS-1
                  DET = DET + (AMP(J)-AMP(J-1))*
     &                  ZEIGEN(I)**(MDELAY(NUMINPUTS)-MDELAY(J))
               ENDDO
               RES(I) = BRES(I,2)*EIGEN(I)/DET
            ENDDO
C
C  IF THE USER SPECIFIES NONZERO INITIAL-CONDITION RESIDUES:
         ELSE
            DO I=1,NCOL
               DET = DCMPLX(0.0D0,0.0D0)
               DO J=MSECDELAY+1,NUMINPUTS
                  DET = DET + (AMP(J) - AMP(J-1))*ZEIGEN(I)**
```

Figure 77. Continued.

```
     &                (MDELAY(NUMINPUTS)-MDELAY(J))
            ENDDO
            M = MDELAY(NUMINPUTS)-MDELAY(MSECDELAY)
            RES(I) = EIGEN(I)*(BRES(I,2)-BRES(I,1)*
     &              ZEIGEN(I)**M) / DET
            RESINIL(I) = BRES(I,2) - (AMP(0)*RES(I)/EIGEN(I))*
     &                   ZEIGEN(I)**MDELAY(NUMINPUTS)
            DO J=1,NUMINPUTS
               RESINIL(I) = RESINIL(I)-(RES(I)/EIGEN(I))*
     &                      (AMP(J)-AMP(J-1))*
     &                      ZEIGEN(I)**(MDELAY(NUMINPUTS)-MDELAY(J))
            ENDDO
            RESINIL(I) = RESINIL(I)*
     &                   ZEIGEN(I)**(-SYSDELAY-MDELAY(NUMINPUTS))
         ENDDO
       ENDIF
C---------------------- END OF RESIDUE CALCULATION -----------------------
C
C
C
C-------------     REORDER EIGNEVALUES AND RESIDUES    -------------------
C-------------    ACCORDING TO CONTIBUTION TO SIGNAL   -------------------
C------------- (IN THE SENSE THAT IT REDUCES THE ERROR -------------------
C-------------  BETWEEN THE ACTUAL SIGNAL (Y) AND THE  -------------------
C-------------        ESTIMATED SIGNAL (YHAT).         -------------------
      NORTEMP = 0
 300  ICOUNT = 1
      ERROLD = 1.0D+35
      DO WHILE (ICOUNT .LE. NCOL)
         IF (NORTEMP .GT. 0) THEN
            DO J=1,NORTEMP
               IF (ICOUNT .EQ. ISAVE(J)) THEN
                  IDELTA = 1
                  GOTO 400
               ENDIF
            ENDDO
         ENDIF
         ISAVE(NORTEMP+1) = ICOUNT
         IDELTA = 1
         IF (DABS(DIMAG(EIGEN(ICOUNT))) .GT. 1.0D-12) THEN
            IDELTA = 2
            ISAVE(NORTEMP+2) = ICOUNT+1
         ENDIF
C
C  CALCULATE YHAT AND THE ERROR ASSOCIATED WITH YHAT FOR
C  ORDER NORTEMP+IDELTA:
         N = NORTEMP+IDELTA
         YDEL = 0.0D0
         YNORM = 0.0D0
C
C-----CALCULATE YHAT FOR K=MDELAY(MSECDELAY)+SYSDELAY TO
C-----K=MDELAY(MSECDELAY)+SYSDELAY-1;
         IF ((INICOND .EQ. 'N').OR.(INICOND .EQ. 'n')) THEN
            M = MSECDELAY
            M1 = MDELAY(MSECDELAY) + SYSDELAY
            DO K = M1, MDELAY(M+1)+SYSDELAY-1
               YHAT(K+1) = 0.0D0
               DO I=1,N
                  L = ISAVE(I)
                  YHAT(K+1) = YHAT(K+1) + DREAL(BRES(L,1)*
```

Figure 77. Continued.

```
     &                          ZEIGEN(L)**(K-M1) - AMP(M)*
     &                          RES(L)/EIGEN(L))
               ENDDO
               YDEL = YDEL + (Y(K+1)-YHAT(K+1))**2
               YNORM = YNORM + Y(K+1)**2
            ENDDO
         ENDIF
C
C-----CALCULATE YHAT FOR K=MDELAY(NUMINPUTS)+SYSDELAY TO K=NSAM-1;
         M1 = MDELAY(NUMINPUTS) + SYSDELAY
         DO K = M1,NSAM-1
            YHAT(K+1)=0.0D0
            DO I=1,N
               L = ISAVE(I)
               YHAT(K+1) = YHAT(K+1) + DREAL(BRES(L,2)*
     &                     ZEIGEN(L)**(K-M1))
            ENDDO
            YDEL = YDEL + (Y(K+1)-YHAT(K+1))**2
            YNORM = YNORM + Y(K+1)**2
         ENDDO
         YNORM = YNORM**0.5D0
         YDEL = YDEL**0.5D0
         ERRNEW = 20.0D0*DLOG10(YDEL/YNORM)
C
C----TEST ERROR;
         IF (ERRNEW .LT. ERROLD) THEN
            ERROLD = ERRNEW
            ISV1 = ICOUNT
            INUM = 1
            IF (IDELTA .EQ. 2) THEN
               ISV2 = ICOUNT+1
               INUM = 2
            ENDIF
         ENDIF
 400     ICOUNT = ICOUNT + IDELTA
      ENDDO
      ISAVE(NORTEMP+1) = ISV1
      ERR(NORTEMP+1) = ERROLD
      IF (INUM .EQ. 2) THEN
         ISAVE(NORTEMP+2) = ISV2
         ERR(NORTEMP+2) = ERROLD
      ENDIF
      NORTEMP = NORTEMP + INUM
      IF (NORTEMP .LT. NCOL) GOTO 300
C
C------------------------ END OF REARRANGEMENT --------------------------
C
C*****************************************************************************
c**   Modified Portion to calculate the RES(0)
c**   First calculat the Zmatrix
c
      if ( (thruput .eq. 'Y') .or. (thruput .eq. 'y')) then
       do j = 1, ncol
          do i = 1, mdelay(numinputs)
              zmatrix(i,j) = zeigen(j)**(i-1)
           enddo
        enddo
c      write(19,319)
c       write(19,349)((zmatrix(i,j),j=1,ncol),i=1,mdelay(numinputs))
c319    format(/,'    ***  Zmatrix data follow  ***  ')
349     format(2x,5(2e8.2))
```

Figure 77. Continued.

```
c      Then calculate new bi's for each interval
       do i = 1, ncol
         bnew(i,1) = res(i)*amp(0)*zeigen(i)**(-sysdelay)/eigen(i)
       enddo
       do j = 1, numinputs - 1
          do i = 1, ncol
             bnew(i,j+1) = bnew(i,j) + (amp(j)-amp(j-1))*res(i)*zeigen(i)
     1                        **(-mdelay(j) - sysdelay)/eigen(i)
          enddo
       enddo
c      write(19,320)
c320   format(/,'   ***  Bnew matrix data for each input section ***')
c      write(19,*)((bnew(i,j),j=1,numinputs),i=1,ncol)
c      write(19,330)
c330   format(/,'  ***  Bold matrix after input has been removed ***')
c      write(19,*)(bres(i,2),i=1,ncol)
c      Now calculate the New Zmatrix and New Ymatrix
       jindex = 0
       do i = 1, numinputs
          do j = 1+jindex, mdelay(i)
             ynew(j) = dcmplx(0.0d0, 0.0d0)
             do k = 1, ncol
                ynew(j) = ynew(j) + zmatrix(j,k)*bnew(k,i)
             enddo
          ynew(j) = dcmplx(y(j), 0.0d0) - ynew(j)
          znew(j) = dcmplx(amp(i-1), 0.0d0)
          enddo
       jindex = mdelay(i)
       enddo
c      write(19,321)
c321   format(/,'   ***  Znew matrix follow *** ')
c      write(19,*)(znew(i), i=1,mdelay(numinputs))
c      write(19,*)
c      write(19,322)
c322   format(/,'   ***  Ynew matrix follow *** ')
c      write(19,*)(ynew(i), i=1,mdelay(numinputs))
c      Thus calculation of New Zmatrix and Ymatrix is over
c
C      Now obtain (znew)'*ynew/((znew)'*znew) to get Q(n+1)
c
       ysum = dcmplx(0.0d0, 0.0d0)
       zsum = dcmplx(0.0d0, 0.0d0)
       do i = 1, mdelay(numinputs)
         zsum = zsum + znew(i)*znew(i)
         ysum = ysum + znew(i)*ynew(i)
       enddo
       qnpls1 = ysum/zsum
c      write(19,*)
c      write(19,323)
c323   format(/,'  ***  Q(n+1) Value ***')
c      write(19,*)qnpls1
c      Now calculate the RES(0) term
       res0 = qnpls1
       do i = 1, ncol
          res0 = res0 + res(i)/eigen(i)
       enddo
c      write(19,*)
c      write(19,324)
c324   format(/,'  ***  RES(0) Value ***')
c      write(19,*)res0
        endif
```

Figure 77. Continued.

```
c
c*   Modified portion is over
C*************************************************************************
C------------------------ OUTPUT TO DATA FILES --------------------------
C
      IF ((INICOND .EQ. 'Y').OR.(INICOND .EQ. 'y')) MSECDELAY=0
C
C  OUTPUT ERR:
      WRITE(17,*)'  N   ERR(N) = NORM(Y-YHAT)/NORM(Y) IN DB'
      WRITE(17,20) TITLE
      WRITE(17,*) 1
      DO I=1,NORTEMP
         WRITE(17,*) I, ERR(I)
      ENDDO
C
C  OUTPUT EIGENVALUES AND RESIDUES TO A DATA FILE SO THAT THE
C  PROGRAM ORDER.FOR CAN READ THESE VALUES:
      WRITE(15,20) TITLE
      WRITE(15,*) TSAM,NUMINPUTS,NORTEMP,MSECDELAY,SYSDELAY
      WRITE(15,*) (MDELAY(I),I=1,NUMINPUTS)
      WRITE(15,*) (AMP(I),I=0,NUMINPUTS-1)
      WRITE(15,1000) NAME
      WRITE(15,*) INPUTTEK
      WRITE(15,*)'  REAL-TIME AND DISCRETE-TIME EIGENVALUES:'
      DO I=1,NORTEMP
         WRITE(15,*) DREAL(EIGEN(ISAVE(I))), DIMAG(EIGEN(ISAVE(I))),
     &               DREAL(ZEIGEN(ISAVE(I))), DIMAG(ZEIGEN(ISAVE(I)))
      ENDDO
      WRITE(15,*)'   TRANSFER-FUNCTION RESIDUES:'
      DO I=1,NORTEMP
         WRITE(15,*) DREAL(RES(ISAVE(I))), DIMAG(RES(ISAVE(I)))
      ENDDO
      IF (MSECDELAY .NE. 0) THEN
         WRITE(15,*)'   INITIAL-VALUE RESIDUES:'
         DO I=1,NORTEMP
            X1 = DREAL(RESINIL(ISAVE(I)))
            X2 = DIMAG(RESINIL(ISAVE(I)))
            WRITE(15,*) X1,X2
         ENDDO
      ENDIF

C*************************************************************************
c**   Modified portion for writing the zeroth Residue
c
      if ( (thruput .eq. 'Y') .or. (thruput .eq. 'y')) then
       write(15,*)'   The Residue corresponding to throughput term:'
        x1 = dreal(res0)
        x2 = dimag(res0)
        write(15,*) x1, x2
      endif
c
c**   end of modified porttion for writing
C*************************************************************************
C
      WRITE(*,*)
      WRITE(*,*)'*********************************************'
      WRITE(*,*)
      WRITE(*,*)'  ERROR.TEK contains the errors associated'
      WRITE(*,*)'  model orders.  Run ORDER to obtain the fit'
```

Figure 77. Continued.

```
      WRITE(*,*)'  for a given model.'
      WRITE(*,*)
      WRITE(*,*)'*********************************************'
      WRITE(*,*)
 1000 FORMAT(A20)
C--------------------------- END OF OUTPUT ------------------------------
C
C
C-------------------------- THAT'S ALL FOLKS ----------------------------
      STOP
      END
```

Figure 77. Continued.

```
C*****************************************************************
C**
C**   Program ORDER
C**
C**   This program reads in the eigenvalues and residues resulting
C**   from PRONYWDELAY.  It then calculates the estimate yhat based on
C**   these residues and compares it with the actual data.  The system
C**   is input by the user.
C**
C**   Output files are PRONYWDELAY.OUT and YHATWDELAY.TEK.  YHATWDELAY
C**   is formatted
C**   for TEKPLOT, and contains the actual output y and the estimated
C**   output yhat.  PRONYWDELAY.OUT contains the residues and eigenvalues.
C**
C**   Written by Dan Trudnowski, OCT. 1989, OCT. 1990.
C**   Modified by Prince Emmanuel, OCT. 1990 to include Residue RES(0) term.
C**
C*****************************************************************
C
      PARAMETER(MAX = 500, NMAX=IINT(MAX/3.0)+1)
      IMPLICIT REAL*8 (A-H,O-Z)
      INTEGER SYSDELAY
      COMPLEX*16 RES, RESINIL, EIGEN, ZEIGEN, res0
      CHARACTER TITLE*60,TITLE1*60,NAME*20
      DIMENSION MDELAY(0:NMAX),AMP(0:NMAX), Y(MAX)
      DIMENSION RES(NMAX), RESINIL(NMAX), EIGEN(NMAX), ZEIGEN(NMAX)
      DIMENSION TEMP(NMAX)
      DATA PIE/3.141592654/MDELAY(0)/0/
      DATA (RESINIL(I),I=1,NMAX)/NMAX*(0.0D0,0.0D0)/
C
C
C
C-------------------------- OPEN DATA FILES -----------------------------
C
C  INPUT FILE:
      OPEN(11,FILE='ORDER.IN',STATUS='OLD')
C
C  OUTPUT FILES:
      OPEN(17,FILE='YHAT.TEK',STATUS='NEW')
      OPEN(18,FILE='PRONYID.OUT',STATUS='NEW')
C------------------------- END OF OPENING FILES ------------------------
C
C
C
C--------------------------- READ IN DATA -------------------------------
C
C  READ IN THE EIGENVALUES AND RESIDUES:
      READ(11,10)TITLE
      READ(11,*) TSAM, NUMINPUTS, NCOL, MSECDELAY, SYSDELAY
      READ(11,*) (MDELAY(I),I=1,NUMINPUTS)
      READ(11,*) (AMP(I),I=0,NUMINPUTS-1)
      READ(11,20) NAME
      READ(11,*) INPUTTEK
      READ(11,10) TITLE1
      DO I=1,NCOL
         READ(11,*) X1, X2, X3, X4
         EIGEN(I) = DCMPLX(X1,X2)
         ZEIGEN(I) = DCMPLX(X3,X4)
      ENDDO
      READ(11,10)TITLE1
```

Figure 77. Continued.

```
      DO I=1,NCOL
         READ(11,*)X1, X2
         RES(I) = DCMPLX(X1,X2)
      ENDDO
      IF (MSECDELAY .NE. 0) THEN
         READ(11,10)TITLE1
         DO I=1,NCOL
            READ(11,*) X1, X2
            RESINIL(I) = DCMPLX(X1,X2)
         ENDDO
      ENDIF
C*********************************************************************
c**
c
      read(11,10)title1
      read(11,*)x1, x2
      res0 = dcmplx(x1,x2)
c     print *, res0
c
c**
C*********************************************************************

 10   FORMAT(A60)
 20   FORMAT(A20)
C
C  READ IN Y:
      OPEN(12,FILE=NAME,STATUS='OLD')
      READ(12,*)
      READ(12,*)
      READ(12,*) M
      I = 0
 100  I = I + 1
      READ(12,*,END=200) T,(TEMP(J),J=1,M)
      Y(I) = TEMP(INPUTTEK)
      GOTO 100
 200  NSAM = I - 1
C
C  CHECK DIMENSIONS:
      IF (NCOL .GT. NMAX) THEN
         WRITE(*,250)NSAM
      ENDIF
      IF (NSAM .GT. MAX) THEN
         WRITE(*,260)NSAM
      ENDIF
 250  FORMAT(/,'  Parameter MAX is too small, increase above ',I3)
 260  FORMAT(/,'  Parameter MAX is too small, increase above ',I3)
C
C  INPUT SYSTEM ORDER:
      WRITE(*,300) NCOL
      READ(*,*) N
 300  FORMAT(/,'  System order (less than or equal to ',I2,') --> ',$)
C-------------------------- END OF DATA INPUT ----------------------------
C
C
C
C----CALCULATE YHAT FOR ORDER N AND OUTPUT TO DATA FILES ----------------
C
C  SET UP TEKPLOT FILE YHAT.TEK:
      WRITE(17,*)'  TIME,  ACTUAL OUTPUT, ESTIMATED OUTPUT.'
```

Figure 77. Continued.

```
      WRITE(17,*)
      WRITE(17,*) 2
C
C  CALCULATE YHAT AND THE ERROR BETWEEN Y AND YHAT IN DB:
      YDEL = 0.0D0
      YNORM = 0.0D0
      MS = SYSDELAY
      DO K=0,NSAM-1
         YHAT = 0.0D0
         DO I=1,N
            YHAT = YHAT + DREAL(RESINIL(I)*ZEIGEN(I)**K)
            DO J=0,NUMINPUTS-1
               IF (K .GE. (MDELAY(J) + MS)) YHAT = YHAT + DREAL(
     &            AMP(J)*(ZEIGEN(I)**(K-MS-MDELAY(J))-1.0D0)*
     &            RES(I)/EIGEN(I))
               IF (K .GE. (MDELAY(J+1) + MS)) YHAT = YHAT - DREAL(
     &            AMP(J)*(ZEIGEN(I)**(K-MS-MDELAY(J+1))-1.0D0)*
     &            RES(I)/EIGEN(I))
            ENDDO
         ENDDO

C*************************************************************************
c**  This portion is modified to take into consideration
c**  the res0 or RES(0) term
c
      do j = 0, numinputs-1
         if(k .ge. (mdelay(j) + ms))yhat = yhat + dreal(
     &        amp(j)*res0)
         if(k .ge. (mdelay(j+1) + ms))yhat = yhat - dreal(
     &        amp(j)*res0)
      enddo
c
c**
C*************************************************************************

         T = TSAM*DBLE(K)
         WRITE(17,*) T, Y(K+1), YHAT
         YDEL = YDEL + (Y(K+1)-YHAT)**2
         YNORM = YNORM + Y(K+1)**2
      ENDDO
      YDEL = YDEL**0.5D0
      YNORM = YNORM**0.5D0
      ERROR = 20.0D0*DLOG10(YDEL/YNORM)
C--------------------- END OF YHAT AND ERROR CALCULATION -----------------
C
C
C
C---------- OUTPUT SYSTEM DELAY, ERROR, RESIDUES, AND EIGENVALUES -------
      WRITE(18,1000)TITLE
      WRITE(18,1005)ERROR
      WRITE(18,1007)SYSDELAY
      WRITE(18,*)'  THE REAL-TIME EIGNEVALUES AND THEIR ASSOCIATED'
      WRITE(18,*)'  RESIDUES ARE:'
      DO I=1,N
         X1 = DREAL(EIGEN(I))
         X2 = DIMAG(EIGEN(I))
         X3 = DREAL(ZEIGEN(I))
         X4 = DIMAG(ZEIGEN(I))
```

Figure 77. Continued.

```
          X5 = DREAL(RES(I))
          X6 = DIMAG(RES(I))
          X7 = DREAL(RESINIL(I))
          X8 = DIMAG(RESINIL(I))
          WRITE(18,1010)I,X1,X2
C         WRITE(18,1015)I,X3,X4
          WRITE(18,1020)I,X5,X6
          IF (MSECDELAY .NE. 0) WRITE(18,1025)I,X7,X8
        ENDDO
C*******************************************************************************
c**   modified part
c
      i = 0
      x1 = 0.0d0
      x2 = 0.0d0
      x3 = 1.0d0
      x4 = 0.0d0
      x5 = dreal(res0)
      x6 = dimag(res0)
      write(18,1010)i,x1,x2
c     write(10,1015)i,x3,x4
      write(18,1020)i,x5,x6
c
c**  modified part ends here
C*******************************************************************************

 1000 FORMAT(/,A60)
 1005 FORMAT(/,'  ERROR BETWEEN YHAT AND Y (in db) = ',D12.4)
 1007 FORMAT(/,'  SYSTEM DELAY IN SAMPLES =',I2,/)
 1010 FORMAT(/,'       EIGENVALUE(',I2,')                = ',
     &       D12.4,' + j ',D12.4)
 1015 FORMAT('       DISCRETE-TIME EIGENVALUE(',I2,')  = ',
     &       D12.4,' + j ',D12.4)
 1020 FORMAT('       TRANSFER-FUNCTION RESIDUE(',I2,') = ',
     &       D12.4,' + j ',D12.4)
 1025 FORMAT('       INITIAL-CONDTION RESIDUE(',I2,')  = ',
     &       D12.4,' + j ',D12.4)
C
C
      WRITE(*,*)
      WRITE(*,*)'*************************************************'
      WRITE(*,*)'**                                             **'
      WRITE(*,*)'**  Data file YHAT.TEK contains the estimated and **'
      WRITE(*,*)'**  actual outputs in TEKPLOT format.           **'
      WRITE(*,*)'**                                             **'
      WRITE(*,*)'**  PRONYID.OUT contains eigenvalues and resiues. **'
      WRITE(*,*)'**                                             **'
      WRITE(*,*)'*************************************************'
      STOP
      END
```

Figure 77. Continued.